

Stimulation Methods in Naturally Fractured Carbonates



Master Thesis
by
Philip Nöbauer, BSc.

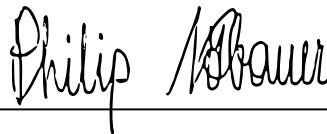
Submitted at the
Chair for Petroleum and Geothermal Energy Recovery
at the
University of Leoben
Leoben, 30th of June 2015

AFFIDAVIT

I declare in lieu of oath, that I wrote this thesis and performed the associated research myself, using only literature cited in this volume.

EIDESSTÄTTLICHE ERKLÄRUNG

Ich erkläre an Eides statt, dass ich diese Arbeit selbstständig verfasst, andere als die angegebenen Quellen und Hilfsmittel nicht benutzt und mich auch sonst keiner unerlaubten Hilfsmittel bedient habe.

A handwritten signature in black ink that reads "Philip Nöbauer". The signature is written in a cursive style with a horizontal line underneath it.

(Philip Nöbauer, BSc.)

Sydney, 5th of October 2015

Executive Summary

Stimulation of carbonate reservoirs is considered a routine operation. However, the presence of natural fractures makes the process more challenging due to several reasons such as fast acid spending rates, high leak-off and non-effective diversion.

As it is the target to reduce the skin factor to the lowest possible value in each zone of the treated section the stimulation job must be carefully designed and optimized. Several kinds of diversion methods have been developed in order to uniformly cover the formation with acid. Those include chemical diversion techniques that alter the viscosity of the acid system, which reduces the invasion of acid into highly permeable zones such as fractures. As a consequence, more acid remains available to flow towards regions with lower permeabilities. This guarantees that the stimulation fluids contact the largest possible reservoir surface area.

Other stimulation techniques hydraulically fracture the formation in order to open closed natural fractures or to create new ones that connect the existing fractures leading to a more complex fracture network. Common techniques include acid fracturing and propped fracturing of rocks.

In performing such stimulation treatments, it is always of highest importance to take special care on all HSSE standards. Before introducing such advanced stimulation treatments in a certain country it has to be checked whether those treatments are in accordance with all local regulations. It is important to take such research into consideration but this is not the main focus of this thesis.

In this thesis a worldwide case study on stimulation in naturally fractured carbonates is conducted. Afterwards it is compared with the stimulation of naturally fractured carbonates in Austria by OMV and observations and suggestions what to improve are illustrated.

Contents

1	Introduction	1
2	Stimulation Theory	2
2.1	Basics	2
2.1.1	Acid washes	2
2.1.2	Matrix acidizing	2
2.1.3	Acid fracturing	2
2.2	Types of acids	3
2.3	Reactions of acid with carbonate rocks.....	3
2.4	Physics	6
2.5	Matrix Acidizing.....	7
2.5.1	Treatment design	8
2.5.2	Retardation.....	9
2.5.3	Treatment placement.....	11
2.6	Acid Fracturing	13
2.6.1	Viscous fingering	13
2.6.2	Viscous acid fracturing	13
2.7	Factors influencing fracturing.....	15
2.7.1	Wellbore placement and lateral length.....	16
3	Naturally fractured reservoirs	17
3.1	Basics	17
3.1.1	Productivity heterogeneity.....	17
3.2	Characteristics	19
3.3	Fracture classification.....	20
3.4	NFR characterization	24
	Core-fracture identification.....	24
3.4.1	Distinguish open/kinematic aperture.....	25
3.4.2	Imaging logs.....	25
3.4.3	Indirect measurements	26
3.4.4	Seismics	29
3.5	Types of NFR characterization.....	32

4	Stimulation in naturally fractured carbonates	34
4.1	Basics	34
4.1.1	Acid Fracturing	35
4.1.2	Coiled tubing	35
4.1.3	Bullheading.....	35
4.1.4	Decision tree.....	36
4.2	Case Studies	36
4.2.1	Bullheading vs coiled tubing.....	36
4.2.2	Packer vs bullheading.....	38
4.2.3	Packer	41
4.2.4	Ball sealer	42
4.2.5	Viscoelastic acid limitations.....	42
4.2.6	Enhanced viscoelastic acid	44
4.2.7	Southeastern New Mexico	45
4.2.8	Coiled tubing acid tunneling.....	48
5	HSE	53
6	Geology of the Vienna Basin	54
6.1	Zoning.....	54
6.1.1	Pre-Neogene Floor: Allochthonous Alpine – Carpathian Floor	56
7	Stimulation of Carbonates in OMV Austria	58
7.1	Main reservoirs in OMV Austria	59
7.2	Division into Areas.....	61
7.3	Strasshof Tief 5a	62
7.4	Evaluation of the stimulation treatments in STR T5a.....	67
7.4.1	Technical evaluation.....	69
7.4.2	Economical Evaluation	70
8	Findings and Conclusion	71
9	Recommendations	72
	References.....	75
10	Appendix	82

List of Figures

Figure 1: Acid penetration distance in dependence of temperature, kind of rock mineral and acid strength	5
Figure 2: Effect of Damköhler number on stimulation efficiency	8
Figure 3: Viscosity profile of 28% HCl containing a viscoelastic surfactant gelling agent	10
Figure 4: Productivity increase ratio as a function of the number of fractures.	15
Figure 5: Fracture development as a function of wellbore orientation	16
Figure 6: FCI distribution in a naturally fractured reservoir	19
Figure 7: Schematic diagram showing the normal and shear stresses.....	20
Figure 8: The shear fracture with the acute angle (θ) in dependence of σ_1 and σ_3	21
Figure 9: Principal stresses and the direction of the stresses	21
Figure 10: The compressive- and tensile strengths of the various kinds of rocks.....	22
Figure 11: Mohr`s circle in dependence of depth and confining stresses.....	22
Figure 12: Seismic azimuthal anisotropy methods.....	29
Figure 13: Principle of microseismics	31
Figure 14: Actual length and direction of the fractures	32
Figure 15: Decision tree for stimulation treatments in carbonate reservoirs.....	36
Figure 16: Percentage of total perforated interval contributing to production.....	37
Figure 17: Comparison between incremental increases in productivity index for viscoelastic acid placed through coiled tubing and pumped in bull heading	37
Figure 18: Comparison between incremental increases in productivity index for hydrochloric acid placed through coiled tubing and viscoelastic diverting acid pumped in bull heading	38
Figure 19: Duration for packer treatments	39
Figure 20: Duration for bullhead treatments	40
Figure 21: Skin before and after treatment for packer and bullhead treatments	40
Figure 22: Skin before treatment and the change of skin for packer and bullhead treatments ..	41
Figure 23: The skin values after treatment	42
Figure 24: Injectivity profile before and after treatment with viscoelastic acid	43
Figure 25: Post-treatment production log.....	44
Figure 26: Pretreatment and post-treatment production log.....	44
Figure 27: Treatment with Enhanced Viscoelastic Acid	45
Figure 28: Stratigraphic chart	46
Figure 29: BHA with one kick-off tool.....	48

Figure 30: Wormholes that occur as the acid leaks off into the formation	49
Figure 31: Before and after treatment production for wells A-E	52
Figure 32: Comparison of production change of the different stimulation treatments	52
Figure 33: The Vienna Basin in the Alpine - Carpathian thrust belt.	54
Figure 34: Generalized cross-section of the Vienna Basin	55
Figure 35: Geological sketch map of the Alpine - Carpathian connection in the Vienna Basin....	56
Figure 36: Carbonate acidizing pre-design workflow	58
Figure 37: Current producing carbonate reservoirs	60
Figure 38: Generalized cross-section of the reservoirs	62
Figure 39: Scheme of STR T 5 and 5a	63
Figure 40: Results of the temperature log.	65
Figure 41: Wellhead pressure and gas rates	66
Figure 42: Production history of Strasshof Tief 5a from 2009 to April 2014.....	69
Figure 53: Graph treatment 4	110

List of Tables

Table 1: Summary of mechanical packer and bullhead treatments in 5 months.....	39
Table 2: Kind of formation, solubility, Young's modulus and Poisson's ratio	47
Table 3: Field data western Venezuela.....	49
Table 4: Conventional treatments.....	50
Table 5: Comparison between matrix acid- and acid tunneling treatments in well 4.....	50
Table 6: Formation characteristics offshore of Spain.....	50
Table 7: Production characteristics of the two pools.....	51
Table 8: Formation characteristics of the Baturaja reservoir	51
Table 9: Formation data	53
Table 10: Production units and reservoir names that the Strasshof wells encounter	61
Table 11: Well test results.....	64
Table 12: The composition of the 28%-, 20%- and 15%- HCl acid system.....	67
Table 13: General data of the acid treatments.	68

1 Introduction

Carbonate rocks play an important role in storing hydrocarbons. Estimates assume that carbonate formations account for roughly 35% of today's worldwide existing petroleum reservoirs that at an approximate estimate contain about 60 – 70% of the world's traditional hydrocarbon reserves [1].

Effective stimulation is an integral part in increasing the recovery and production rate of oil and gas reservoirs [2].

Carbonate rocks have usually a low porosity and permeability and are naturally fractured but offer two particularly useful and often overlooked properties: mechanical integrity and high solubility in acids. Typical solubility of carbonate minerals in hydrochloric acid exceeds 95% and is often even higher 99.5% [1].

As a consequence, hydrocarbon wells producing from carbonate reservoirs are often stimulated with acid. Compared to sandstone acidizing an increase in production is almost guaranteed as the chemical reactions involved are simple and hence predictable. In most of the cases relevant increases in hydrocarbon production are obtained. However, this does not mean that the well was properly stimulated and the ideal producing conditions have been reached [3].

This is even truer in naturally fractured carbonate reservoirs, where stimulation is quite challenging because treatment fluids tend to enter fractures and avoid less permeable regions. In recent years great progress has been achieved as new acid recipes and execution methods have been developed. Those include more effective fluid diversion techniques that ensure that stimulation fluids contact the largest possible reservoir surface area [4]. Further progress has been made in the retardation of acid systems, which relies on delaying chemical reactions so that the penetration distance and number of wormholes is increased. Completely new methods such as acid tunneling also evolved [1].

This thesis consists of following main chapters: It is introduced with the theory of stimulating carbonates followed by presenting on how to characterize naturally fractured reservoirs. Chapter 3 presents several worldwide field cases of stimulating naturally fractured carbonates and their success rates. Chapter 4 focusses on the stimulation of naturally fractured carbonates in the Vienna Basin conducted by OMV and in chapter 5 the findings are presented. Chapter 6 gives a recommendation on how to improve and finally it is concluded with a discussion.

2 Stimulation Theory

2.1 Basics

In general, the purpose of stimulation is the reduction of skin value and pressure drawdown and the maximization of productivity. In the case of carbonates this is achieved by bypassing damage and the creation of new flow paths in the formation [5].

There are three possible treatments which are acid washing, matrix acidizing and acid fracturing [5].

2.1.1 Acid washes

The smallest volumes of fluid are pumped for acid washes, usually through coiled tubing on newly drilled wells. The objective in naturally fractured carbonates is the maximization of the communication between the wellbore and the natural fracture network. The fluid volumes are between 0.3 and 0.8 m³ per meter of perforated interval, usually [3].

2.1.2 Matrix acidizing

Matrix Acidizing acts only in the near wellbore region. The flow capacity is improved by bypassing damage. This is achieved by dissolving rock of the damaged region. Certain acids are used that dissolve calcite or dolomite and so create open and conductive channels. By extending those channels, wormholes develop [5].

To increase the length and numbers of wormholes retarded acid systems can be used. Those include gelled acid, chemically modified acid, surfactant-retarded acid, emulsified acid and foamed acid [5].

This treatment is only effective if some damage exists, which can be bypassed as this technique does not go deeper into the formation. An exception would be naturally fractured carbonates, where the acid can move more easily along the fractures [5] [6].

2.1.3 Acid fracturing

Acid fracturing does not only bypass formation damage, but also stimulates the formation. Conductivity is achieved by creating a fracture and etching it with an acid. Two methods exist, which are viscous fingering and viscous acid fracturing, which are applied in dependence of rock heterogeneity [5].

Viscous fingering works by first creating a fracture by a non-reactive, viscous water pad. In the next step an acid with a low viscosity is pumped. Due to the low mobility of the acid it fingers rapidly and unevenly through the viscous pad and etches the formation. This technique can be applied in all carbonates as the uneven and deep flow paths do not depend on formation heterogeneity [5].

Viscous acid fracturing on the other hand requires heterogeneous carbonates such as dolomites or impure limestones. Only one fluid system is needed to do both, creating the fracture and differentially etching the fracture surface. Gelled, emulsified, foamed or chemically retarded acid are usually used [5].

2.2 Types of acids

Hydrochloric acid (HCl), acetic acid (CH₃COOH) and formic acid (HCOOH) are the most common acids used for carbonate stimulation [5].

The most common acid used is HCl. It is the cheapest one and has the highest strength. It is typically used in concentrations of 15% or 28% [5].

Acetic acid is organic. It is weakly ionized, slowly reacting and of the three acids mentioned the one that can be most easily inhibited against corrosion. Due to this, it can be used as a perforation fluid in carbonate wells. Furthermore, as corrosion rate is higher at increased temperatures, this acid is also better suited for stimulating formations with high temperatures [5].

It naturally sequesters iron and so less inhibition against iron precipitation is needed. Concentrations used are typically 10% [5].

Formic acid is also organic but has a higher strength than acetic acid. Treatments with formic acid are more vulnerable to corrosion. However, the corrosion is in the non-pitting category and so it can also be used at high temperature operations. Concentrations are in the range of 9% and 10% [5].

2.3 Reactions of acid with carbonate rocks

The spending rate of acid with carbonate formations is influenced by following factors [7]:

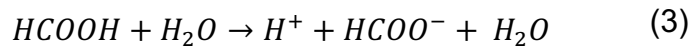
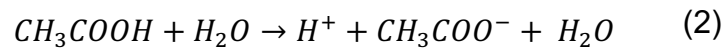
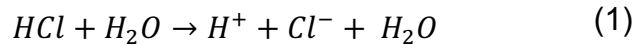
- Pressure
- Temperature
- Acid type, velocity and concentration
- Reaction Products
- Surface area to volume ratio
- Formation composition

Pressure: Up to about 500 psi (34 bar), the higher the pressure the higher the reaction rate, but above it the pressure does not influence the rate anymore [5].

Temperature: The higher the temperature the higher the reaction rate. E.g., at 150°F (66°C) HCl reacts with limestone two times as fast than at 80°F (27 °C). There is also a dependence

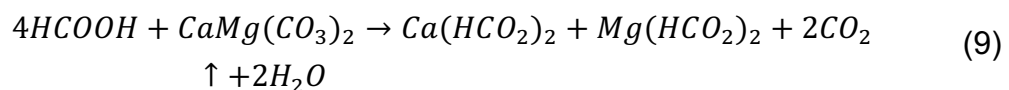
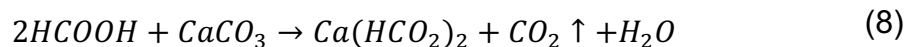
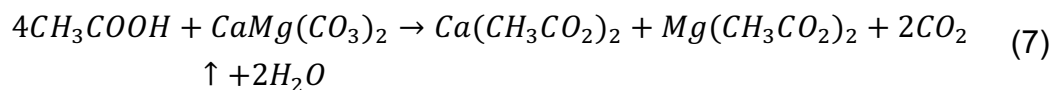
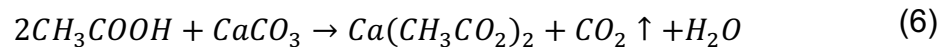
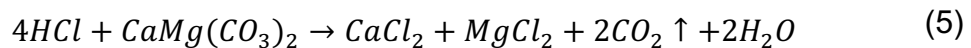
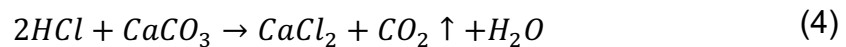
on the kind of rock. Up to 250°F (121°C) the reaction rate of limestone with HCl is higher than with dolomite. Above 250°F their rates are almost equal [5].

Acid type: Acids have the property to dissociate (ionize) in aqueous solutions. The ionic strength measures the amount of ions, which go into solution. In the case of acids, the ionic strength is an indicator to which degree acid ionizes to hydrogen ion. The hydrogen is the reactive species with carbonate minerals and not the acid molecule. For hydrochloric- (1), acetic- (2) and formic-(3) acid the dissociation reactions are following:



As can be seen only hydrochloric acid is completely ionized to the hydrogen ion and its corresponding anion in water. Opposed to that the organic acids ((2) & (3)) are only weakly ionized, as already described. Due to that they have a lower spending rate and additionally, because of higher equivalent weights, organic acids have less dissolving power at equal percentage acid solution [5].

Formation composition: The acid spending rate, with which the acid penetration distance is derived, is highly dependent on the physical and chemical composition of the formation and the type of acid used. The possible reactions of the different kinds of carbonate minerals and the acids are shown below [5]:



As can be seen from stoichiometry, twice many moles are needed for the reactions of acid with dolomite ($\text{CaMg}(\text{CO}_3)_2$) compared to calcite (CaCO_3) (compare equations (4) and (5), e.g.). Therefore, the dissolution power in limestone acidizing is higher than in dolomites.

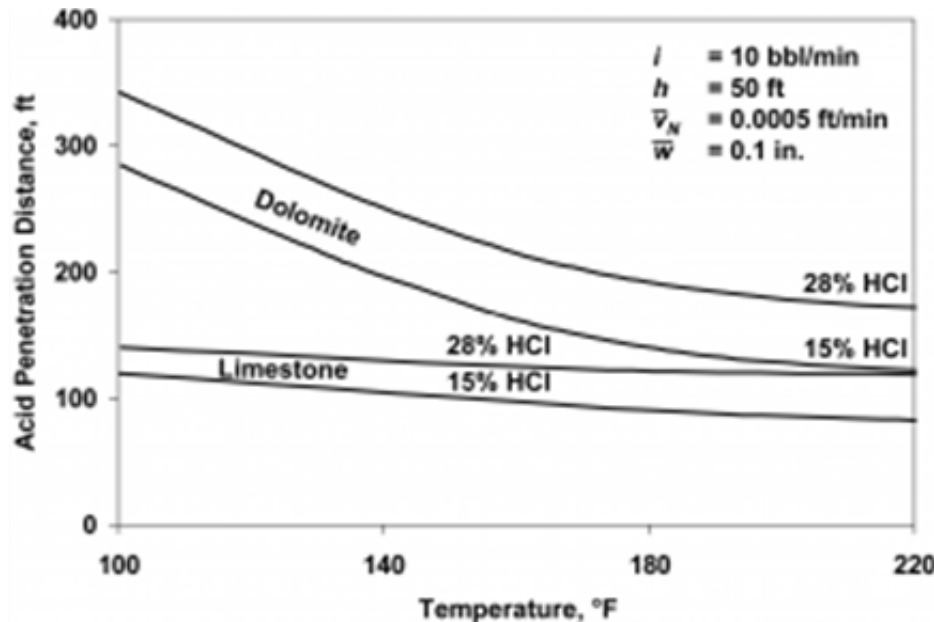


Figure 1: The acid penetration distance in dependence of temperature, kind of rock mineral and acid strength [8].

As described, reaction rate in limestones is twice of that in dolomites at low temperatures. In general, high reaction rates reduce penetration. Consequently the deepest penetration can be achieved at low temperatures in low soluble dolomites (fig.1).

The dissociation of the weaker, organic acids is suppressed by the generated CO_2 , which itself is an acid in solution. In HCl-organic blends the influence of organic acid is very low, especially at high temperatures. Only when the HCl is already spent the organic acid starts to react with the minerals.

Acid concentration: Higher acid concentrations increase the dissolving power and therefore spending. However, acid concentration should not be too high. Beyond a certain concentration, spending decreases again. The reason is that at higher concentrations more and more reaction products in solution are generated which hinders further reaction. According to Kalfayan [5] this optimum, where HCl spending has its maximum is at a concentration of about 20%.

Acid velocity: In fracture acidizing a higher acid velocity gives higher live acid penetration [5].

Surface-area-volume ratio (SVR): The higher the surface area of the rock, with which a certain volume of acid is in contact, the higher the spending rate. A high SVR can be found at matrix acidizing and because of that the penetration is not deep. In order to increase the penetration depth, it is necessary to retard the acid to slow down the rapid spending. In naturally fractured formations the SVR is low and a deep penetration is possible. In acid fracturing the penetration is even deeper. In order to maximize that, reacting and leak-off can be reduced with certain additives [5].

2.4 Physics

In fracture acidizing the success of the job depends on the created fracture length and its conductivity. The fracture length is a function of the penetration distance of the live acid, whereas the conductivity is a function of the etching pattern imparted on the fracture walls and the resulting flow channel stability [5].

The acid penetration distance can be increased by reducing acid reaction rate and fluid loss (leak-off) from fracture to matrix. This works by decreasing mass transfer or by reducing diffusion from the acid to the fracture wall surface, where the reaction takes place.

Parameters influencing fluid loss are [5]:

- permeability
- porosity
- viscosity of the acid
- compressibility of the formation fluids
- differential pressure between matrix and fracture

Fluid loss can effectively be reduced by reducing the number of wormholes or by blocking them. To block the holes gelled pad fluid is used which diverts the acid deeper into the fracture [5].

The etching pattern is controlled by following [5]:

- mass transport from the body of the fracture to its wall
- reaction of the acid on the rock surface
- acid leak-off from fracture to matrix
- heat transfer in the fracture

Increasing the viscosity of the acid improves several parameters [5]:

- the rate of diffusion is decreased → reaction rate is decreased
- less fluid loss
- the width of the fracture is increased

The different systems to increase viscosity are discussed in chapter 2.5.2 “Retardation”:

2.5 Matrix Acidizing

As mentioned, in matrix acidizing it is tried to create wormholes, which go from the wellbore into the formation. Their structures are quite complex, which depend on injection rate and acid reactivity with the rock minerals, itself a function of temperature and the properties of the stimulation fluid. Based on this the target is to find the best suited injection rate of the acid and its reactivity (can be decreased by retardation, e.g.) [5]. Following categories of wormhole structure exist [9]:

- face dissolution
- conical wormholes
- dominant wormholes
- ramified wormholes
- uniform dissolution

Where from top to bottom injection rate increases, reactivity decreases and from no wormholes in face dissolution the amount of branching increases more and more to highly branched dissolution at ramified wormholes and finally in uniform dissolution the wormholes disappear again [5].

Experimental studies [10] [11] [12] showed that the number of pore volumes of acid to breakthrough a core (proportional to the reciprocal of the acid efficiency) reaches a minimum with a certain value of the reciprocal of the nondimensional Damköhler number (proportional to the pump rate per interval height). At this value highly conductive wormholes with narrow and unbranched structures are generated (fig.2) [3].

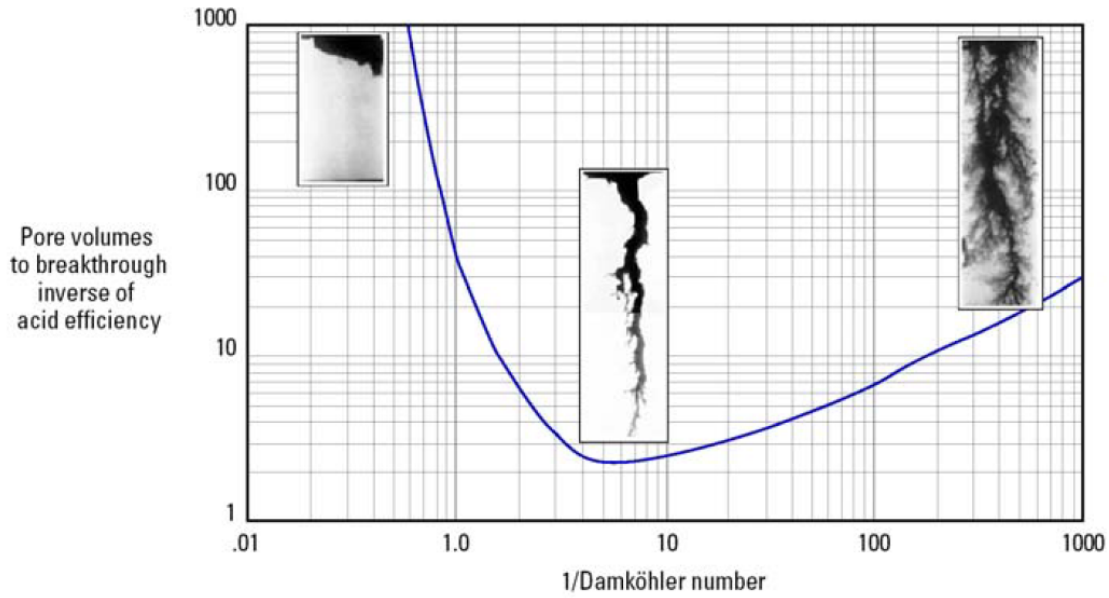


Figure 2: Effect of Damköhler number on stimulation efficiency [3] [12].

2.5.1 Treatment design

The conventional treatment design looks as follows:

- Pickling
- Preflush
- Acid stage
- Overflush

Pickling: The first stage is the pickling stage, where either 5-15% inhibited HCl or other special pickling solutions are used to clean the injection string. A standard is 7.5% HCl acid including an iron control agent and a corrosion inhibitor. If organic deposits or other kinds of debris are in the pipe, typically a dispersion of acid, an aromatic solvent and also a corrosion inhibitor is required [5].

Preflush: It is needed to remove scale from the wellbore tubing before acid injection. Hydrocarbon deposits can be removed by an aromatic solvent, such as xylene. Asphaltene elimination works by the application of a terpene based solvent solution. 5-7.5% HCl acid is used to get rid of rust and inorganic scale. However, at temperatures above 60°C it may be better to use a non-acid solution for cleaning of the rust. In the near wellbore region oil must be displaced as it could form emulsions or sludge. This works by using xylene or water and a surfactant [5].

Acid Stage: This is the main stage of the treatment, which bypasses the damaged regions. Volumes pumped range from 10 to 300gal/ft depending on porosity and depth of damage.

When taking HCl acid normally only concentrations of 15 % are taken, as higher concentrations increase the risk of forming emulsions, sludges or insoluble precipitations. High strength acid with concentrations up to 28% should only be used when absolutely required, which could be in high permeability formations with very deep damage or in acid fracturing. As mentioned the application of organic acids should be preferred at higher temperatures. Mixes of HCl and organic acids may extend live acid reaction as the full dissolution capacity of both types of acids is utilized [5].

Overflush: Finally, an overflush is required to displace the acid to the perforations. In this stage most likely fresh water is used. In oil wells filtered crude oil or diesel can also be pumped but there is a risk of incompatibilities with acid. In gas wells nitrogen gas is effective as overflush fluid [5].

2.5.2 Retardation

Acid retarders are slowing down acid reaction and are reducing acid leak off. Because of that they increase acid penetration depth and extend the flow channels (chapter 2.4). Retarded systems are able to form smaller and more branched wormholes. To some degree this is beneficial as long as the branching is not too extensive, as it would finally result in ramified wormholes or even uniform dissolution, which is not desirable [5], as explained in chapter 2.5.

There are three possible retardation systems: acid retardation by using surfactants, chemical- and physical retardation [5].

Surfactant retarded acid: Oil-wetting surfactants are added to the organic or inorganic acid, which coat the pore surfaces and hinder acid attack. This decreases reaction rate there. These systems can also be applied in wells with high temperatures [5].

Chemical retardation: Acid reaction can be retarded by adding organic acids (react slower than HCl) or reaction products (CaCl_2 , CO_2) of HCl. CaCl_2 is useful in anhydrite (CaSO_4) formations as it decreases anhydrite solubility. Through this, less anhydrite re-precipitates, as acid spends. Further CaCl_2 has the advantage that it can be used as a weighting agent. CO_2 as retarder slows down reaction in two ways, which are due to its cooling effects and it changes reaction equilibrium and kinetics [5].

Physical retardation: The principle of physical retarding systems lies in increasing acid viscosity. The target is to reduce the rate of acid diffusion to the rock surface and to reduce leak-off of the acid from the wormhole to the unreacted matrix that in turn ensures a large penetration distance [13].

- Emulsified acid achieves deepest possible penetration. Those are either oil-external or acid-external. As oil-external emulsions have a higher dissolving capacity they

are more effective. However, emulsified acids exert high friction during pumping, which leads to high pressure losses. This may impart a problem in very deep wells. Their application in matrix acidizing is not ideal.

- Polymer-gelled acids may be a better solution due to lower friction, but their ability for retardation is rather low.
- Foamed acid helps in increasing fracture length and improves contact in long treatment intervals, but per volume of fluid it can only take a rather low amount of acid. They are well suited for damaged gas wells.
- Surfactant-gelled acids (viscoelastic acid systems “VES”) provide viscosity in dependence of the pH-value, which itself is governed by acid concentration. As the acid spends, acid concentration declines (the pH increases) and subsequently the surfactant generates viscosity, leading to a retardation of the reaction. When concentration declines below a certain value the surfactant starts to reduce viscosity again [14]. This is shown in figure 3. This technique has several advantages: it serves as in-situ diversion, penetration distance is increased and cleaning-up is improved. The drawback associated with shear thinning is that through this, leak-off is increased and this again could decrease acidized fracture length. Surfactant-gelled acids are often used in matrix acidizing or are applied in diverters for acid fracturing [5].

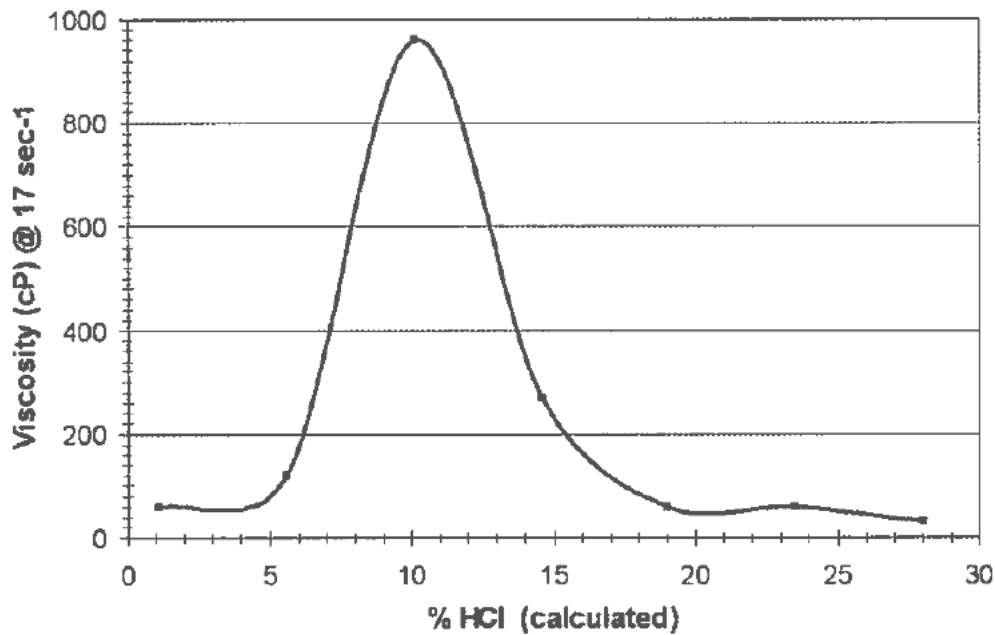


Figure 3: Viscosity profile of 28% HCl containing a viscoelastic surfactant gelling agent [3].

2.5.3 Treatment placement

The placement or diversion of acid is more complicated in carbonate matrix acidizing than in sandstone acidizing due to the high reactivity of acid with carbonate minerals [5].

When it is intended to stimulate large sections with high permeability contrasts and natural fractures the diverting agent is a critical component of the acid system [3].

Diversion is important to treat the entire interval as uniformly as possible to ensure that the lowest possible skin is achieved. Perforated intervals exceeding 6 meters generally benefit from diversion. This ensures uniform acid coverage across the interval [3].

There are chemical and mechanical methods for diversion. Mechanical methods include packers and balls sealers, chemical ones use gelled- or/and foamed acid [5].

Types of packers used are retrievable treating packers and retrievable bridge plugs or multi-settable straddle packers. They are run on tubing and several sets of perforations are treated selectively [5].

Packers are very efficient in diversion but have several drawbacks [5]:

- more time is needed (several days)
- stimulation fluids may not reach the target interval if the cement bond quality is of low quality
- the formation could be damaged because the well must be killed after each interval is treated; due to this, new treated perforations are exposed to foreign fluids for a long time and when in contact with formation crude and spent acid, emulsions or sludges might be generated

Ball sealers have shown to be reliable for diversion. They are injected at high rates through tubing [5].

They are small spheres that are pumped at the surface with the stimulation fluids in order to seal the perforations. Non-buoyant (drop into the rathole as soon as injection halts) and buoyant types (are caught in ball catchers at the source as soon as injection halts) exist, whereby the buoyant type has shown to be more efficient. To be efficient a sufficient pump rate has to be maintained during the treatment to ensure a consistent pressure differential across the perforation to keep the sphere in place. The conditions of the perforation holes, such as smoothness and shape, also influence the efficiency of the ball sealers [3].

Foamed acid is a non-damaging method in zones with high permeabilities (does not penetrate as deep due to a high viscosity and a low density) or low pressures. For weighting the acid to get it into a high-pressure zone, dissolved salts, such as CaCl_2 can be used, but care must be taken that the total dissolved solids remain below saturation. Diversion

efficiency can be increased by pumping a surfactant slug ahead of the foam stage [15] [16]. Cleanup of spent acid is also much easier when using foams [3].

Brines with viscoelastic surfactants are generated by adding viscoelastic surfactants to ammonium chloride brines. They contain no solids and polymers [17], making them non-damaging. They can be easily broken by adding a mutual solvent to the overflush or when they are contacted by hydrocarbons during the flowback process. Additionally, they can be used in high water cut wells. There they divert the acid from the water zone to the hydrocarbon-bearing zone, thus preventing stimulation of the water zone [18] [3].

Viscoelastic acid: Viscoelastic surfactants are added to hydrocarbon-acid-based systems. When acid is spending, fluid viscosity increases significantly, achieving diversion from high to low permeability sections. They also do not contain solids or polymers and thus are non-damaging to formation. The breaking works in the same way as for systems described above [19] [3].

Enhanced HCl acid systems are equal to the systems described above, but additionally degradable fibers are added. It combines chemical diversion (viscoelastic acid) with a bridging agent (fibers). This system has an extraordinary ability in diverting the acid from natural fracture dominated section sections without natural fractures. This achieves uniform coverage. The fibers degrade as a function of temperature with time. The requirement for their degradation and hydrolysis is the presence of water [3].

Another method is the pumping of alternating stages of gelled (viscous) acid and regular (non-viscous) acid through coiled tubing. The injection rates are lower than at the other methods. The gelled stages achieve lower reaction rates and due to their high viscosity, fluid injectivity and fluid loss are decreased in the treated interval [20]. Because of this the following acid stage is diverted to another zone. This succession can be continued until the complete interval of interest is treated.

The **gelled acid** can be:

- polymer-gelled
- surfactant-gelled
- crosslinked polymer-gelled

Polymer-gelled acid breaks at high temperatures, and it is possible that a residue remains behind damaging formation. Surfactant-gelled acid breaks more cleanly in oil. In gas wells an additional breaker is necessary [5].

2.6 Acid Fracturing

2.6.1 Viscous fingering

As explained, in viscous fingering a nonreactive, high viscosity gel, e.g. cross-linked gelled water (contains 20-40 pounds per thousand gallons of guar or modified-guar polymer) is pumped with a pressure high enough to create a fracture by overcoming compressive stress of the earth and tensile strength of the rock. A fluid loss additive increases efficiency, such as 100 or 200 mesh sand. With this pad the desired geometry, including length, height, width and direction of the fracture is created and the formation is cooled to slow down reaction for the acid following in the next stage.

The pumped acid has a much lower viscosity and due to the high viscosity difference between the two stages, a mobility contrast results. Due to this, the acid fingers through the created fracture subsequently. As a rule of thumb the viscosity difference between the two fluids should at least be 50 cP [21].

As opposed to matrix acidizing the application of high strength acid up to 28% HCl is much more common here. However, 15% HCl is most often used. High strength HCl has the advantage that it is more viscous than the low strength variant and so leak-off of acid is decreased. In general, it is recommended to viscosify acid for fluid-loss control, especially HCl. Care must be taken that a high enough viscosity contrast between pad fluid and acid is maintained. At higher temperatures, again, organic acids or organic-HCl mixtures may be preferred. In acid fracturing the only reliable diversion technique is the pumping of ball sealers. An alternative would be natural diversion by pumping alternating stages of viscous pad and non-viscous acid [22] [5].

2.6.2 Viscous acid fracturing

Viscosified acids are used, which do both creating the fracture and differentially etch it. This technique is only reliable in impure formations. Today it is the most likely applied acid fracturing method [5].

Three stages are used [5]:

- preflush,
- viscous acid stage
- overflush

In the **preflush** the fracture is initiated with slightly gelled water, which serves also for cooling [5].

The **viscous acid stage** is the main part of the treatment. The fracture is propagated and its walls differentially etched. Most treatments are carried out with gelled acids. A possibility

would be Xanthan as a gelling agent but unfortunately can only be used for HCl concentrations up to 15%. Above it, Xanthan would be degraded too fast. On the other hand below 200°F (27°C) it does not degrade entirely. The most common gelling agent is Polyacrylamide that has several advantages. It is efficient in a high temperature range and crosslinking is possible, which increases viscosity and system stability. Further, also generation or in-situ destruction of viscosity is feasible. Crosslink between the polymers can be created in the beginning of the pumping to achieve high acid injection viscosity or also delayed crosslinking. In delayed crosslinking the injection rate is high in the beginning as acid viscosity is low. The viscosity increases as the acid starts to react with the formation face. Similar to VES, viscosity is provided in dependence of pH of the fluid (viscosity is generated in the range of pH 2-4.5). At a certain high pH the gel starts to break again. Through the thinning and regeneration of low viscosity, flowback in the subsequent stage is improved. A problem with this technique is that there may remain a potential damage to the formation [5].

The **overflush** is used to remove acid from the wellbore and pushing it forward into formation, through which penetration distance is further increased. The combination of viscous acid and a large overflush volume efficiently increases etched fracture length. In general a high rate is desirable. The overflush is a crucial step in viscous acid fracturing. Plain acid should only be used when the bypassed formation damage is very shallow. The reason is that plain acid reacts rapidly, through which large volumes of rock near the wellbore are dissolved. This leads to a very low penetration distance. Plain acid makes high overflush volumes necessary. Formation stimulation requires viscous acid, which increases etched fracture length also [5].

More sophisticated methods of viscous acid fracturing are alternating stage- and alternating acid methods. They should only be used in already known fields, as those methods are more complicated to design and the prediction of the result is harder [5].

In the alternating stage method alternatively acid and gelled water are pumped. This has following functions [22]:

The gelled-water stages have a high viscosity and so wider fractures are formed. Further these stages are cooling the formation, which was heated during previous acid reactions (exothermic; heat generation). Due to the lower temperatures the subsequent reactions are slower and so penetration distance is increased (fig. 1). Penetration distance is even more extended due to the alternating pumping stages with a retarded acid and the gelled water that decreases fluid loss of acid from the fracture to the matrix [5].

In the alternating acid method two acids with opposite characteristics are pumped alternately. One acid system is reaction-retarded, the other one is non-retarded and reacts

very rapidly, mainly in the near wellbore region. Through this differential etching is improved and the dissolution of formation near the wellbore is also higher [5].

2.7 Factors influencing fracturing

Near wellbore tortuosity can be caused by the creation of T-shaped fractures, reoriented fractures and multiple fractures. These conditions can cause additional friction pressure loss during the injection or production phase of a well. However with powerful, deep penetration charges, the near wellbore tortuosity and pressure losses due to inefficient perforations are minimized [23].

Excellent drilling and perforation techniques are essential to minimize such pressure loss and create a good communication between the well and the virgin reservoir to ensure full well potential. These can be achieved by the proper choice and placement of perforations or advanced multistage fracturing in horizontal wells. Horizontal wells with advanced multistage fracturing have proven to be very productive. Depending on the well trajectory and azimuth, several fractures can be induced in sequence in selected intervals to augment the flow path between the reservoir and the wellbore. The number of stages in the advanced multistage fracturing completion depends on reservoir development, stress profile and wellbore trajectory [23].

For example, from fig.4 it is clearly seen in an analytical solution of the productivity index that increasing the number of hydraulically created fractures from 5 to 7 in a horizontal well with a net pay thickness of 200 ft, can approximately double its productivity index. Hence the productivity ratio increases as a function of the number of fractures and depends on the net pay thickness of the treated interval (H_{NET}) and the vertical to horizontal permeability ratio (k_v/k_h) [23].

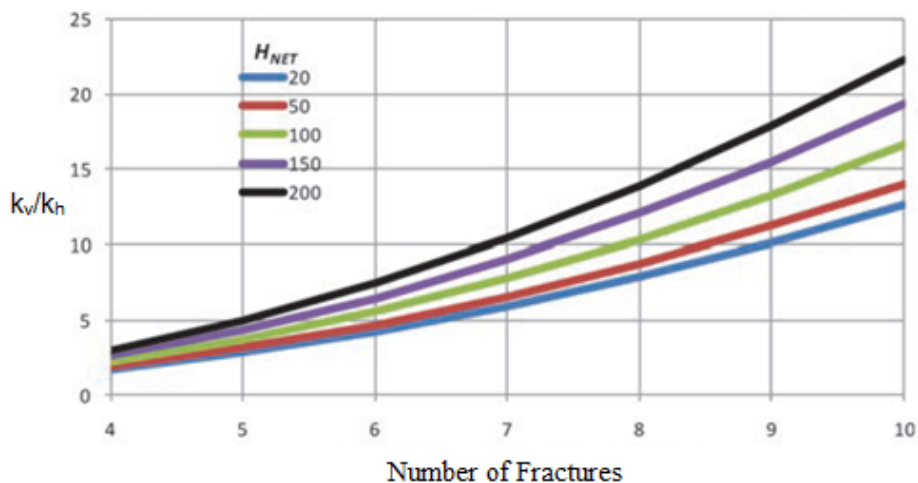


Figure 4: Productivity increase ratio as a function of the number of fractures [23].

Improper placement of perforations can cause the fracture to grow outside the reservoir interval. To avoid sanding using the indirect fracture, placing perforations below the zone of interest is usually a better option [23].

2.7.1 Wellbore placement and lateral length

Wellbore placement is another factor that can have a major impact of the performance of the hydraulic fracture treatment. Placing a wellbore along the direction of minimum in-situ stress (σ_{\min}), there will always be a possibility that the induced fractures will overlap each other because the fracture plane goes in the direction of the maximum horizontal in-situ stress (σ_{\max}) which is perpendicular to σ_{\min} and meaning that multiple, independent fractures can be placed along the wellbore [23].

On the other hand, when the well trajectory is in the σ_{\max} direction, the induced fractures will be longitudinal along the wellbore plane, thereby significantly reducing the number of hydraulic fractures that can effectively be created and hence this will not favor the induction of fractures. It is therefore conceivable that only between two and four fractures can be placed longitudinally in a wellbore that is more than 1,000 ft long. There is practically no limitation on the number of orthogonal fractures created in wellbores perpendicular to σ_{\max} . As a result the maximum number of fractures is dictated by the reservoir flow capacity, wellbore trajectory, reservoir contact, and completion limitation [23].

The well inclination and azimuth can have an effect on the fracture initiation pressure. Drilling the wellbore in the direction of the least horizontal stress, T-shaped fractures are likely to occur because the tensile zone created around the wellbore in the direction of σ_{\max} causes the fracture to initiate in σ_{\min} direction, but as soon the fracture turns, the propagating axis changes, and the fracture develops toward the σ_{\max} direction [23].

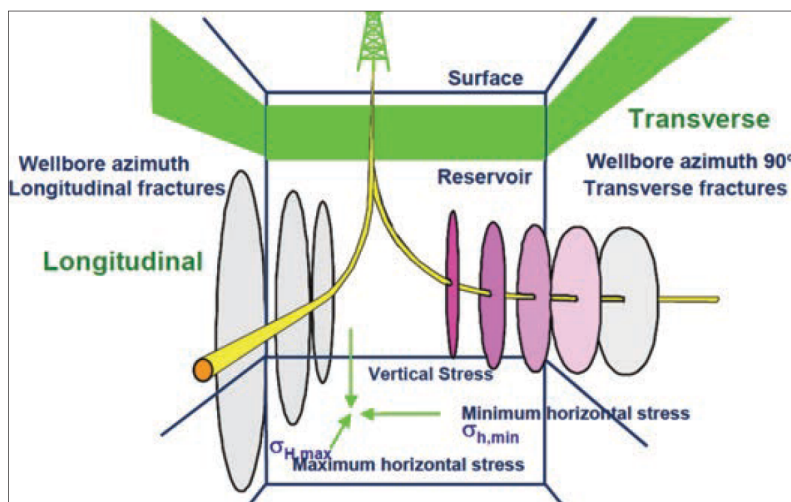


Figure 5: Fracture development as a function of wellbore orientation [23].

3 Naturally fractured reservoirs

3.1 Basics

“A natural fractured reservoir (NFR) is a reservoir in which fractures enhance the permeability field, thereby significantly affecting well productivity and recovery efficiency.” Almost all reservoirs contain fractures. What differs is the degree to which fractures influence fluid flow through the reservoir [24]. A fracture is a mechanical discontinuity or parting that is caused by brittle failure. The scale of their occurrences is in a far-reaching range, from microcracks to features having a length of several kilometers. They can do both, act as super-highways to fluid flow, if they are open and permeable, or act as flow barriers, if their openings have been secondary mineralized or filled with other fine-grained material. As a consequence, they can dramatically improve hydrocarbon production or prevent its economical recovery. Because of that the influence of fractures must be investigated in an as early as possible stage. Fractures affect processes such as drilling, well completion, data collection, stimulation, well placement and enhanced-recovery methods. Not characterizing natural fractures early can lead to heavy losses in field-development options in the future. Evaluating the natural fracture in an early development stage could not only increase overall recovery, but could also prevent wasting resources on unnecessary infill drilling in the future [24] [25].

In 2001, Nelson [26] published a classification scheme of naturally fractured reservoirs, which is based on the relative contribution of matrix and fractures to the total fluid production. Following, only fractures enhancing permeability are considered.

3.1.1 Productivity heterogeneity

To classify a reservoir as naturally fractured, it is necessary that a majority of wells have fracture-enhanced production. It is up to the experts whether the number of wells with fracture-enhanced effects is sufficient to classify the reservoir as an NFR. In general, there is a wide scope of discretion and is case dependent. It is common in NFRs that there is significant heterogeneity. As the transition between conventional reservoirs and NFRs is continuous judgment is hard [25].

Field heterogeneity can have several causes, such as thin, continuous, high permeability strata or vugs that are connected in various ways. It is also a main characteristic of NFRs and, when occurring, is seen as an evidence of a possible fracture involvement. [25]

Following fieldwide, well-specific productivity parameters can be analyzed to retrieve heterogeneity: productivity index (PI), cumulative production (Q), permeability thickness (kh), flow capacity index (FCI), absolute open flow [26].

The statistical evaluation of those parameters in a NFR differentiates significantly to a conventional one, as its variability between the wells is much larger. Concerning this, the 80/20 rule of thumb exists, which states that 80% of the field production is from 20% of the wells. It has already been proven to be a good reference point [25].

Also when looking on the spatial distribution of the well productivity a variable mix can be observed. E.g. one well which intersects a fracture is very productive, whereas a well not far away has very low production due to not intersecting any fractures. Compared to that a field without any fractures has uniform production and only gradual changes in productivity occur [25].

The **FCI** parameter is an important tool in recognizing and quantifying the flow enhancement caused by natural fractures. It relates observed well performance with the predicted one. Following equation by Reiss is used [27]:

$$FCI = \frac{kh_{well}}{kh_{matrix}} \quad (10)$$

Where

- h_{well} is the productive height of the well
- h_{matrix} is the productive height of the matrix

kh_{well} is measured from a well test, whereas kh_{matrix} is computed based on matrix permeabilities determined for the rocks from the well completion zone. A ratio significantly greater than unity indicates fractures, but could, as already mentioned, be a consequence of thin permeability beds or connected vug networks. When plotting the FCIs of several wells in a histogram it becomes obvious that the FCIs of NFRs are wider distributed than those of conventional reservoirs (fig.6). The spread is hereby the widest in horizontal wells, as they intersect with more fractures, which are usually vertical [25].

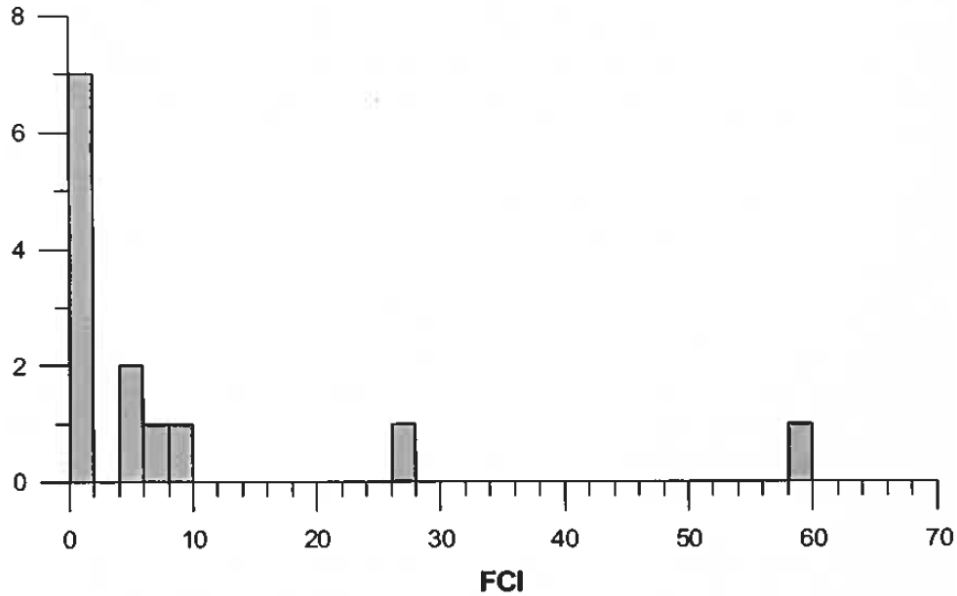


Figure 6: FCI distribution in a naturally fractured reservoir [25].

In NFRs the determination of the productive height (h) might be quite challenging as production is usually not from the entire open interval. In low-matrix-permeability NFRs this effect is even more significant. The production might be almost only from the fractures, occurring only in a small part of the total height of the total open interval. A possibility to determine producing height is by a PLT tool (see chapter 3.4.3). After adjusting h , the FCI value becomes even larger [25].

3.2 Characteristics

When starting production from an NFR with low matrix permeability, initial productivity (IP) is very high, as production comes from those highly permeable fractures. Fracture porosity is very low and so only little amounts of hydrocarbons can be stored there. Additionally, as the rock matrix is not able to respond fast enough to support the high production rate of the fractures, the production rate declines rapidly. Eventually the main part of production originates from the matrix and stabilizes at a low and steady rate [25].

It is common that fractures occur in extensive, consistent and parallel sets oriented in a certain direction in dependence on the stresses occurring in the subsurface. This is confirmed when drilling several wells in that field and flow anisotropy can be observed in the direction of the stresses. After depletion of the fractures and hydrocarbons were produced from the hydrocarbons stored in the matrix, Elkins [28] observed that pressure declination occurred not only in flowing wells but also in already shut-in wells. Additionally, pressure measurements of newly drilled wells in the vicinity of producing wells had the same pressure. This indicates that a well-connected fracture network exists, which improves communication within the field [25].

Another characteristic of NFRs is that due to rapid pressure drawdown, the GOR rises already in the beginning very fast, which is highest near the fracture face [25].

3.3 Fracture classification

To successfully develop and model an NFR it is of importance to fully understand the characteristics of its fractures and fault systems [29]. The classification of the natural fractures is achieved with descriptive, genetic and geometric methods. By gaining knowledge about the existing fracture types in the field, fluid flow simulation models are improved, as the conduction of fluids is dependent on the type of fracture [24].

It is critical to link gathered data from field observations with data from controlled laboratory measurements to get the best possible understanding of the fracture system [30]. In the laboratory the fracture types are divided roughly into two principal types, according to their mode of generation [24]:

- shear fractures: form with shearing parallel to the created fracture
- tension fractures: form with shearing perpendicular to the created fracture

These fractures form in dependence of the direction of the three principal stresses, with σ_1 being the maximum compressive stress, σ_2 the intermediate stress and σ_3 the minimum compressive stress [31].

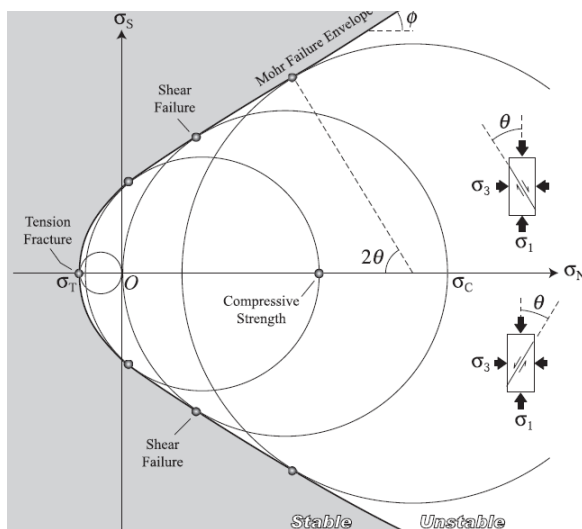


Figure 7: Schematic diagram showing the normal and shear stresses at which the cylindrical specimens of the same rock are fractured by axial stresses ($\sigma_3=\sigma_2<\sigma_1$) [31].

Shear fractures are formed under high differential stresses ($\sigma_1-\sigma_3$), whereas tension fractures are created at low differential stresses, as can be seen from the Mohr circle (fig.7). Shear fractures occur in conjugate pairs (fig. 8 & 9), forming an acute angle (2θ) with σ_1 . The tension fracture is oriented perpendicular to σ_3 [31].

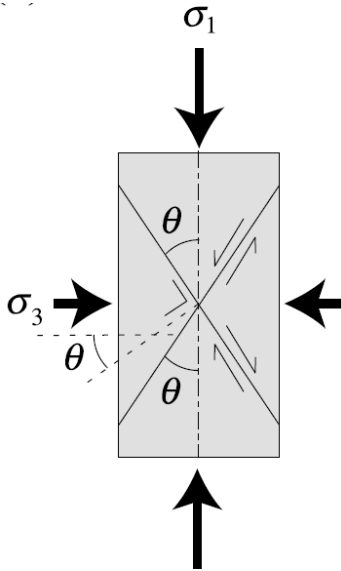


Figure 8: The shear fracture with the acute angle (θ) in dependence of σ_1 and σ_3 [31].

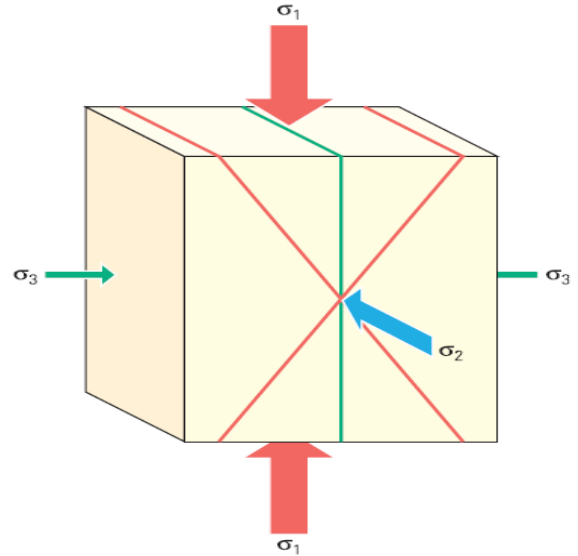


Figure 9: Principal stresses and the direction of the stresses. The diagram shows the direction of the 3 principal stresses and the resulting fracturing. The tensile fractures (green) form parallel to σ_1 and σ_2 . The shear fractures (red) are parallel to σ_2 [24].

The laboratory tests to obtain a Mohr circle are conducted by applying axial load (σ_1) and confining pressure ($\sigma_2 = \sigma_3$) by a triaxial testing apparatus on the test sample. Normal and shear stresses exerted on the plane just before fracturing can be calculated by measuring the fracture plane angle θ [31].

This angle is equal to the orientation perpendicular to the fracture plane from the σ_3 axis, so that the normal and shear stresses are indicated by the point that makes an angle of 2θ from $(\sigma_2, 0)$ along the Mohr circle (fig. 7). The point represents the critical condition for shear fracturing. A series of experiments conducted for a specific type of rock with various confining pressures provide a series of such critical points in the Mohr diagram. By connecting those points, the failure envelope for the sample material is obtained. The envelope is symmetric with respect to the horizontal axis of the Mohr diagram, because the specimens and the applied stress have axial symmetry. Accordingly, the envelope is expressed by a one-valued function $\sigma_s = f(\sigma_N)$. Failure takes place when the Mohr circle expands with increasing differential stress so that it is just tangent to the envelope. According to experiments on rock failure, the shear stress needed to produce failure increases as the confining pressure increases [31].

Figure 10 shows the compressive and brittle strength of the various types of rocks. Carbonate rocks and halite have lower yield strength than plutonic rocks.

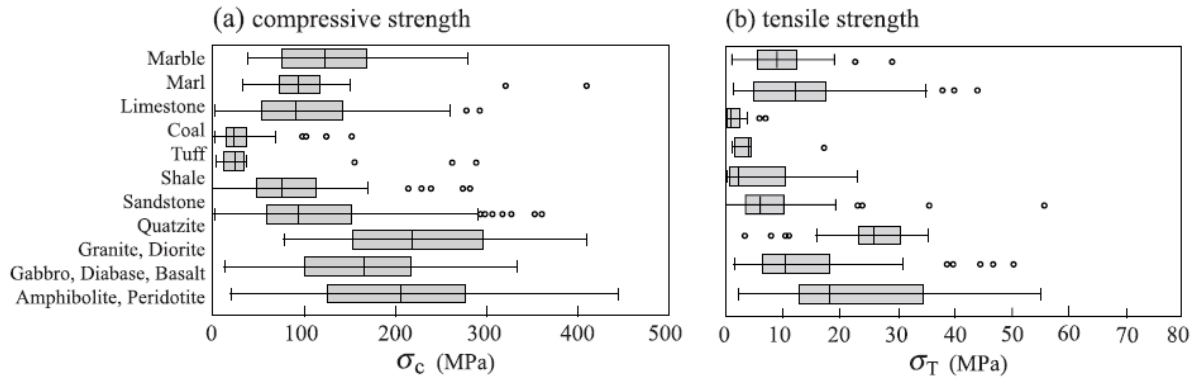


Figure 10: The compressive- and tensile strengths of the various kinds of rocks.

The normal stress designated by the intercept is called tensile strength σ_T . When the uniaxial stress with $\sigma_N < \sigma_T$, tension fracturing occurs, which could also occur when compressional load and low confining stresses are applied [32].

Figure 11 shows the type of failure in dependence of depth in carbonates.

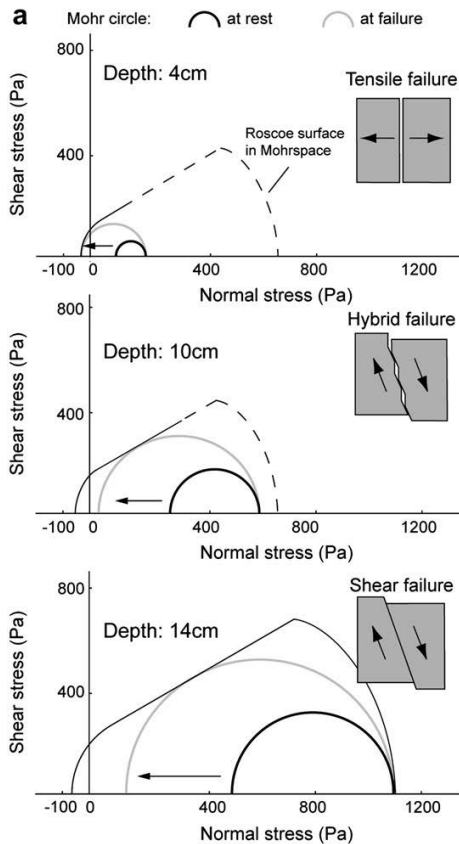


Figure 11: Mohr's circle in dependence of depth and confining stresses [31].

Comparing laboratory experiments with reality shear and tension fractures have natural occurring counterparts. Shear fractures correspond to faults, tension fractures to joints [33]. Faulting in nature requires high differential stresses that commonly occur during significant tectonic events. The range of scales of tectonic faults is wide, having displacements from millimeters to kilometers. The large ones can be detected by seismics, the smaller ones can be observed by analyzing borehole data. This will be discussed in more detail in chapter 3.4.

Faults are non-stratabound, which means that they cut without problems through stratigraphy [24] [25]. Opposed to that, joints are usually stratabound and so their propagation is stopped at bedding surfaces. They are at a high angle to layering, often perpendicular to bedding. They often form a so-called “joint set”, which is a group of parallel, spaced joints [24]. Commonly there are long and continuous sets of joints, termed “systematic joints”. They are joined by a perpendicular array of cross joints, which connect the systematic joints [34]. Through that an interconnected network is created. Joints enhance fluid transport in most NFRs reservoir wide. Their orientation is usually consistent over large areas, but local variations are possible across distances in the order of 100 meters [25].

Non-stratabound joints also exist. They occur in a wide range of scales and are spatially clustered [35]. Consistency in orientation is not dependent when crossing different rocks.

Determination of joint origination is often hard to obtain. But, as explained, must have originated due to a low effective σ_3 . This could either be at shallow depth, where tensile stress possibly occurs or if generated at higher reservoir depths, the existence of high pore pressures is a prerequisite due to the fact that only compressional stresses are present there [24].

The detection of joints is only possible with data from the wellbore, as detection by seismics requires displacement that offsets bedding.

Differentiation between joint and faults is hard to obtain in some cases [24].

Fractures are not only created by external forces but also by volume-reduction of rock. Of highest importance in oil and gas production are syneresis fractures and mineral-change fractures. Syneresis is a chemical process causing dewatering of rock that leads to a reduction of volume [24].

As already described in chapter 2.3 carbonate minerals are very easily dissolved in acids [36]. The corrosion of the rock might already start shortly after deposition by near-surface acidic water [37] but also by sulfide-rich fluids that are associated with hydrocarbon migration leading to enlarged fractures [38]. Often the dissolution is concentrated to form caves or vugs, which results in increased porosity. This is termed karst and is of special importance in fractured carbonates as porosity is especially enhanced along the fractures

[24]. However, the high fracture conductivity can be destroyed too. This occurs, if the open fractures are secondarily mineralized, which means that they are completely filled with minerals, such as calcite, dolomite or quartz [24]. Carbonates have also the characteristic to dissolve at high pressures through which subsequently stylolithes are created. Those are uneven surfaces of the insoluble residue. They are oriented normal to σ_1 . Stylolithes reduce permeability and act as flow barriers [24]. Stylolithes and thin shaly intervals as little as one foot thick can stop most of the propagating fractures [39].

3.4 NFR characterization

Core-fracture identification

With a core the most direct description of geological details is possible. It shows unmistakably the relationship between the rock properties and the specific fractures. Subsequently origin, geometry and occurrence of fractures can be determined that can be used for routine and advanced engineering analysis. The core is also the solely source of information about geochemical modification of the fracture that happened after it was generated. This data is absolutely crucial for obtaining the time when the fracture was created, the probability to find them at certain localizations, their degree of sealing due to secondary sealing or enhancement by the movement and reaction with corrosive fluids [25].

By knowing the orientation of the fractures the fracture induced flow anisotropy can be acquired. When the core is taken the dip of the fracture relative to the core axes and to bedding and the relative orientation of the fractures can be measured. With the following four techniques the core can be oriented:

- To get the orientation of the core with respect to azimuth a downhole camera compass is used during coring [40].
- If borehole and bed orientation are known (from a dipmeter log or a structure contour map) standard structural geological tools can be used [41] to get orientation of the core.
- Specialized laboratories measure the paleomagnetic field of the core from which geographic orientation is determined [42] [43].
- The core and corresponding features on an image log that records accurate orientation information, are directly compared [25].

In order to get fracture density, fracture porosity and further fracture characteristics it is vital to measure fracture height and aperture from the core. However, as aperture is usually variable a value is hard to obtain [25].

3.4.1 Distinguish open/kinematic aperture

Routine core analysis includes the cutting of the whole core into several slices (plugs) to get a clean and flat surface. It is important to do the fracture description from the whole core. Problems associated with core drilling are that in most cases they are taken from vertical wells. As most fractures are also orientated vertically, the probability to intersect fractures is at its lowest. As a consequence, cores should preferentially not be taken from vertical wells. A drawback of core analysis is that in high fractured zones core recovery losses might occur [25].

Fractures in cores can have two origins, which are the natural fractures that have already existed in the reservoir before drilling the well and those which were induced during drilling or when taking the core. According to Kulander [44] the distinguishing between those types is not challenging anymore. Natural fractures can be mineralized, weathered or have symptomatic surface markings, which have a point of origin beyond the well region. Induced fractures occur geometrically, symmetric around the core, in a curved shape and the surface markings indicate a point of origin at the edge of the core, or a propagation along the core axes [25].

3.4.2 Imaging logs

Imaging logs are a further direct source of information about subsurface fractures which is even more commonly applied. Lots of information obtained from image logs overlap with information from cores, however they are not regarded as a replacement of cores as both supply unique data. Following image logs exist: resistivity- and acoustic image logs. Whereas the resistivity image log measures small variance in resistivity to generate the borehole wall image, the acoustic image log utilizes a transducer that emits and collects reflections from the borehole wall. The resistivity log is more accurate in low resistant mud, e.g. WBM, the acoustic log works better in high resistant mud, e.g. OBM. For best results they should be used in combination, to deploy the advantages of both tools. Finally, the image logs give a flat representation of the wellbore. If a fracture intersects the circular cylinder of the wellbore an ellipse is formed. When unwrapped and flattened the shape is transferred into a sinusoid shape. With a standard interpretation software a sine curve is fitted. With the additional data from the wellbore survey and the tool orientation the orientation of the interpretation planes is derived [25].

Drawbacks of image tools are that they may fail to notice very narrow fractures. Highly fractured zones are opposed to cores no problem [25] [45].

If water based mud had been used resistivity image logs are the best option in order to distinguish between open and closed fractures. Conductive mud filtrate enters void space and so the open fractures have very low resistivity compared to closed ones, which are

mineralized (most minerals are non-conductive). If oil based mud is used the distinguishing is more challenging [25].

As the resolution of the resistivity image log is very high, also fracture aperture can be computed [46]. The absolute value has been disputed but they provide a fairly consistent relative ranking of aperture sizes within a certain well. However, well-to-well correlations remain uncertain. In order to compute fracture porosity, it is necessary to have values for aperture and fracture spacing. Cores are a good check if the values derived from the image logs are consistent [25].

Imaging logs can be used to measure fracture height. Generally, the height of tall fractures is underestimated. With the fracture height, the fracture porosity and -density is computed. Intersected fracture length can be measured in highly deviated wells, if its trajectory is parallel to the fracture. At large fractures the determination of the true height or length of the fractures is not possible, instead it must be estimated from observations of the fracture character in outcrop analogs [25].

Imaging tools give also information of in-situ stress orientation in the present day reservoir. This can be obtained from drilling induced fractures or borehole breakouts [25].

In a vertically drilled well the plane of the minimum stress is mostly parallel. Consequently the induced tensile fractures strike parallel to the maximum stress direction [25].

On the other hand, breakouts, which are compressive-stress-induced failures, strike perpendicular to the maximum stress direction [25].

3.4.3 Indirect measurements

The analysis of cores and image logs provides a significant collection of fracture statics, but this often does not aid in the understanding of the dynamic flow behavior of the reservoir. To get a wider knowledge of the dynamically coupled systems the observed fracture information is combined with dynamic data from other sources, which are discussed in the following subchapters [25].

The basic questions, which have to be answered, are whether the individual fractures are open or closed and, more importantly, whether they are connected to an extensive, hydraulically conductive network [47]. The latter one is required to know, if the fractures are effective, meaning, to be able to transport fluid in sufficient quantity to alter the flow within the reservoir and to the well, finally.

Stoneley Wave log: By processing full-wave sonic data the reflected Stoneley wave can be derived. The amplitude is attenuated in open fractures in dependence of the aperture [46]

[48]. However, they should be run in combination with an image log (or cores) to confirm open fractures, as they could give false positive reading from vugs and washouts [25].

PEF log: The PEF log peaks near zones with open fractures. False, positive readings could be due to vugs or borehole rugosity and so it should be used only in conjunction with other open fracture identifying tools. An example would be the application in oil based mud, as resistivity image logs are not able to identify open fractures [25].

Porosity logs: Fracture porosity is usually very low in reservoirs (<0.1%) but could have a maximum at borehole walls, which is especially true for fractures with big apertures. They should also be used in addition to other tools [25].

PLT: The production logging tool measures flow and temperature within the borehole. It is the best solution, in order to identify, whether the fractures have the capacity to transport significant amounts of fluid into the wellbore and by interference, which distance they extend into the reservoir. When the tool passes a flowing fracture during pulling upward, the flowmeter will record an increase in flowrate and a change in temperature. E.g., as gas is entering the wellbore, there will be a cooling effect, which is due to the rapid pressure drop from rock to reservoir that results in an expanding gas [25].

Lost Circulation: The data recorded on lost circulation, including the rates of fluid loss, recorded in the driller`s report aids in the recognition of effective fractures. As fluid loss into open fractures is abruptly, as compared to linear fluid drainage to rock matrix, the report gives a good indication. Challenges in analyzing the recordings of the drillers are, that they are often not precise, but still, by comparison with other sources identifying fractures can be a confirmation. However, as monitoring is more and more automatized and hence, accuracy improved, it is possible to determine fracture size and effective aperture, based on recorded fluid loss rate [49] [50]. In this process several points have to be considered: As mud properties change during drilling the wellbore, fluid loss is altered, which has to be recognized, when building the fracture model. This is especially relevant, when lost circulation material is added to the mud system. Due to this, newly encountered effective fractures may clog fast, and so will not be recognized, as no fluid loss occurs. When dynamic hydraulic properties change a misinterpretation of fracture location could happen. A previously clogged fracture from a level above the bit might be opened, leading to lost circulation. As a consequence, it is falsely expected to have the fracture at bit depth. A gas kick, which decreases mud level abruptly, also leads to misinterpretations. To counteract this, lost circulation data should be used in combination with core or image log data [25].

Mechanical indications: Open fractures can be indicated by mechanical effects, but only their presence and not very reliably. When the drill bit enters areas with natural fractures, borehole wall can break off [51]. This can be recorded by a caliper log, where data will spike.

However, orientation of the tool is not equal to the orientation of the fractures, as the borehole wall fails in dependence to fracture-borehole geometry [25].

Further mechanical effects appear during drilling. When open fractures are encountered, rate of penetration increases, whereas torque decreases. Narr, Schechter and Thompson speculate that this is due to the bit dropping into a cavity of rock. This effect is especially noticeable in carbonate rocks, as corrosive fluids enlarge fractures by dissolution, most commonly [25].

Analog: NFR characterization requires information from an analog, especially to get a generalized view, which is usually not obtainable during development. Some of that data is only rough, other values are only determinable from analogies such as bedding-fracture relationship, fracture lengths and fracture-fracture relationships. Two types of analogs exist, which are outcrops and producing fields [25].

Outcrop analogs: The perspective of an outcrop is 2D and by modeling only a limited 3D view of the fracture system is available. When doing an outcrop study, it would be best if the rock of the outcrop was identical to the reservoir rock formation or at least have similarity in respect to the reservoir lithology, stratigraphic setting, rock properties, age, structure, etc. Outcrop analog studies have a large variety of applications. Those include the understanding of variations in fracture densities related to the geometry of an oil-size fold, constraining the distance between major fractures (which is important for planning the wellbore trajectory of horizontal wells that target the fractures; how fractures relate to lithology and stratigraphy or the investigation of areal variations of the fractures. As in the subsurface it is hard to obtain fracture length and connectivity [25].

What has to be considered are alterations in the characteristics of the fracture system during uplifting from burial depth to the surface. Overburden and tectonic stresses are reduced, temperature is reduced and pore pressure also changes [52] [53]. Due to the changing stress field on the rock, it is probable that existing fractures are extended and new fracture sets are created. When doing the outcrop study it is therefore important to filter those late-acting processes from the natural fractures observed at the outcrop [25].

Producing field analogs: With the aid of field analogs it is possible to set constraints on producing characteristics, such as recovery factor, productivity, production heterogeneity and water influx. It is crucial that the fields are geologically similar, which includes lithology of the reservoir, structural and tectonic settings, burial depth, geologic history or pore pressure. The associated difficulty however, lies in the fact that fracture systems are very diverse and only sparse information about them exists [25].

Dynamic Data: Dynamic data provides a better understanding of the NFR on the large scale. Further with the gained data the geology-based fracture model can be calibrated and

transferred into a more useful reservoir simulation model. This data is obtained by doing well tests. Single well tests derive kh , dual porosity and whether linear or dual flow occurs. With multiwell interference tests it is possible to get in-situ-flow anisotropy, k , kh , ϕh , etc [25].

However special discrete-fracture-network models are required to calibrate well tests and the geological model efficiently. The conventional well-test analyses software that works with the standard dual-porosity formulations just constructs ideal mathematical constructions of the reservoir but no realistic fracture network is mirrored [25].

3.4.4 Seismics

It has the advantage that with this technique fractures can already be classified in one of the earliest stages of field development and so economic risk is reduced. Asset teams are able to plan optimum horizontal well direction, which subsequently maximizes production and recovery. Compared to the other already discussed techniques the resolution is very low. The wavelengths used are up to 100m long. Natural fractures are obtained with the azimuthal anisotropy analysis [54] [55], which does not detect them directly. Thereby the average response across a large volume of rock is analyzed. Parameters such as the fracture intensity or the fracture orientation can be deduced by measuring travelttime differences between the fast and the slow shear waves and additionally by the polarization direction of the fast shear wave. To characterize fractures a variety of seismic techniques exist, including velocity anisotropy determination, azimuthal amplitude variation with offset and the normal moveout variation with azimuth [24], which are shown in fig.12.

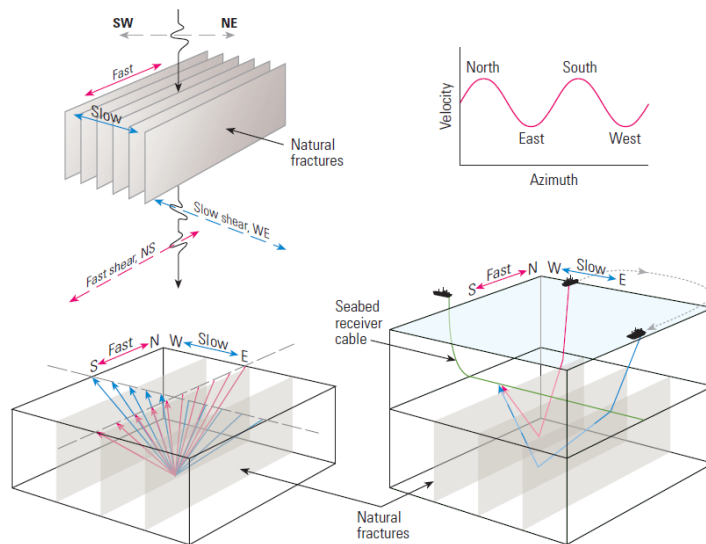


Figure 12: Seismic azimuthal anisotropy methods. The diagrams show land and marine seismic acquisition methods used to detect fracture-induced anisotropy. The fracture diagram (top left) shows vertical fractures striking north-south in the example, causing shear-wave splitting that helps to determine the fast-shear direction (north-south red polarization

vectors) and the slow-shear direction (east-west blue polarization vectors). The sinusoids show how anisotropy can be determined from compressional and shear velocity variations with the azimuth (top right). The land seismic diagram (bottom left) shows the rays for common midpoint gathers from two-source-receiver directions. The seabed seismic diagram (bottom right) demonstrates the effects of seismic anisotropy by showing two rays: a south-going fast ray from a source position to the north of the seabed receiver cable; and a west-going slow ray from an east source position above the seabed receiver cable. In a 3D survey, all azimuth directions are interrogated [24].

Techniques investigating NFR such as multioffset, multiazimuth vertical seismic profiles (VSP), or walkaway-and walkaround-VSP methods that analyze velocity anisotropy and amplitude variation with offset and azimuth (AVOA) allow a higher resolution than with surface seismic methods. These techniques help to calibrate results obtained from surface seismic results. To optimize the VSP configuration it is necessary to integrate all available data for extracting high-quality anisotropy information. This information is used to design 3D surface seismic surveys to cover areas remote from well control [56] [57] [24].

The fast compressional- (P-) wave direction aligns with the direction of the maximum compressional stress, which is, as already explained, parallel to the natural fractures. The slow P-wave is aligned normal to the fracture strike [58]. Fracture filling fluid affects the velocity. Seismic attributes, e.g. the reflection amplitude depends also on the azimuth and so fracture azimuth can be determined [24].

When analyzing azimuthal variations velocity-based methods respond to the accumulating effects of overlying strata, whereas amplitude variation methods also detect local azimuthal variations [59]. This leads to higher vertical resolutions.

The reflection amplitude depends on the effective elastic properties of the fractured rock. Due to changes of the P- and S- velocities in the fractured rock, the AVO response is influenced by the fracture azimuth [60] [61] [62].

The azimuthal variation of P-wave normal moveout velocity is another technique. Three azimuthal measurements are performed that show the NMO in all directions. This method helps to measure additionally dipping beds, where the fractures are not vertical. The disadvantage is the lower vertical resolution [63].

Those techniques are already in an advanced stage of development. Carbonate reservoir studies showed wide agreement between the results obtained by seismic and those by FMI images [64].

3.4.4.1 Microseismics

When fluid is produced or injected into rocks in the subsurface the net stress varies in the fractures, which induces small shear events that emit acoustic signals. Nearby monitoring wells, equipped with sensitive multicomponent seismic recording equipment is used to measure those emissions. Due to the different arrival times at the certain sensors the exact location and time of the events can be deduced (fig.13). Due to the possibility of the measurement of those microseismic events also the creation of hydraulic fractures in a stimulation operation can be recorded [65].

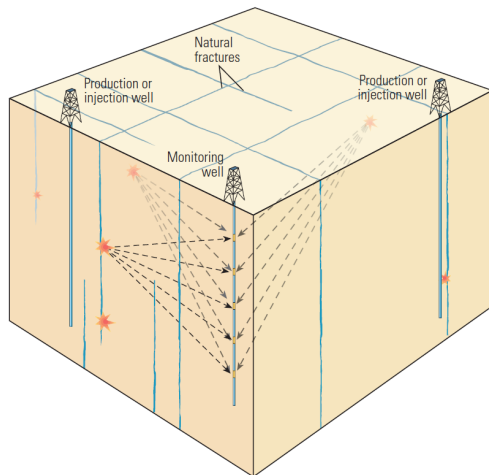


Figure 13: Principle of microseismics. The shear events, production/injection wells and monitoring wells are illustrated [24].

As explained before for horizontal completions the key to maximize the stimulated reservoir volume (SRV) for low to ultralow permeability formations is to drill lateral in direction of σ_1 within the reservoir to provide essentially transverse fractures when the multistage hydraulic fracture stimulation treatments are pumped. Therefore, it is crucial to understand the basic fracture directions, how deep the fractures penetrate formation and to determine if the designed perforation spacing is sufficient to produce the intended fracture coverage during the multistage fracturing treatments. The only existing technique that provides that is microseismics [66].

The following example shows the importance of microseismics. The path of the lateral well and the desired direction of the fracture plane is illustrated in the left graph (fig.14). However, the result was unsatisfactory. The right graph illustrates the generated fractures measured by microseismics (fig.14). To get transverse fractures, which are perpendicular to the wellbore, the next well was drilled perpendicular to the fracture plane witnessed by the first well. This yielded in a two-fold better production rate and economic ultimate recovery (EOR)

than well 1. The other wells drilled in that area were planned as the second well but used in addition longer lateral sections and more stages for fracture stimulation [66].

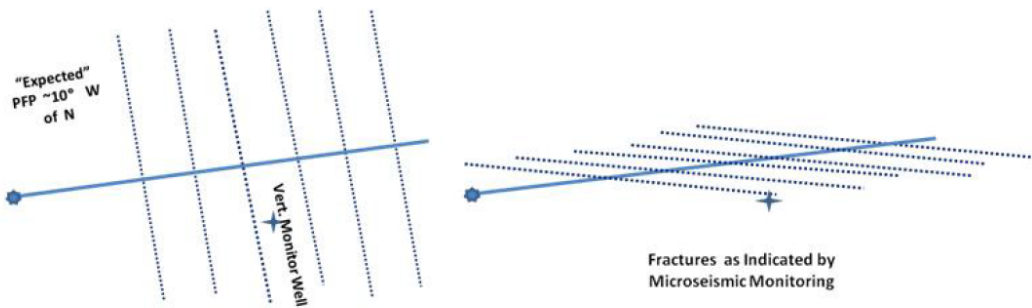


Figure 14: The intended well path was transverse to the fractures (left). At the right the actual length and direction of the fractures recorded by microseismics is shown [66].

3.5 Types of NFR characterization

Reservoir characterization in NFRs is more challenging than in conventional reservoirs as they are more complex. In NFRs it is necessary to characterize [67]:

- 1) fractures and matrix
- 2) matrix-fracture interaction

Following fracture parameters have to be characterized: inter-fracture spacing, length, orientation, porosity, connectivity, aperture and permeability. For the complete NFR also vertical and areal heterogeneity must be considered [67].

There exist two approaches in NFR characterization, which are the geological- and the engineering approach [67].

Geological (forward) approach: Geologists try to compile fracture statistics on spacing, fracture height, orientation, aperture and length. In a successive step those parameters are scaled up to represent an effective fracture porosity and permeability. It is also termed “forward approach” as it aims to characterize the reservoir from a perspective of what caused or created the geological setting [67].

Fracture parameters such as its spacing, aperture, length and connectivity are controlled by [67]:

- porosity
- lithology
- structural position
- rock brittleness

The aim of the fracture model is to set up empirical/analytical relationships that integrate the parameters of the fracture listed above with its variables. Those parameters are obtained by doing a certain amount of reservoir sampling. For setting up the empirical/analytical relationships and to get valuable data of the parameters it is crucial to do outcrop studies. Problems associated with outcrops however are that it is possible that the petrophysical parameters may be altered due to weathering and stress effects [67].

Cores are another data source. As already discussed, it is more probable to intersect fracture systems with horizontal wells, as they are drilled perpendicular to those systems mostly. Furthermore, they also give an insight into inter-fracture spacing and length. Mainly in vertical drilled wells it is probable that the derived number of cores is not sufficient to cover the fractured sections. Fracture parameters and empirical relationships cannot be derived by coring but only from outcrop studies or field analogies [67].

Averaging of fracture spacing and aperture is according to Long [68] useful. However, field evidence does not support this. Moreover it seems that only a few fractures are hydraulically active and fluid may largely only flow through the best conducting fractures [67].

Engineering (inverse) approach: The inverse approach goes the other way round. It measures dynamic effects from the large-scale project and tries to conclude smaller scale characteristics. Well test and production data is used to derive permeability and fracture conductivity to understand the nature of the fracture system [67].

When analyzing the tests reservoir heterogeneity is often not considered. Build-up pressure-transient- and long term production tests are in practice not conducted zone specifically. As a consequence those tests are not suitable in characterizing reservoir heterogeneity effectively [67].

In 90% of the naturally fractured reservoirs, the pressure build-up performance does not mirror dual porosity behavior. Still many NFR field examples have shown that a reasonable match can be obtained by applying a single porosity model. Therefore a higher effective permeability, compared to matrix permeability had to be set [67].

However, by ignoring fracture heterogeneity simulation models often underpredict watercut, water breakthrough time and the amount of oil being bypassed in the reservoir [67].

As both approaches have their drawbacks due to undersampling of in-situ fracture systems it is tried to build more accurate and realistic models of NFRs by combining both approaches [67].

“It is critical to identify, early in the reservoir study [67]:

1. what created the fracture system (i.e., regional, faulted or bended environment)

2. characteristics of the matrix-fracture system (i.e., fracture types, length, height, spacing etc.)
3. matrix permeability and porosity
4. the degree of communication between the matrix and fractures”

4 Stimulation in naturally fractured carbonates

4.1 Basics

As already explained hydrocarbon production in naturally fractured carbonate reservoirs occurs with a dual-porosity mechanism through sections with natural fractures and with a matrix flow where fractures are not existent. When a well intersects such fracture networks (either by drilling induced fractures or with perforations) it is possible to achieve negative skin values. When stimulating such wells diversion plays a critical role in order to obtain well production as closely as possible to its ideal conditions as it aids in establishing a more uniform production of the different intervals by distributing the acid across the production interval (with variable permeabilities and fractured- and non-fractured zones) during stimulation.

Especially in thick, heterogeneous sections optimum fluid placement is more challenging as the lowermost interval tends to receive more fluids as a result of a higher hydrostatic pressure. Further, due to heterogeneity in such reservoirs, reservoir pressure varies significantly as a result of heterogeneous depletion from virgin conditions [3].

Typical fluid volumes in stimulation treatments are between 1.0-1.8 m³/m of perforated interval, in dependence of the matrix properties. Higher volumes (up to 3 m³) did not achieve higher hydrocarbon gains.

Acid treatments in Kazakhstan were able to achieve well skins as low as -4.8 with acid volumes less than 1.0 m³/m of perforated interval. A hydrochloride acid system pumped through coiled tubing was used. A plausible cause for this is that natural fractures dominate and the fracture network was invaded by drilling fluid during drilling. After perforating the entrance to the network was cleaned again, which was leading to an improved communication between wellbore and reservoir.

As a matter of fact, by properly designing the drilling process low productivity in naturally fractured reservoirs can be prevented. Especially in horizontal wells, mud could get static, leading to a gelled mass which enormously increases skin [3].

In reservoirs that are fracture dominated the simplest placement method in newly drilled wells would be to perforate low permeability sections first, treat them, and to proceed subsequently with higher permeability zones. The disadvantage is the huge amount of time needed for that process [3].

The general principle of other diversion techniques was already discussed in chapter 2.5.3 and is the same in the application of treating naturally fractured carbonates.

4.1.1 Acid Fracturing

Acid fracturing serves in the creation of new paths connecting to the natural fracture network. It is especially helpful where the number of natural fractures is low. The challenge is that fractures compete for the pumped fluid and so the higher the number of fractures the higher the required rate [3].

After a fracture is initiated it grows up to a certain point until the growth stalls. The remaining part of the treatment is pumped in matrix mode. It is probable that this is, because the created fractures are intersecting a natural fracture network and all the fluid is lost to it. Additionally, the acid dissolves the rock resulting in decreased closure stress around the created fracture area. It is possible that the fracture still remains open although the propagation has stopped because the pressure in the fracture is below the closure stress of the far field [3].

4.1.2 Coiled tubing

Before viscoelastic surfactants were introduced coiled tubing operations were the preferred mean for the diversion of hydrochloric acid in formations with high permeability contrast. Due to the fact that the well does not have to be killed after the operation a potential source of formation damage is excluded. In low pressure wells flowback can be initiated immediately after the treatment which accelerates live acid recovery. This is achieved by the injection of nitrogen, which lightens the hydrostatic column. In fracture dominated reservoirs coiled tubing operations are suitable for cleaning up the fracture network from drilling induced damages. In reservoirs with non-dominant fractures the objective is to create wormholes. As discussed, they need optimum pump rate to minimize acid volume and thus creating highest possible conductivity. A further advantage of coiled tubing operations is that less equipment is needed. The overall equipment is even smaller than in bullheading operations at high rates.

Disadvantages regarding coiled tubing are that those pumping operations need more time. Due to the fact that crossflow occurs in thick carbonates more likely during heterogeneous depletion the pipe is exposed to acid and H₂S longer [3].

4.1.3 Bullheading

Many operators used bullheading techniques in a thick carbonate reservoir in Kazakhstan, described later. Alternating stages of 24% or 28% hydrochloric acid and viscoelastic diverting agents were pumped. Experience was also gained with treatments pumped above the fracture pressure but often could not be maintained for very long despite the use of fluids with appropriate leak off characteristics. The reason is the same as explained in chapter 4.1.1 [3].

4.1.4 Decision tree

A decision tree about the kind of stimulation treatment in dependence of the permeability contrast in carbonates is provided below (fig.15).

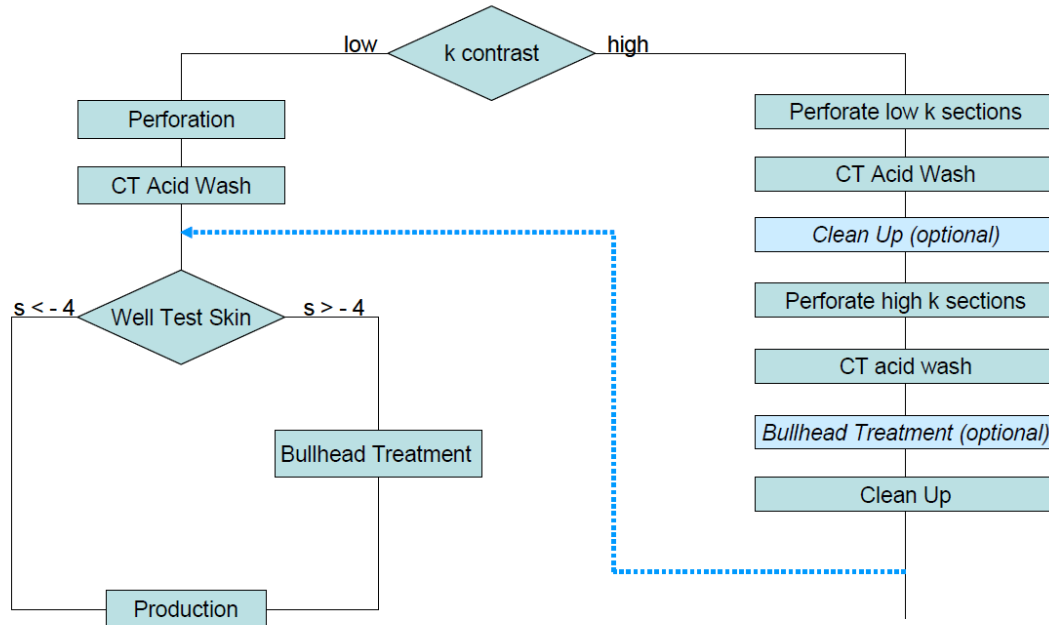


Figure 15: Decision tree for stimulation treatments in carbonate reservoirs based on permeability [3]. In naturally fractured reservoirs the permeability contrast is always high.

4.2 Case Studies

4.2.1 Bullheading vs coiled tubing

The first analysis compares the effects of hydrochloric acid treatments pumped through coiled tubing and viscoelastic treatments pumped in bullheading [69]. All wells are located in a field in Kazakhstan and all were treated with the same acid volume per unit of perforated length. The intervals are multiple perforated with total lengths of 75 m usually spread over 500 m.

As the available data is insufficient to get reliable skin values only the length of the perforated interval contributing to production was analyzed before and after treatment. Those producing lengths were determined by the use of production logs. The results are shown in fig.16 [3].

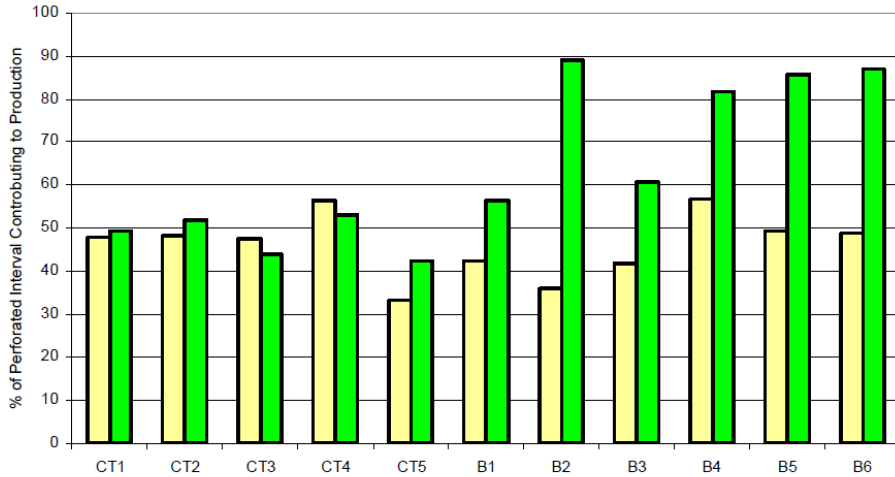


Figure 16: Percentage of total perforated interval contributing to production before (yellow) and after (green) coiled tubing [3].

It is obvious that a bullheading treatment with a diversion agent is more promising as the length of the producing section is increased to a higher extent than in the coiled tubing cases. Consequently, this leads to a more homogeneous depletion of the reservoir.

Another analysis was executed on treatments performed in a 5-month period in the same field. Coiled tubing-conveyed viscoelastic acid treatments were compared with bullheaded viscoelastic acid treatments. Again the same volume per unit length was taken and to make the result better comparable also acid strength was equal. The percentage of productivity index is shown in figure 17.

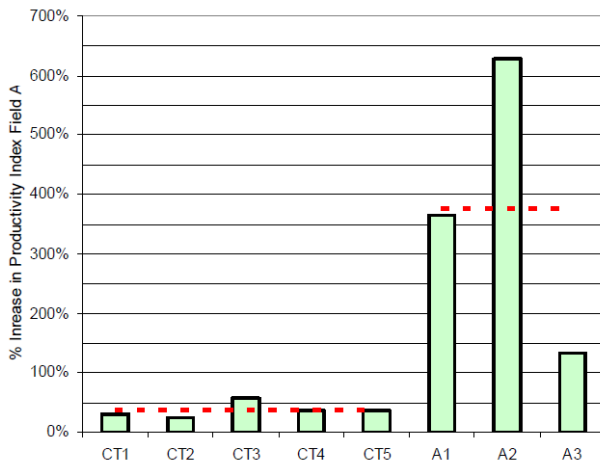


Figure 17: Comparison between incremental increases in productivity index for viscoelastic acid placed through coiled tubing and pumped in bull heading [3].

Also in this field case bullheaded treatments yielded better results than coiled tubing operations.

In another field a further analysis was carried out, comparing productivity indexes before and after treatment. Hydrochloric acid systems were pumped through coiled tubing and hydrochloric acid systems were bullheaded in stages with viscoelastic acid at high rates. The results are shown in fig.18.

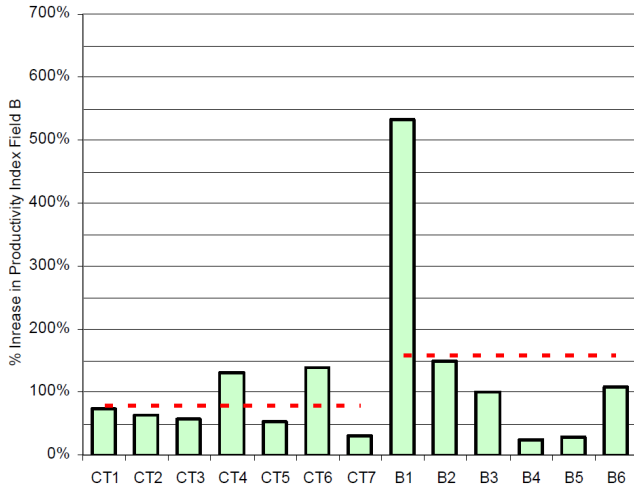


Figure 18: Comparison between incremental increases in productivity index for hydrochloric acid placed through coiled tubing and viscoelastic diverting acid pumped in bull heading [3].

Again the average increase of the productivity index is higher in the wells treated by bullheading although the bullhead cases already had a very low skin due to the fact that they were treated with hydrochloric acid through coiled tubing in the previous years. The wells CT4 and CT5 were severely damaged by previous workover operations and so they had a higher potential for improvement. In the wells treated by bullheading it is remarkable that all, except the wells B4 and B5, are above the coiled tubing samples. This is due to the fact that they already had before the treatment a skin factor of -4.5 and so the potential to decrease that value further was low. The wells B3 and B5 were proven to have sections with highly conductive fractures by production logs. In B3 the entire production was coming from less than 10% of the production interval [3].

4.2.2 Packer vs bullheading

16 treatments using mechanical packers or bullheading techniques on both, producer and injectors are compared. This was done in a field in Western Kazakhstan. It consists of 14 producing layers, whereby the two bottommost layers are known to have natural fractures. The wells have more than 70m of perforations spread over 400m. Due to heterogeneous depletion during production the layers have its own unique pressure regime. As a result, crossflow is occurring between the layers.

All wells were treated with the same amount of acid per unit of length of perforated interval. As mentioned, with mechanical devices more time is needed than with bullheading techniques. This is confirmed in tbl. 1 and fig.19 & 20

Table 1: Summary of mechanical packer and bullhead treatments in 5 months. Treatments that used viscoelastic acid are highlighted in grey [3].

Well	Treatment	Days	Skin Before	Skin After
P1	M.Packers	5	New	+2.0
P2	Bullhead	2	+7.0	-0.9
P3	Bullhead	3	+21.0	-0.2
P4	M.Packers	2	New	+2.2
P5	M.Packers	2	New	+1.5
P6	M.Packers	10	New	-4.0
P7	Bullhead	2	7.2	-3.2
P8	Bullhead	2	+11.5	-2.0
P9	Bullhead	3	New	-2.5
I1	Bullhead	2	-3.0	-4.5
I2	M.Packers	2	-3.0	-3.0
I3	Bullhead	2	+19.0	+5.0
I4	M.Packers	4	-4.0	-4.0
I5	M.Packers	6	-4.5	-4.5
I6	M.Packers	14	-4.5	-5.0
I7	M.Packers	4	-2.5	-3.5

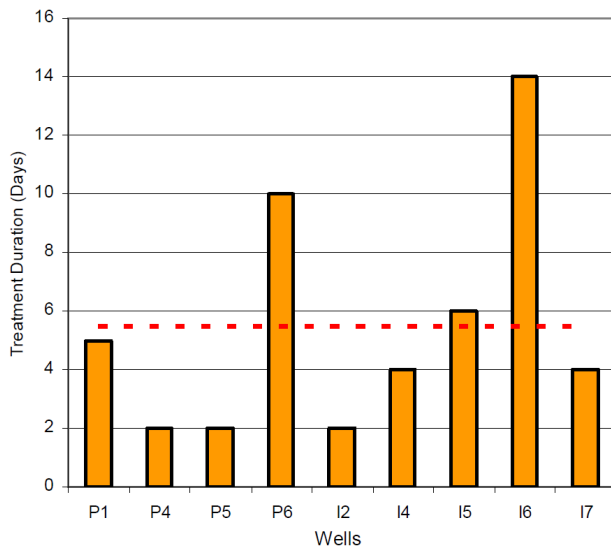


Figure 19: Duration for packer treatments [3].

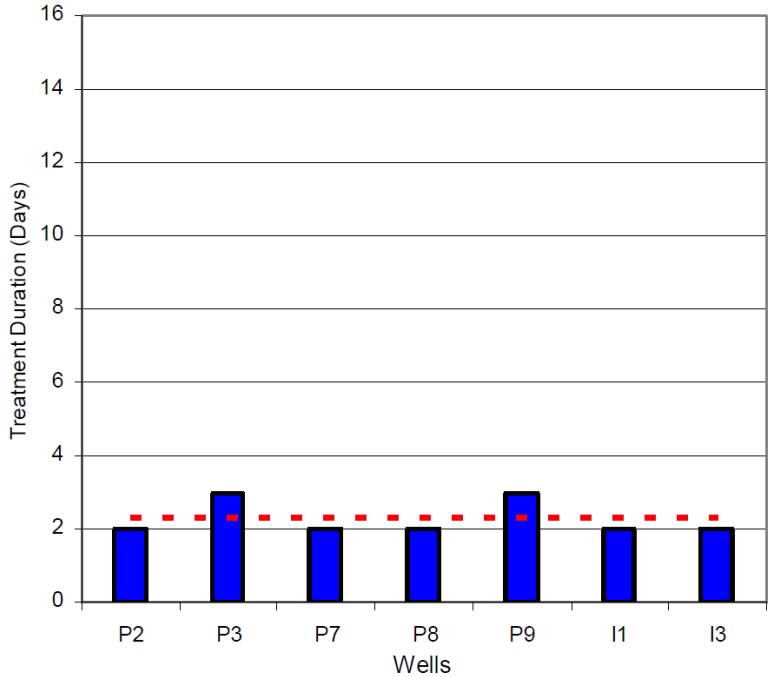


Figure 20: Duration for bullhead treatments [3].

The average of the bullheaded cases gave a value of 2.3 days, whereas the treatments performed with a packer took 5.4 days.

Further, after analyzing tbl.1 it can be concluded, that the bullheaded treatments achieve a more significant reduction of skin values, although only certain wells (in grey, tbl.1) were treated with a diverter. The result is shown in fig.21.

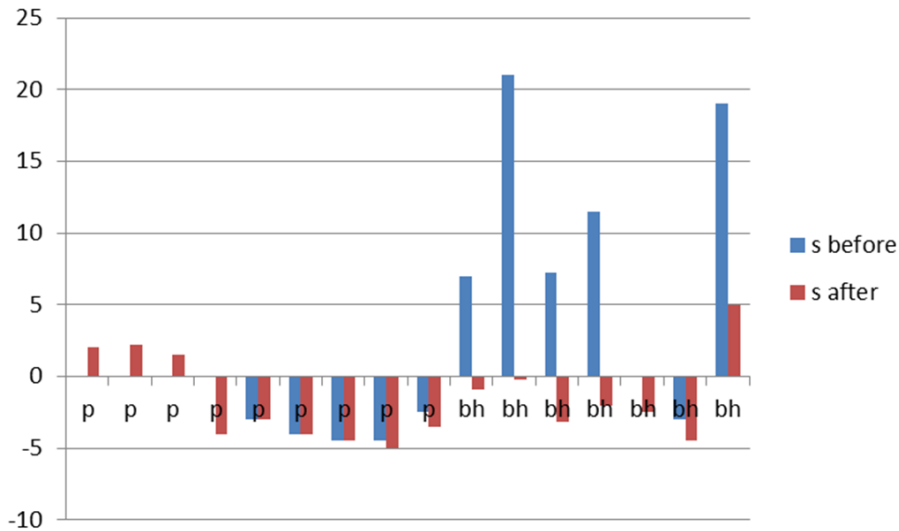


Figure 21: Skin before and after treatment for packer and bullhead treatments.

Due to the author this can only be attributed to the fact that no fluids were placed in the treated reservoir in the bullheaded treatments, which avoided damage after the stimulation treatments were completed.

However, after analyzing the data further it must also be mentioned, that the wells treated by bullheading, had higher skin values pre-treatment (fig.22) and so there was a higher potential for skin reduction.

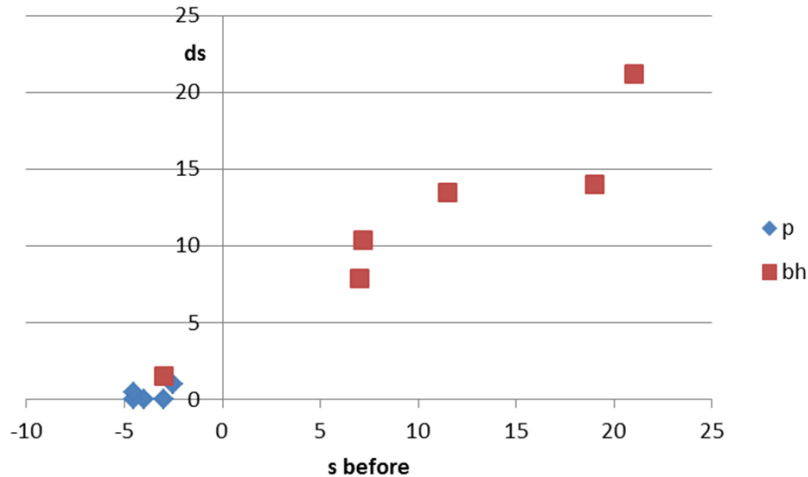


Figure 22: Skin before treatment and the change of skin for packer and bullhead treatments.

4.2.3 Packer

In another Western Kazakh field, it was tried to minimize time of treatments, where mechanical packers were used, by treating a relatively large section at the same time. To yield best results a brine-based viscoelastic surfactant was used for diversion. When measuring the bottomhole treating pressure the effects of the diverting agent were evidenced, as the bottomhole pressure was increasing when the diverter entered the formation. This effect was in some cases mitigated by the presence of streaks with natural fractures.

As explained, in mechanical packer applications it is sometimes necessary to kill the well to remove the packer, which often results in damage as the kill fluid enters the formation. Also here, post-treatment production tests showed that the wells were not ideally producing.

In one well a heavier killing fluid had to be used. This resulted in the requirement of a workover rig to swab the well for two months to resume production. Finally, a skin of 0.5 was achieved, which is a non-optimum condition.

However, in one well a foam-based hydrochloric acid system was pumped through coiled tubing which yielded the best result of all treated wells in that field. The volume of acid pumped was only 0.6 m³ per meter of perforated interval.

4.2.4 Ball sealer

Another field, consisting of a pay zone of 340m with 12 zones, of which two were known to have natural fractures. The typical perforated intervals were in excess of 60m. Non-buoyant ball sealers have been used as a diverting agent of the hydrochloric acid system in the stimulation of the newly drilled wells. However, the results obtained were disappointing. The ideal situation of skins would have been about -5, the average skins achieved were -1.5 (fig.23).

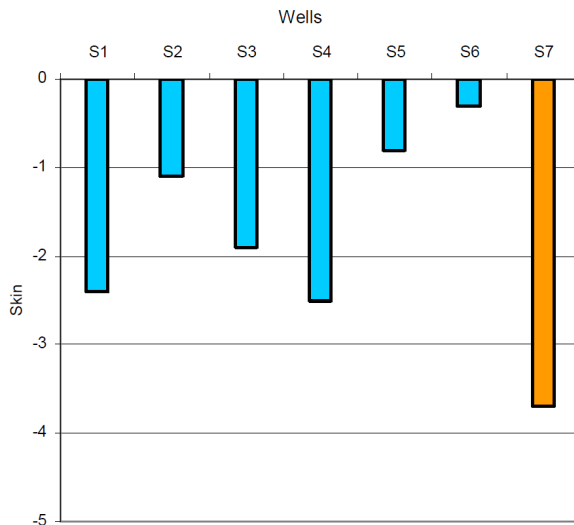


Figure 23: The skin values after treatment. In blue the ballsealer treatments are shown, in orange the foam treatment [3].

Well S7 has already been drilled several years earlier. It was treated with a viscoelastic diverting agent conveyed with coiled tubing. The post-treatment skin achieved is much lower than at the other wells treated with ball sealers. However, it could also be a statistical outlier, as there are no further data points.

As mentioned, due to safety issues remotely operated ball sealers have to be used additionally, which increases logistics on large-size treatments.

4.2.5 Viscoelastic acid limitations

When treating formations with extremely conductive natural fractures the diversion achieved is in many cases insufficient. As mentioned viscoelastic acid systems increase viscosity when they spend but are still reactive. Another characteristic is that they are a shear thinning fluid. Consequently, opposed to treatments using polymer-based agents no pressure increase can be observed with VES treatments. The only way to evaluate the success of a treatment with viscoelastic acid system is the comparison of the production logs before and after the treatment.

Following three wells are analyzed:

- Well A: This well, with perforation of 139m spread over 575m, is used for water injection and was treated with hydrochloric acid in stages with viscoelastic acid. Due to that the injection rate increased by 8%, the pressure has not changed. In fig.24 the pre- and post-treatment injection profiles are shown. The layers 20, 21, 25, 26 and 28 are known to have natural fractures. Only layer 24 was additionally opened with the treatment. In the lower section of the perforated interval the overall injectivity into the fractured layers improved.

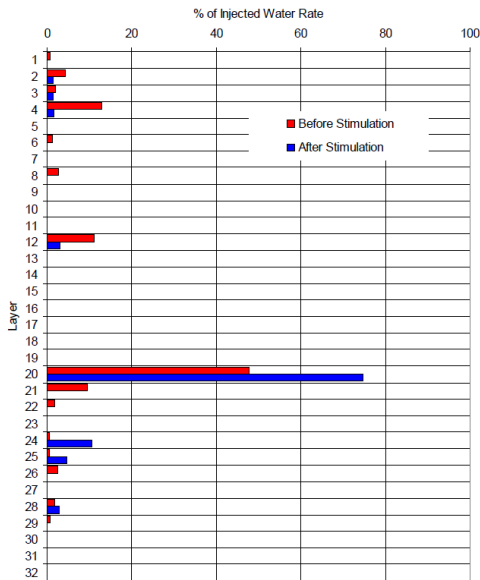


Figure 24: Injectivity profile before and after treatment with viscoelastic acid for well A [3].

- Well B: This well has 60m of perforations straddled over approximately 180m. FMI logs showed several sections with natural fractures. The treatment was performed with a viscoelastic system. A post-treatment well test showed an oil production increase by 12 times. The post-treatment production log shows that still, most of the production is from the zones with natural fractures, whereas as the zones without fractures contribute only to a very limited amount to overall production (fig.25).

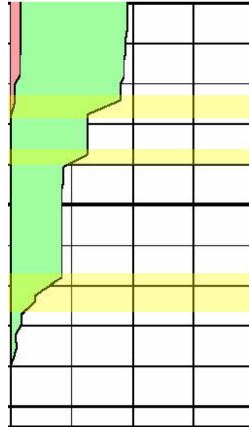


Figure 25: Post-treatment production log on well B (sections in yellow have natural fractures) [3].

- Well C: This well has 78 m of barefoot completion but production is from only 4 m of a highly conductive zone with natural fractures. To reduce the inflow of the fractured zone a viscoelastic brine solution was pumped. In a next step stages of hydrochloric acid and viscoelastic stages were pumped. This treatment yielded an increase in production of 29%. The increase in producing height was only 2 m so still 72m did not contribute to production. Pre- and post-treatment productions are shown in fig.26. The extension of the producing zone in the lower zone and the opening of the zone above can be seen.

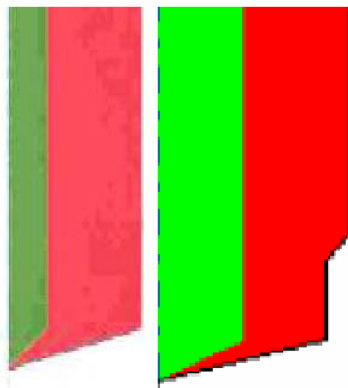


Figure 26: Pretreatment and post-treatment production log on Well C [3].

4.2.6 Enhanced viscoelastic acid

In a field in North West Kazakhstan acid fracturing with enhanced viscoelastic acid treatment was conducted. The well has an open-hole section with a 330 m drain. It consisted of a dual-acid technique. To provide retardation and deeper penetration into the fracture hydrochloric acid was emulsified in diesel. For fluid-loss control and fracture-to-fracture diversion an enhanced viscoelastic system was pumped. To prevent contact, which would lead to degradation and a loss of the specific properties, a spacer (15% hydrochloric acid) was

pumped for separation between the two systems. For monitoring the treatment bottom-hole pressure gauges were mounted 618m above the horizontal section.

The stages of the treatment were as follows:

1. 15% hydrochloric acid prewash for displacement of H₂S away from the wellbore
2. Enhanced viscoelastic acid pumped at high rates
3. Spacer
4. Emulsified acid-in-diesel system
5. Enhanced viscoelastic acid at lower rates

The reason for step 2 is the plugging of the existing fractures. In step 5 the rate was decreased, because diversion efficiency is higher at a lower pump rate. The viscoelastic acid diverts fractures already stimulated and creates new fractures in other locations along the open-hole section. [3]

The open-hole pressure response clearly indicates the diversion effectiveness of the VES. The productivity increase was from 0.9 m³/d/bar before the treatment to 7.1 m³/d/bar afterwards, which is due to a creation of additional fractures that intersect the network of natural fractures and fissures. Because of that the well accesses more reservoir and the effective length of the horizontal section is increased.

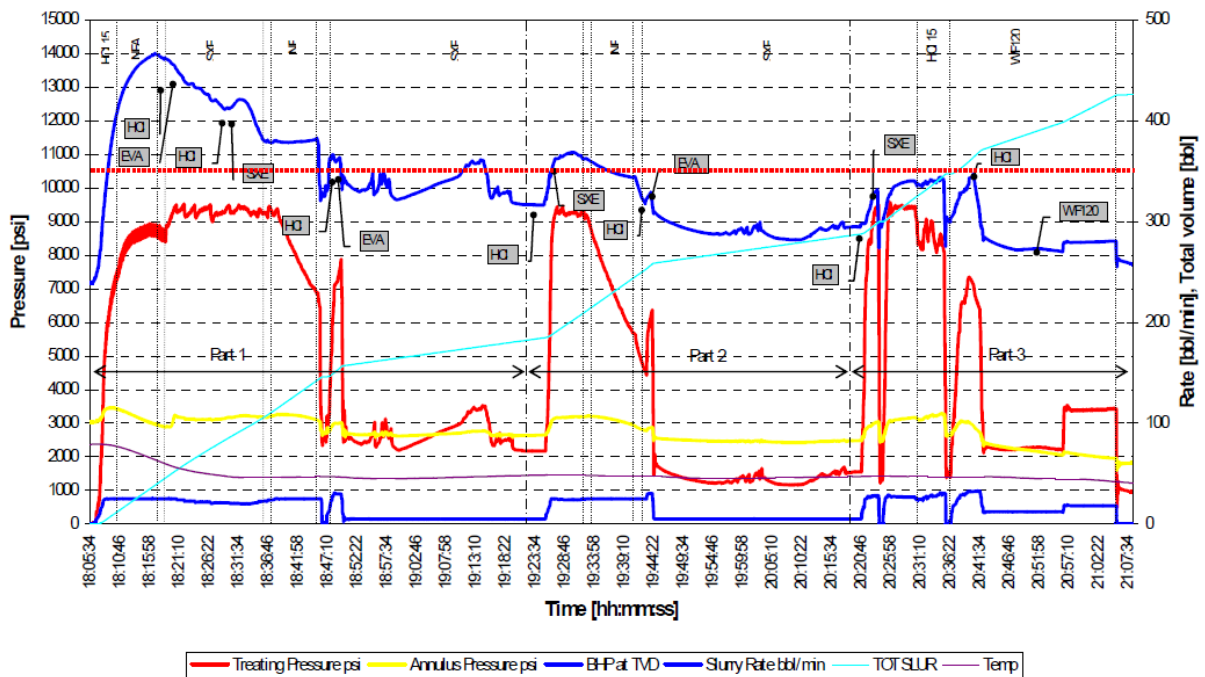


Figure 27: Treatment with Enhanced Viscoelastic Acid [3].

4.2.7 Southeastern New Mexico

The following case histories are from the Warren Unit in Southeastern New Mexico. The wells are producing from the Yeso (part of the Leonardian series) and Grayburg San Andres

(part of the Guadalupian series) formation, which both are thick, tight, lenticular fractured carbonates (fig.28) [70].

(b)

System	Epoch/ Series/ Stage	Time (m. y.)	Delaware Basin	NW Shelf New Mexico	NW Shelf Texas	Central Basin Platform	Midland Basin					
PERMIAN	Ochoan	251	Dewey Lake	Dewey Lake	Dewey Lake	Dewey Lake	Dewey Lake					
			Rustler	Rustler	Rustler	Rustler	Rustler					
			Salado	Salado	Salado	Salado	Salado					
			Castile	Castile	Castile							
	Guadalupian			Delaware Mountain Group	Bell Canyon	Tansill	Tansill	Tansill	Tansill			
						Yates	Yates	Yates	Yates			
					Seven Rivers	Seven Rivers	Seven Rivers	Seven Rivers				
					Queen	Queen	Queen	Queen				
				Cherry Canyon	Grayburg	Grayburg	Grayburg	Grayburg				
					Upper San Andres	Upper San Andres	Upper San Andres	San Andres				
				Brushy Canyon				Brushy Canyon				
					Cutoff	Lower San Andres	Lower San Andres	Lower San Andres				
				Leonardian			Bone Spring	1st carbonate	Glorieta	Glorieta	Glorieta	Spraberry
								1st sand				
	2nd carbonate	Paddock	Upper Clear Fork					Upper Clear Fork	Dean			
	2nd sand	Blinebry	Middle Clear Fork					Middle Clear Fork				
	3rd carbonate	Tubb	Lower Clear Fork					Lower Clear Fork				
	3rd sand	Drinkard	Lower Clear Fork					Lower Clear Fork				
	Lower carbonate	Abo	Abo	Abo/Wichita								
	Wolfcampian			Wolfcamp	Wolfcamp	Wolfcamp	Wolfcamp					

QA13434b.jx

Figure 28: Stratigraphic chart [70].

A paper [71] from 1996 investigated how to treat the Warren Unit, specifically the Leonardian series, best. They took a closer look on the Drinkard- and Tubb formation. Both formations have oil zones and a perceived gas cap [72]. Laboratory test gave a high solubility of the rock of the Drinkard in mineral acid. The formation consists of two zones, where the upper one is dolomite with vugular porosity making it non-productive. The lower one contains interbedded limestone and dolomite, where production is from natural fractures and vuggy

porosity. The oil zone has a porosity of 12%, the gas zone 10% on average. The thickness of the formation is 200 ft.

The Tubb formation is above the Drinkard (fig.28), where the pay zone consists of dolomite and sandy dolomite. The oil pay zone has a net pay thickness of 54 ft, the gas cap 28 ft. Porosity is between 7 and 18% (averaging 9%). Formation data is summarized below (tbl.2):

Table 2: Kind of formation, solubility, Young's modulus and Poisson's ratio are summarized in dependence of the Unit [71].

Warren Unit No.	Formation	Solubility in 15% HCl	Young's Modulus, psi	Poisson's Ratio
WU BT#111	Blinebry	---	2.31×10^6	0.370
WU BT#111	Drinkard	92.5	$2.35 \text{ to } 2.92 \times 10^6$	0.335 to 0.395
WU#54	Blinebry	19.4 to 93.2	$4.68 \text{ to } 10.31 \times 10^6$	0.23 to 0.39
WU#54	Tubb	80.8 to 07.6	$7.42 \text{ to } 7.59 \times 10^6$	0.27 to 0.32
WU#28	Drinkard	99%	6.63×10^6	0.23

Results [71]:

- Crosslinked 15% hydrochloric acid gel treatments were economical and effective; they achieved higher production rates for new well completions compared to sand fracturing and special fluid loss control acid in the Tubb formation
- Reservoir quality is the major control parameter; results were similar when changing job size and staging variations in the Drinkard formation
- Re-stimulation yielded similar results regardless of the type of treatment employed in the Tubb formation
- No production enhancement was achieved with heated acid stages or by adding CO₂ to the stimulation fluids
- Crosslinked 15% hydrochloric acid gel and gelled acid provided improvement in retardation of reactivity in vugular and naturally fractured dolomite formations and provide better leak-off control than gelled or neat acid

4.2.8 Coiled tubing acid tunneling

Since 2005 a new stimulation termed “coiled tubing acid tunneling” has been applied in carbonate formations. It can only be applied in open-hole completions .The tunnels are created by pumping HCl through a specially designed jetting bottom assembly (fig.29) conveyed by coiled tubing. On the surface conventional acid pumping equipment is used. The objective of acid tunneling is to create lateral production tunnels with its own network of wormholes (fig.30), which can interconnect natural fracture networks in carbonate formations, which yields a negative skin [1].



Figure 29: BHA with one kick-off tool

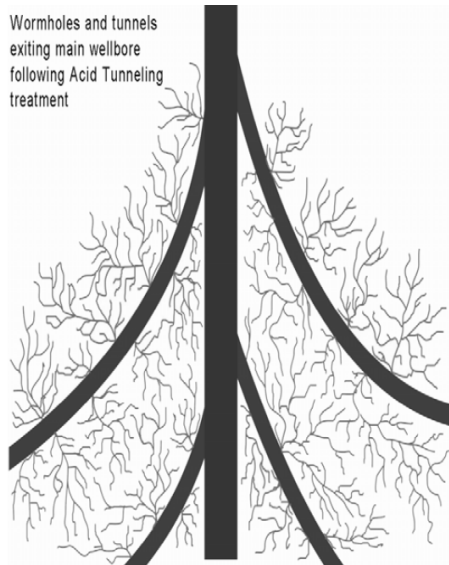


Figure 30: Wormholes that occur as the acid leaks off into the formation while tunnels are created

4.2.8.1 Venezuela

The Mara field in Western Venezuela contains massive naturally fractured carbonate formations (up to 1000 vertical feet), having low porosity and permeability values. The production is from about 400 wells. The characteristics of the formation are listed in tbl.3.

Table 3: Field data western Venezuela [1]

Porosity	3-10%	Permeability	1-5mD
Average reservoir temperature	150-200°F	Initial reservoir pressure	2771psi
Average flowing pressure	870psi	°API crude	15
Average depth	6000ft		

16 wells with open hole completions have been treated by acid tunneling with 10% HCl and 15% HCl, yielding in a total production increase of 5000 bopd. The objective was to bypass sections damaged from invasion of muds, cements and fluid loss control material and to interconnect the present micro-fractures [1]. Before using this technique conventional treatments were applied, which were as follows (tbl.4):

Table 4: Conventional treatments [1]

1.5 ft penetration with solvent mixture	13-15% HCl acid treatment
9% formic and acetic acid treatment	Foam diversion
Acid penetration >3 ft	Nitrogen lifting after treatment

The acid values pumped were 100-150 gal/ft compared to 60-130 gal/ft pumped in the acid tunneling treatments.

In Well #4 with an open hole completion from 4,439 to 6,150 ft, a direct comparison of matrix acid treatment and acid tunneling is possible (tbl.5).

Table 5: Comparison between matrix acid- and acid tunneling treatments in well 4 [1]

Matrix Acid Treatment	Acid Tunneling Treatment
400 bbls of solvent, 225 bbls of 13%HCl + 9% formic acid	455 bbls of 10%HCl, 571 bbls of 15%HCl
Foam diverted and nitrogen induced	7 tunnels with a cumulative length of 138 ft, 7-16 ft/hr penetration rate
Initial production rate was 380 bopd	Initial production rate was 918 bopd
15 days payback	6 days payback

4.2.8.2 Offshore Spain

In this field acid tunneling was applied at high bottomhole temperatures (greater 300°F) and a high reservoir depth (greater 7000 ft). The naturally fractured carbonate formation consists mainly of highly soluble calcite. The formation characteristics are summarized in tbl.6.

Table 6: Formation characteristics offshore of Spain [1]

Initial reservoir static pressure	3,745 psi
Current reservoir static pressure	3,950 psi
Bottomhole temperature	302 °F
Reservoir fluid compressibility	5.1 E-6 psi ⁻¹
Reservoir fluid viscosity	1.1 cP
Initial GOR	75 scf/STB
Gas gravity	0.959
Water gravity	1.03
API gravity	31°
Initial water saturation	22.7 %

Bubble point pressure	400 psi
H2S content	100 ppm

The acid tunneling treatment was used to re-open a 40m section of the original mother borehole, which could not be entered probably due to a collapse of the formation or due to hole roughness, and to additionally create a 5.8m long lateral tunnel. Due to the high temperatures an HCl-acetic acid blend was pumped. After the acid tunneling process, a bullheaded acid treatment and scale inhibition treatment was performed. Production increased from 110 to 246 bopd [1].

4.2.8.3 Indonesia

The production in Baturaja reservoir is from the NEASD- and the GRH pool. Some statistics are summarized below (tbl.7):

Table 7: Production characteristics of the two pools [1]

Pool	NEASD		GRH	
Peak production	30 wells	12,500 bopd	24 wells	6,500 bopd
Current production	21 wells	1,750 bopd	15 wells	1,100 bopd

In the paper it is not mentioned whether the reservoir is naturally fractured. Formation characteristics are shown in tbl.8.

Table 8: Formation characteristics of the Baturaja reservoir [1]

Rock	Carbonate reef
Porosity	15-25%
Permeability	220-4,150 mD
Solubility in 5% HCl	>90%

Several HCl treatments have been performed, but with limited success. The purpose of the acid tunneling process was to create multiple laterals from a 6 m open hole section. 5 wells are summarized. The constructed laterals had a length of only 2 to 7 m, as they should not go too close to the water zone. The success of the job was significant. Before the treatment the average production was 280 bopd, and increased to 860 bopd after the treatment. Water production increased from 680 bpd to 1,930 bpd, which yields in a decrease of the water cut from 71 % to 69%. The average payout was 1 month. The figures of all treatments pre- and post-treatment are shown in fig.31.

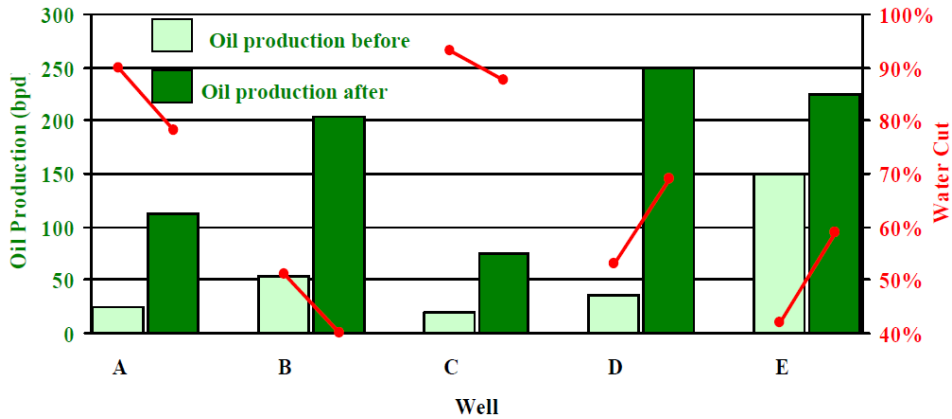


Figure 31: Before and after treatment production for wells A-E [1].

Well B was before the acid tunneling treatment also conventionally treated. The results are shown in fig.32.

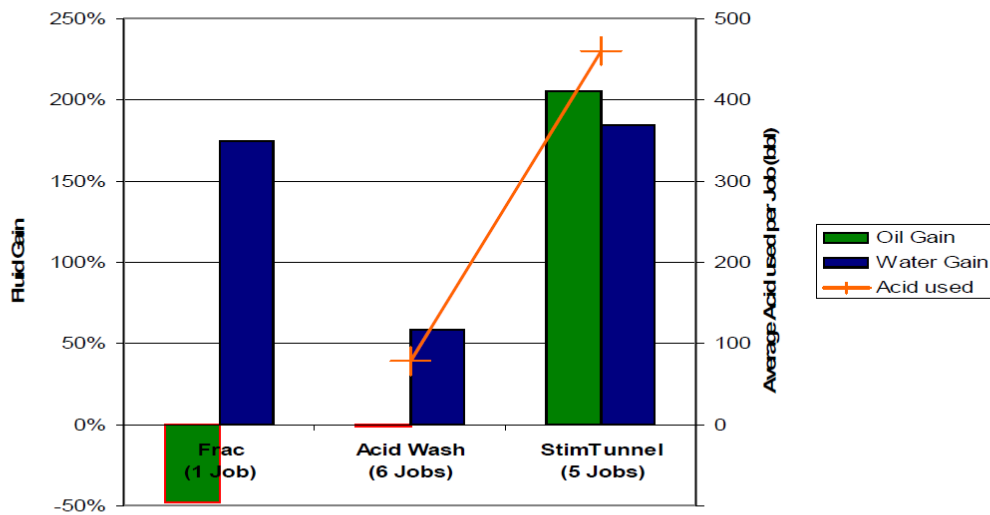


Figure 32: Comparison of production change of the different stimulation treatments [1].

As can be seen acid tunneling performs by far best. Proppant fracturing yielded an oil production decrease from 50 bopd to 30 bopd and water production increase from 130 bpd to 350 bpd [1].

In addition to Wells A to E further 7 wells were treated by an acid tunneling technique. In total, the 12 wells increased from 955 bopd to 1,670 bopd, which is an increase of 75% [1].

4.2.8.4 Oklahoma

The field was producing since 1924. It is not mentioned whether the formation is naturally fractured. The purpose was to create three tunnels. The initial increase in production was 110 %, the sustained increase was 80 % and additionally also gas production increased [1].

4.2.8.5 Romania

Romania's oil fields including large areas of carbonate formations are traditionally stimulated by bullheading acid. Six horizontal and four vertical wells in four fields are analyzed. The data is shown in tbl.9.

Table 9: Formation data

Kind of well	Vertical	Horizontal
Average TVD	3,050 ft	5,730 ft
Average open-hole section	108 ft	1,640 ft
Permeability	5 mD	14 mD
Temperature	142 °F	171 °F

15 % HCl was pumped. 43 tunnels with a cumulative length of 1,300 ft were created, which yielded an average production increase of 30% in the 10 wells. The horizontal wells were more successfully treated [1].

4.2.8.6 Summary

The paper summarized acid tunneling treatments of 47 wells in 9 countries. In total 299 tunnels with a cumulative length of more than 10,000 ft were created, where longest one has been 120 feet. The penetration rates were between 3 and 45 ft/h. Usually 10 to 15% HCl was pumped. Temperatures ranged from 140 to 302 °F at depths from 3,000 to 16,799 feet. Sweet and sour gas was treated. The permeability ranged from 0.5 to 4,200 mD [1].

A summary of the literature review on all papers dealing with naturally fractured carbonates is illustrated in tbl. A - 1.

5 HSE

Due to the nature of acidizing fluids and the high pressure occurring during stimulation treatments an experienced crew with a well-established chain of command and strict adherence to safety and execution guidelines is extremely important. Those HSE guidelines will not be further discussed as it will mainly be focused on stimulation of naturally fractured carbonates.

6 Geology of the Vienna Basin

The Vienna basin was formed during the early Miocene when the Alpine-Carpathian thrust front reached the European forelands. Along the Alpine-Carpathian thrust front, thrust ages become younger from west to east, because at the Alpine-Carpathian junction, the Bohemian Massif has been recessing. There the thrust units advanced progressively, whereas to the west of the reentry the thrust movement stopped earlier [73].

Final thrusting of the easternmost Alpine nappes (8) stopped where the Carpathians start, whereas the Romanian Carpathians (6) continued thrusting beyond the Pannonian. [74] (fig.33)

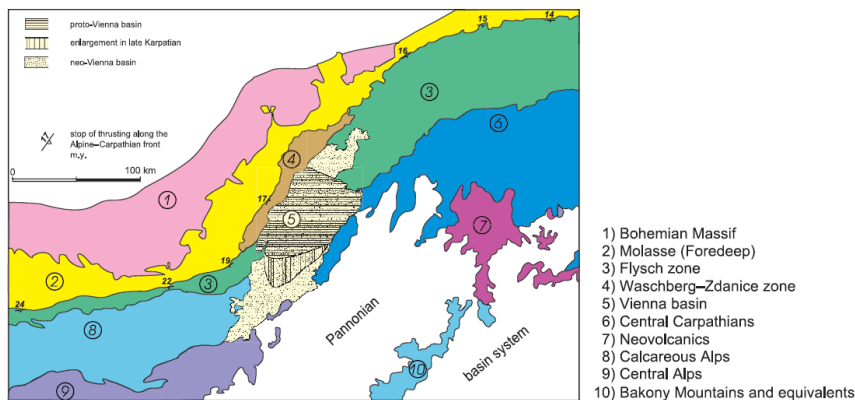


Figure 33: The Vienna Basin in the Alpine - Carpathian thrust belt [73].

This led to a very complex sequence of thrusting, wrenching and normal faulting along the Alpine-Carpathian junction, which is a typical feature of a pull-apart basin [75]. The Vienna basin developed between a system of sinistral transfer faults. The shape of the basin is a rhombohedrum. In the south the basin is bounded by a strike-slip fault system with typical transtensional patterns (e.g. negative flower systems, small pull-apart basins) trending to the northeast. This zone is characterized by increased seismicity [73].

6.1 Zoning

The Vienna Basin consists of three "floors" (distinct sequences, each with a separate structural history). Floor 1 is made up of Neogene sediments, which are an infill upon the subsided Second Floor. Floor 2 consists of allochthonous Alpine-Carpathian thrust sheets, which are thrust over the Third Floor. Floor 3 is the autochthonous Tertiary and Mesozoic basement cover [76]. The cross-section is shown in fig.34.

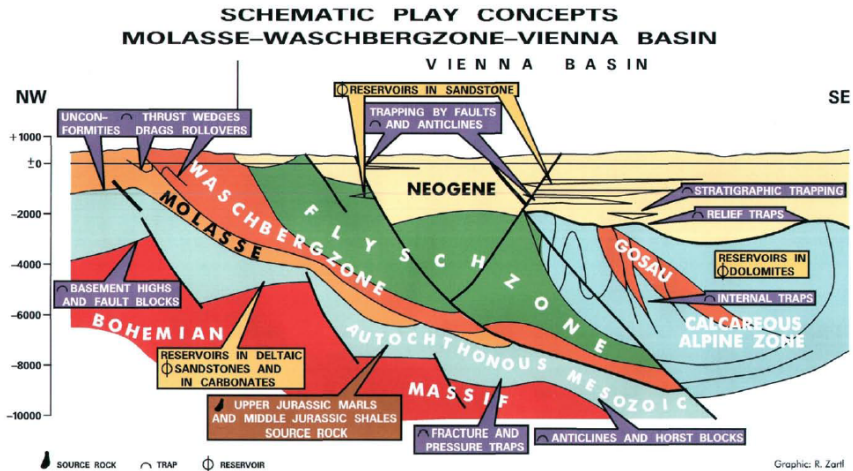


Figure 34: Generalized cross-section of the Vienna Basin. Note that the wells, which will be discussed in the last chapter all produce from the calcareous alpine zone [76].

Floor 1 was discovered the earliest and contributes to the highest amount to oil and gas production. Matzen, the largest field of Central Europe, is also located in that floor [76].

Shales, sands, and conglomerates of open-marine or restricted marine origin in the north were deposited concurrently with shallow-marine or terrigenous sediments along the southern margin of the trough [76].

In the end of the 50s gas was discovered in dolomites of the Northern Calcareous Alpine Zone of the Second Floor [74] [76] [77] [78] [79] [80]. From the western border of the basin to the Carpathians three main thrust units of the Calcareous Alps exist. Each of these units contains gas and oil in fractured Upper Triassic Hauptdolomite or Dachstein Limestone. They are sealed by either Miocene marls (such as in the Aderklaa Tief, Schoenkirchen Tief, Prottes Tief and Baumgarten fields) or by internal cap rocks (such as Schoenkirchen-Gaenserndorf Uebertief). The first, called relief deposits (buried hills), produce from depths up to 2,600 m, while the latter, called internal deposits, were encountered between 5,000 m and 6,350 m depth [76].

As all stimulated wells analyzed in this paper were producing from Floor 2, this floor will be discussed in more detail in the next chapter.

Floor 3, which is the lowermost one, requires ultradeep drilling into depths of at least about 5000m to 8500m. Malmian marls provide a large source rock potential. Oil and gas while drilling prove a supply of free hydrocarbons [76].

continental collision by the end of the Eocene. The Calcerous Alps have the highest reservoir potential of the units of the second floor, which ranges stratigraphically from Permoskythian to Paleocene. They are dominated by Middle to Upper Triassic limestones and dolomites. Their primary thickness goes up to several thousand meters. The stratigraphic profile can be found in tbl. A - 2. The most important reservoir rock for hydrocarbons is the Norian Hauptdolomite [73].

Along the northwest border the frontal and tectonically deepest element is the intensively deformed Frankenfels–Lunz nappe. Its master unit is the Bajuvarikum.

The Giesshubl Gosau overlies unconformably folds and internal secondary thrusts of the Frankenfels-Lunz nappe. Its time span ranges from Upper Cretaceous to Paleocene. The Upper Cretaceous varies from river-dominated facies with conglomerates (>1000 m; >3300 ft) to marine facies with sands and marly limestones. The Paleocene was deposited in deep-water, in an environment similar to the Flysch. The rocks, formed in that age, act as a seal rock of the internal reservoirs. The Goller nappe, which belongs to the Tirolikum, overthrusts the Giesshubl Gosau. This nappe carries the Glinzendorf Gosau as a postdeformational layer group. Its stratigraphy is from the Upper Cretaceous only and shows a variety of different facial settings from predominantly limnic to shallow-marine and even minor, open-marine deposits. *The tectonically highest structures are a deep-reaching syncline and an isolated body of Lower to Middle Triassic. The syncline consists mainly of Wetterstein (Ladinian) and Dachstein limestone (Norian). The Triassic rocks are piled up against the Glinzendorf Gosau in the area of Tallesbrunn. Accordingly, these structures are equated to the Tirolikum system outside the basin [73].*

In the south (southwest), on the rear side, the Calcareous Alps show a sedimentary contact to their former Paleozoic basement. The wedge-shaped sliver consists mainly of low metamorphic, terrigenous layers and is therefore of minor interest in an exploratory sense. The Greywacken zone ends at the Slovak part of the basin without any comparable continuation further to the northeast [73].

Most of the hydrocarbons are stored in central highs, with Hauptdolomite, which is from the Upper Triassic, being the main reservoir rock. These dolomites reach thicknesses of up to 500m. The hydrocarbons are trapped by relief- or thrust internal traps, which developed in the imbricated system [73].

For the first type, Neogene marls act as a cap rock, whereas for the second, tight sediments of the Calcareous Alpine complex (Cretaceous to Paleocene shales and sandstones) seal the reservoirs. The Schönkirchen Tief and Prottes Tief oil- and the Aderklaa, Baumgarten, Zavod, and Borsky Jur gas fields are relief pools, whereas the Schönkirchen Übertief, Reyersdorf, and Aderklaa Tief gas fields are internal traps. Remarkably, the gas derived from the internal reservoirs is sour gas. Schönkirchen is of particular importance, because

the Schönkirchen Tief pool is the second largest oil reservoir, and Schönkirchen Übertief is the second largest gas reservoir of Austria [73].

Whereas in the beginning oil and gas were produced only from Floor 1 the importance of the second floor is increasingly rising [73]. The Strasshof Tief wells discussed in the next sections are all producing from that floor. The geological section through the Vienna Basin and its pre-Neogene floor is illustrated in fig. A - 1.

7 Stimulation of Carbonates in OMV Austria

The pre-design workflow of carbonate acidizing is summarized in the decision tree below:

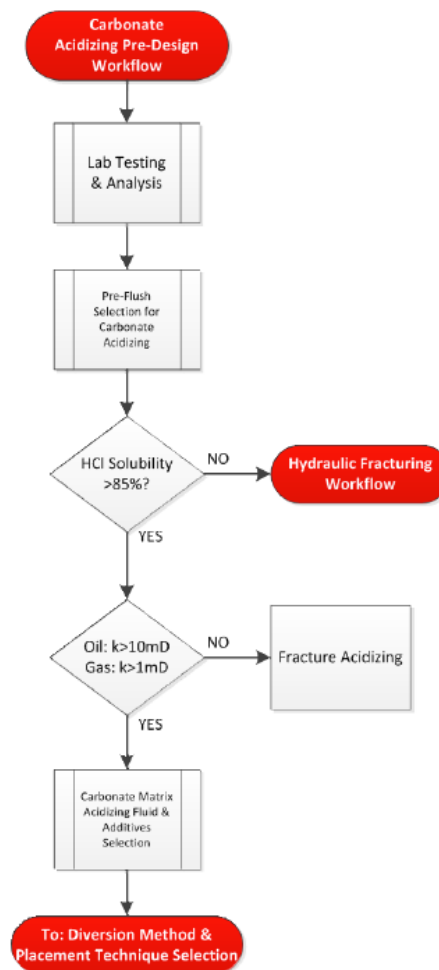


Figure 36: Carbonate acidizing pre-design workflow. The criteria, whether to matrix acidize or fracture acidize is based on permeability [82].

The first step to a successful carbonate acidizing treatment is to carry out necessary lab testing in order to determine the optimum type and concentration of acid to be used during the treatment. Tests include:

- ▶ Mineralogy analysis
- ▶ Acid solubility
- ▶ Acid etching
- ▶ Rotating disk

The main criteria to select the type of stimulation in carbonates are acid solubility and formation permeability. In general, in carbonates with an acid solubility smaller than 85%, hydraulic fracturing is applied. If additionally, permeability of oil and gas is greater than 10 and 1mD respectively, acid fracturing is used, if they are lower than the benchmark, carbonate matrix acidizing is selected. These rules of thumb are commonly used but can vary depending on reservoir conditions. In the next step acid type and pre-flush are designed and the necessary additives must be selected [82]. The principles are the same as already discussed or are explained in the MSc thesis of Rodriguez Chavez [83].

The selection of the diversion method or the placement technique also does not differ of that explained in the theory section (chapter 2.5.3.)

7.1 Main reservoirs in OMV Austria

The main carbonate reservoirs of the Vienna basin are in the rock formations of the Northern Calcerous Alps. The so far discovered fields, including their reservoirs, type of produced hydrocarbons and start of production are summarized in tbl. A - 3.

The only field, which is still producing is Matzen. Figure 37 shows all the current producing carbonate reservoirs.

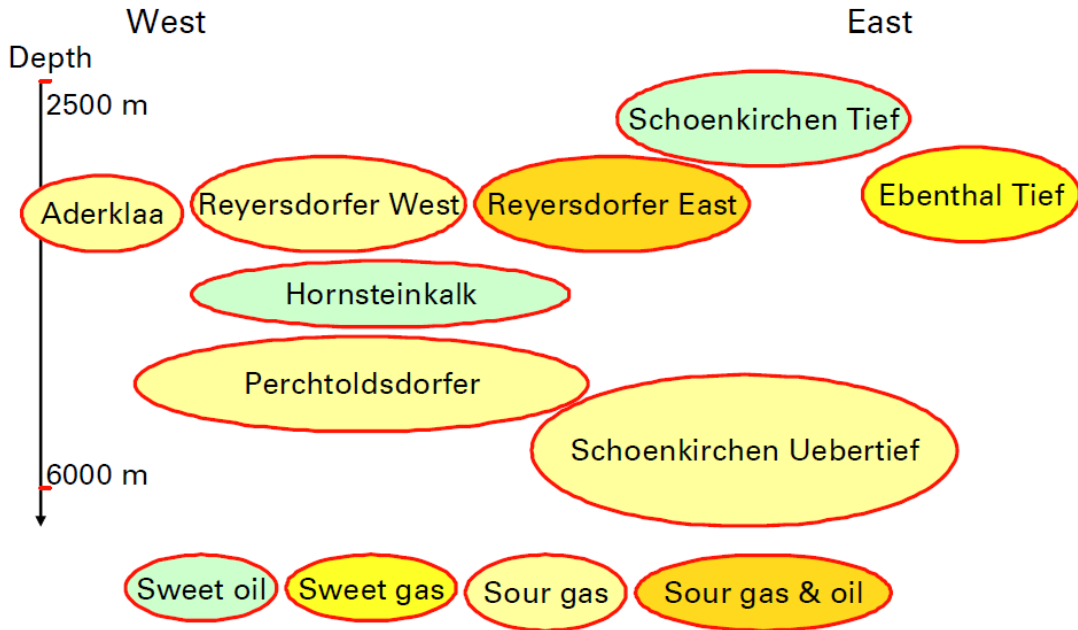


Figure 37: Current producing carbonate reservoirs. The hydrocarbon type and the location is illustrated [84].

Schoenkirchen Tief (A015-800-10) is the best producing sweet oil reservoir of the entire basin. It has a weak aquifer, excellent permeabilities up to several Darcies and a good interconnection between the different parts of the reservoir.

Prottes Tief, Prottes Tief Sued and Prottes Tief West are connected with the same underlying aquifer. Schoenkirchen Uebertief (A015-635-10) is a volumetric sour gas reservoir. The three wells, S T 32, S T 42 and S T 62, located close to each other, produce OMV's deepest reservoir. It has good permeabilities of around 200 mD and its parts are interconnected well.

Ebenthal Tief (A015-800-50) is a highly permeable sweet gas reservoir with a weak aquifer or maybe even volumetric behavior. The Eastern Reyersdorfer Dolomite is an oil reservoir (46 m oil column thickness) with a large gas cap of ~400 m height and a good aquifer support. Since the 1980s the last well S T 38a produces the gas cap. The permeability of ~50 mD is sufficient for a stable gas production. The Western Reyersdorfer Dolomite (A015-800-16) is comparable in aquifer drive, permeability and gas composition, but may be more compartmentalized.

Since 2005 several new reservoirs were discovered, which are the Western Reyersdorfer Dolomite (A015-800-16), the Perchtoldsdorfer Dolomite (A015-848-16, A015-850-16 and A015-850-17), Ebenthal Tief (A015-800-50), Prottes Tief Sued (A015-800-13) and Prottes Tief West (A015-800-14). Relatively new is also the Hierlatz- / Hornsteinkalk (A015-700-16) formation which is a Jurassic limestone reservoir. Both, Hierlatz- / Hornsteinkalk and

Perchtoldsdorfer Dolomite have probably large HC-volumes, but have a low permeability (<1 mD) and are compartmentalized. Hierlatz- / Hornsteinkalk has sweet oil content, Perchtoldsdorfer Dolomite contains sour gas. Its poor performance is comparable to the already depleted Aderklaa Dolomite reservoirs.

7.2 Division into Areas

In OMV Austria it is produced from 9 different areas, where only 1 is not located in the Vienna basin but in Upper Austria (fig. A - 2& tbl. A - 4). The youngest producing area is Strasshof Tief (Area 13), which was discovered in 2006 by the well STR T4. Its structure is very complex and all its carbonate reservoirs are located in the second floor, which is from the Pre-Neogene. With increasing depth the following reservoirs are encountered (tbl.10) :

Table 10: Production units and reservoir names that the Strasshof wells encounter. The code of the horizon is based on the geological time the rock was deposited (7xx – Jurassic, 8xx – Triassic).

Field-Horizon-Production unit	Reservoir name
A015-800-16	Western part of the Triassic Reyersdorfer Dolomite
A015-700-16	Jurassic Hierlatz-/Hornsteinkalk
A015-848-16	Triassic Rhaetian Perchtoldsdorfer Dolomite
A015-850-16	Eastern Triassic Norian Perchtoldsdorfer Dolomite
A015-850-17	Western Triassic Norian Perchtoldsdorfer Dolomite

Fig. 38 illustrates a schematic cross section of the Strasshof Tief Area and its currently existing wells are shown. In tbl. A - 3 it is illustrated from which reservoirs the wells are producing including their hydrocarbon content.

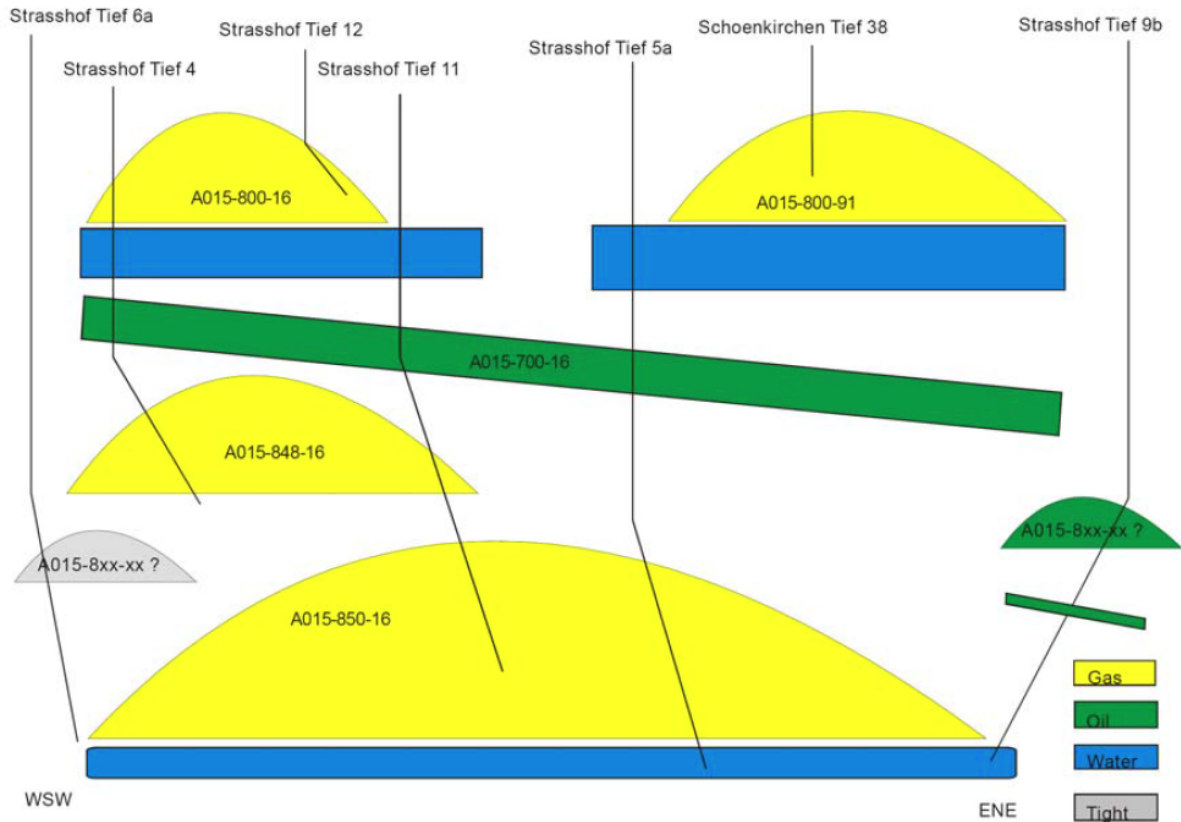


Figure 38: Generalized cross-section of the reservoirs that the Strasshof wells produce from. The kind of the produced media is indicated [84].

7.3 Strasshof Tief 5a

Following the history of the well STR T 5a will be discussed in more detail as it has encountered those zones that are naturally fractured to the highest degree and the acidized section is also very long.

In 2006 the appraisal well STR T 5 found the Norian Perchtoldsdorfer Dolomite (A015-850-16) (illustrated in tbl. A - 5 & fig. A - 4)

It was perforated from 5275-5285 m MD, which yielded in the production of water. A test with an additional perforation from 5050-5080 m MD yielded gas and water (fig.39). Calculations of the GWC gave a value of 5159m MD. Later the lower perforations in the water zone were plugged to decrease the water production.

A well test consisting, of five 12h lasting production periods, indicated a negative skin (no or little formation damage and enhanced production from fractures), a poorly developed radial flow (kh and pressure extrapolation have to be seen with care), a kh product of about 15 to 20 md*m, a calculated average permeability of around 0.7 md, crossflow with the HH-formation (fig.39) 400m above (the initial pressure and the extrapolated average pressure at gauge depth differed by ~30 bar). Pseudo steady pressure did not develop.

Due to the fact that the production liner of STR T5 was very bad the well was plugged-back and technically sidetracked up dip into the Perchtoldsdorfer Dolomite.

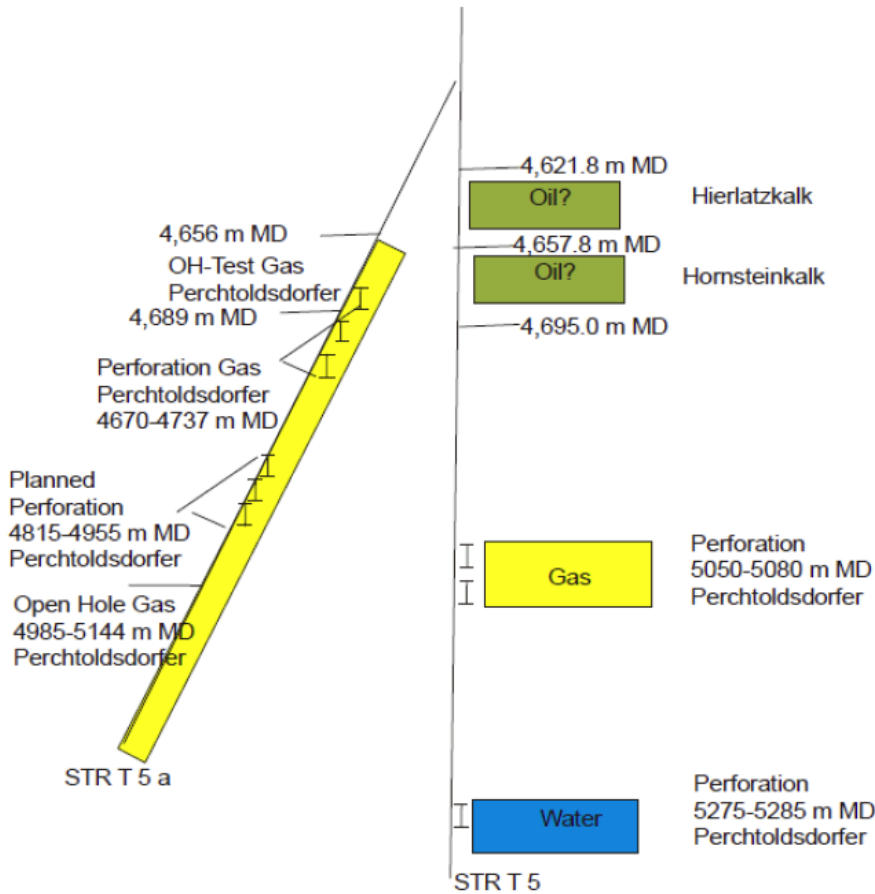


Figure 39: Scheme of STR T 5 and 5a. The kind of formations and fluid contents are shown. Note that the planned perforation from 4815 – 4955 m MD was actually perforated from 4813 – 4885 m MD [84].

In May, 2006 STR T 5a was kicked off below the 9 5/8" casing of STR T 5 to penetrate the Perchtoldsdorfer Dolomite in a structurally updip and therefore better position. An additional target was to gather more reservoir data, such as the GWC, e.g.

The well was drilled to a TD of 4747 m MD GL. An unstimulated open-hole straddle test with a side wall anchor (test interval 4656-4689 m MD) was successfully conducted in the 8 3/8" open-hole section between October and November 2006. As can be seen from the geological cross-section (fig. A -4.) it would make sense that the oil bearing Liassic Hierlatz-Hornsteinkalk formation would extend from the interval in STR 5 to STR T5a. However, except from the water cushion and occasional slugs of mud, no liquids were produced at the surface in the welltest but only natural sour gas and so the tested formation was geologically

revised to be part of the Perchtoldsdorfer Dolomite, A015-850-16. The lithological profile is shown in tbl. A - 6.

The memory gauge data is in tbl. A - 7.

The pressure build-up showed infinite acting radial behavior, with a kh product of 12 mD*m and an average permeability of 0.46 mD. No long term predictions were possible. The gas composition is different from A015-850-16 PD of STR T 5 but similar to A015-848-16 PD of STR T4 (see tbl. A - 8). This may be as the produced amount of gas may have not been large enough to be representative.

After the OH-test, the well was extended to 5400m MD in the same formation and completed as a production well (fig. A - 5). The top view of the trajectory (fig. A - 6), the side view of the trajectory (fig. A - 7) the inclination plot (fig. A - 8) and the dogleg plot (fig. A - 9) are in the appendix.

In November 2006 a welltest was conducted in the open-hole section (4985-5144 m MD) of STR T 5a, which yielded a permeability of 0.9 to 1.3 mD, which is slightly higher but comparable to STR T 5. The results are listed in tbl.11.

Table 11: Well test results

Gauge measurement depth	4643 m MD GL
Bottom hole temperature	145.5 °C
pwf	451 bar-g
pws	480 bar-g
pres	483 bar-g
k*h	150-230 mD*m
s	-2.7
Producible gas (aquifer drive)	1 bn m ³

PLT runs from 4985m MD to 5144m MD in the open-hole have shown that the entire section contributes to dry gas production. The highest deliverability is from 5030-5090 m MD, whereby higher permeable fractures are at 5055-5057 m, 5081 m and 5089-5090 m MD. Influx of free water was not observed. The measurement results from the logs and the inflow distribution measured by the PLT runs are shown in fig. A - 10 & A - 11.

2.5 years later, in February 2009, STR T 5a went on production. Only 45 days later the well started to produce reservoir water. Dynamic PLT runs detected water entry below at about 5040 m MD (fig. A - 12). This is exactly where also some of the more conductive fractures are located.

After that the well was shut-in for a week for pressure build-up. However, the wellhead pressure did not increase as fast as expected and the GWC stayed the same, which should

have been pushed down due to a higher wellhead pressure. The scheme of the well and the water coning is illustrated in fig. A - 13.

It was concluded that this due to the fact that the highest conductive fracture at 5050 m MD is able to transport the reservoir water into the wellbore but the less conductive fractures below are not able to let the water return back downwards after shut-in.

To increase the GWR the well was perforated structurally higher from 4670-4737 m MD in October 2009. Additionally, an HCl wash was conducted.

Further, it was assumed that this would lead to a sharp pressure increase, which was not achieved. This indicates that the perforated interval belongs to the same reservoir as the open-hole section. The gas influx from the two sections is shown in the dynamic temperature log (fig. 40).

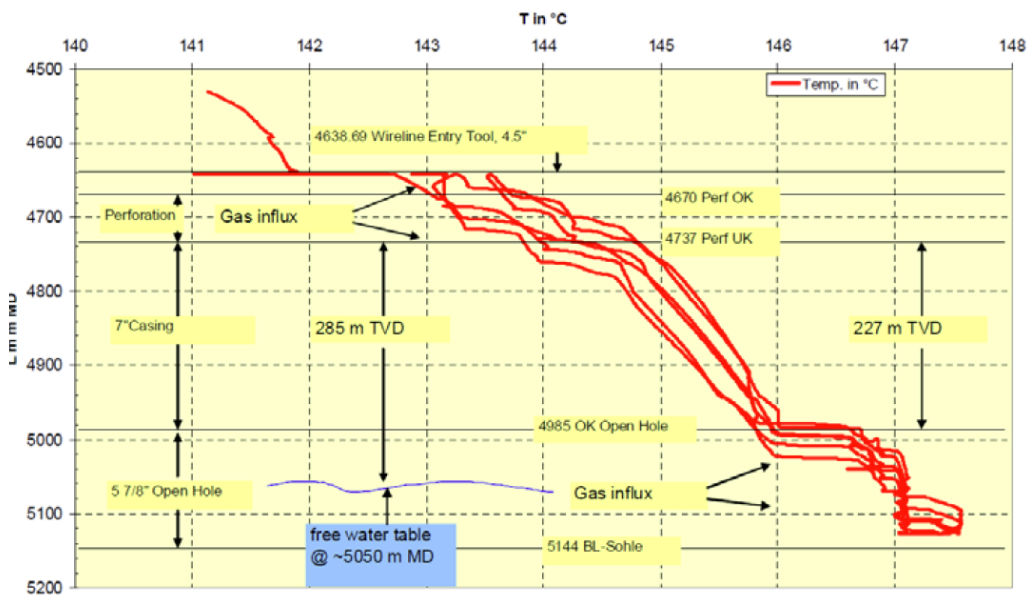


Figure 40: Results of the temperature log. It is surprising that above and below the free water table the influx of gas was observed [84].

From August to December 2009 the well produced with a low, but increasing water cut. To stall this again the open-hole section was closed by a bridge plug, set at 4940 m MD slightly above the casing shoe (4985 m MD). The impact of the perforation and the shut-off of the open-hole on production and pressure can be seen in fig. 41.

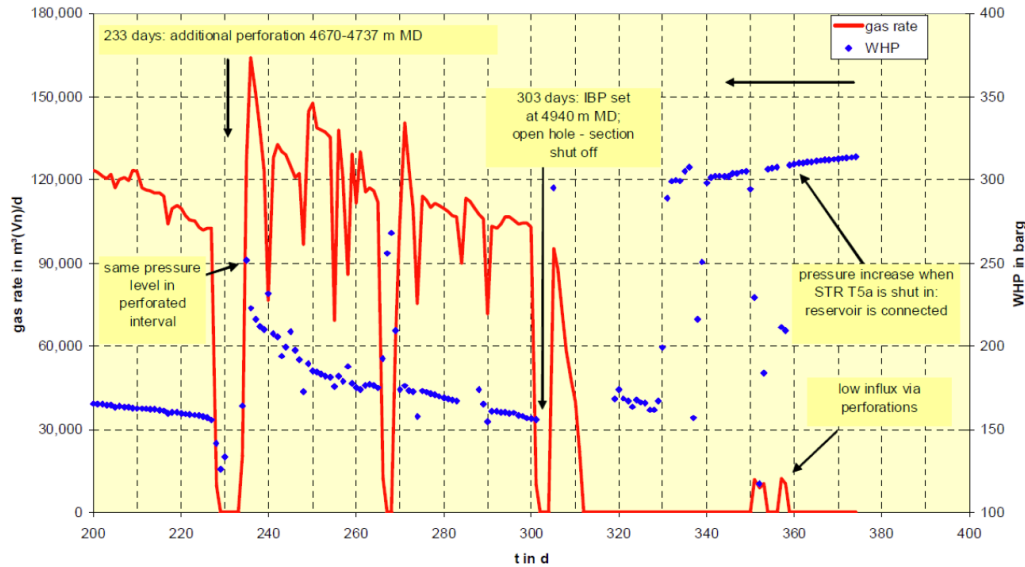


Figure 41: Wellhead pressure and gas rates. The well was additionally perforated in October 2009 and shut-in again in December [84].

As illustrated in fig.41 the shut-off yielded in a declining rate and pressure which made further perforations and stimulations of the dolomite horizons with HCl necessary.

In June 2010 it was additionally from 4814-4829 and 4865-4885 m MD perforated. Afterwards it was stimulated with an HCl blend.

The scheme of the completion is shown in fig. A - 14.

In November 2011 it was acidized again to increase production. This time a similar blend but more than twice the volume was taken (tbl.13). It is remarkably that although the section is very long (88 m) and is also fractured no diverters or retarders were used. This led to an increase in gas- but also water production which was the highest in 2013. This may be a result of the acid flowing very well along the fractures, connecting them to an underlying aquifer. Still, compared to the foregoing stimulation in the same section with a similar acid recipe only 1.5 years ago there was a much a higher improvement in production.

Finally, the production from the perforated section was only intermittent with a high water cut. As a consequence, in January 2014 the perforations of STR T 5a were finally plugged and the lower open-hole section opened again. As this section previously has shown to have a high gas production but also a high water inflow from the fracture system a multizone completion was planned.

The multizone completion is as follows: 3 ½ tubing with swelling packers (from/to):

- 5018 – 5027 m
- 5045 – 5054 m
- 5076 – 5085 m
- 5100 – 5109 m

Between those packer sections SSDs were installed to get access to the open-hole section. The schematic of the current installed multizone well is illustrated in fig. A - 15. The general wellbore information including reservoir and well data is listed in tbl. A - 9 & A - 10.

After running the tubing string it was tested with slick-line and test equipment. The stimulation procedure was the following: all SSDs were closed except the bottommost where the HCl blend was injected. It was proceeded by closing the SSD of the already stimulated section and to acidize the next one until all intervals were treated. Finally, each interval was cleaned selectively and tested. The ultimate target was not only to treat selectively all intervals to guarantee a uniform coverage of the 88m section, but what was even more important to find an optimum SSD-constellation for a high gas production and a low water cut.

As all zones except the uppermost one yielded a high water inflow, currently the lower 3 SSDs are closed.

7.4 Evaluation of the stimulation treatments in STR T5a

In general, the acid recipes in stimulation treatments in the Vienna basin are a 15%-, 20%- or 28% HCl – acid system. The used recipes are summarized in tbl.12.

Table 12: The composition of the 28%-, 20%- and 15%- HCl acid system is shown.

HCl	28 %	20 %	15 %
Citric Acid (iron control)	5 %	3.6 %	2 %
A 201 (85% Formic Acid as Stabilizer for Cronox)	3.6 %	3.6 %	3.6 %
Cronox 242 ES (corrosion inhibitor)	2 %	2 %	2 %
A 255 (H ₂ S scavenger)	0.2 %	0.2 %	0.2 %
Non-ionic surfactant (e.g. Sapogenat)	optional	optional	optional
Mutual Solvent	optional	optional	optional

As explained, from 2006 to 2014 five acid stimulation treatments were performed. As the fracturing pressure was in none of the treatments exceeded the treatments are classified as matrix acidizing or acid washes (treatment 1 & 2). The stimulated intervals, the used acid recipe and volumes are summarized in tbl.13.

Table 13: General data of the acid treatments.

Treatment	Date	Treated interval [m MD]	Recipe	Volumes (KCl-preflush/ acid solution/KCl-postflush) [m ³]
1	28.10.2006	4985-5144 (OH)	24% HCl 2% Cronox 0.4% SCA 130	0/55/5
2	08.10.2009	4670-4690 (CH) 4697-4717 (CH) 4724-4737 (CH)	15 % HCl 2% Citric Acid 2% Cronox 3.6% Acetic Acid	0/24.1/2.2
3	11.06.2010	4670-4690 (CH) 4697-4717 (CH) 4724-4737 (CH) 4813-4828 (CH) 4865-4885 (CH)	15 % HCl 5% Citric Acid 2% Cronox 3.6% Acetic Acid 0.5% Sapogenat	0/96.1/17.1
4	09.11.2011	4670-4690 (CH) 4697-4717 (CH) 4724-4737 (CH) 4813-4828 (CH) 4865-4885 (CH)	20 % HCl 2% Cronox 20% Acetic Acid 0.5% Sapogenat	5/196.8/41.3
5	13.-17.1.2014	4985-5144 (OH) selectively	20% HCl 2% Citric Acid 3.6 % A201 2% Cronox 0.2% M295"	0/190/0

Treatments 1, 2 and 5 were squeezed through 1.9" coiled tubing, the treatments 3 and 4 bullheaded through 4 ½ " production tubing.

In order to evaluate the success of the operations a technical and an economical evaluation was conducted. The production history and the time of the treatments 2 to 5 is shown in fig. 42.

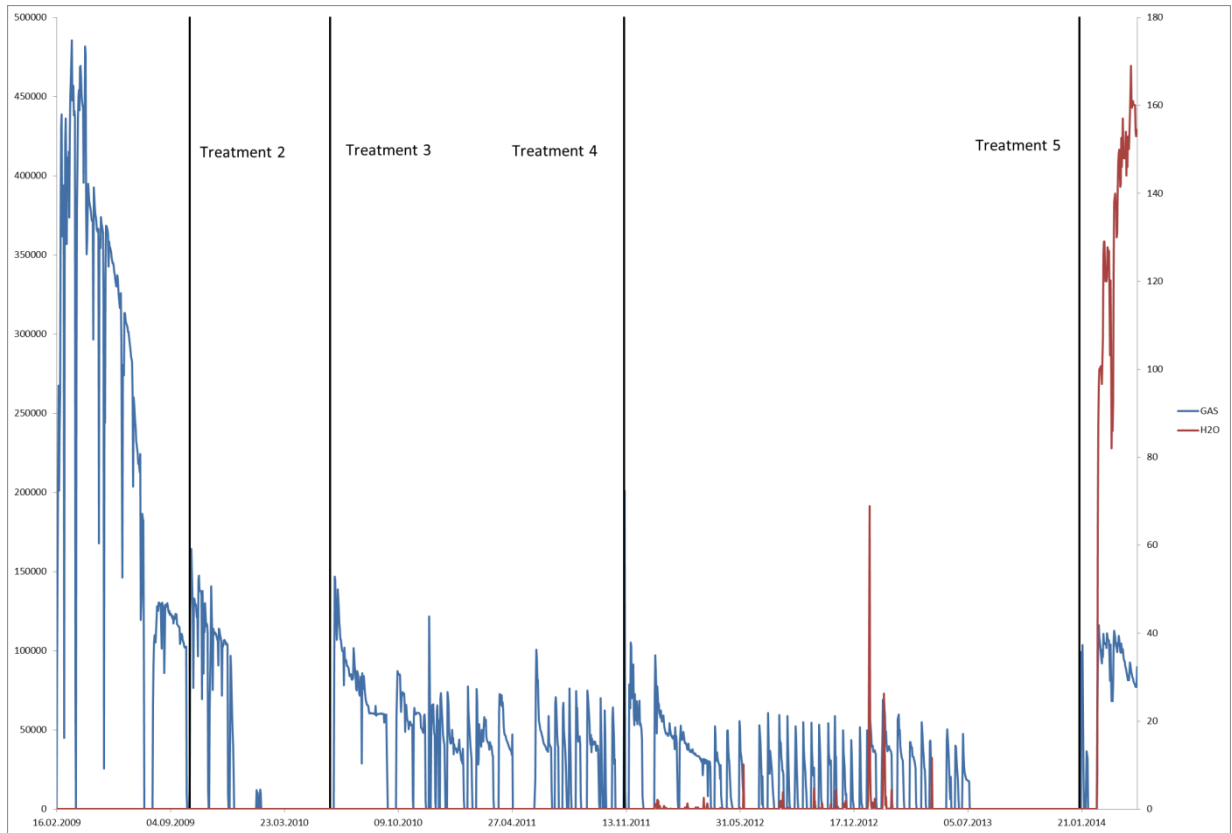


Figure 42: Production history of Strasshof Tief 5a from 2009 to April 2014. After each treatment gas production increased but only few months later decreased again. Note that the water rate is not accurate as it was not recorded every day.

7.4.1 Technical evaluation

The technical evaluation was performed by calculating the improvement in injectivity during the acid treatment.

The injectivity parameter is defined, as follows:

$$II\left[\frac{m^3}{bar \times day}\right] = \frac{Q\left[\frac{m^3}{day}\right]}{p_{wf}[bar] - p_e[bar]}$$

With this equation the improvement in injectivity was calculated:

$$Injectivity\ Improvement[\%] = \frac{II_{final} - II_{initial}}{II_{initial}}$$

The initial values for each parameter were derived, when the acid was hitting the formations, the final ones when it was started to pump the KCl-postflush-solution, which is the point in time when the acid reaction was almost completed. In general, in a success case the injection rate increases whereas the wellhead pressure decreases during the treatment.

Treatments 1 to 4 all yielded in an injectivity improvement, and in treatment 5 each, except one of the four selectively treated sections showed an improvement in injectivity and so are regarded as technical success cases. The treatment graphs, including injecting rate, wellhead pressure and well flowing pressure for all treatments are in figures A - 17 to A - 23. The results of the technical evaluation are in table A - 12.

7.4.2 Economical Evaluation

However, the economical evaluation is more complicated than the technical one as the conditions have to be compared before- and after the stimulation treatment. As a consequence, there must already be an existing production history and the well must not have been re-perforated within the same work-over or shortly before the stimulation treatment. The perforation history of STR T 5a is summarized in tbl. A - 11.

The first perforation was conducted only shortly after treatment 1. Because of this the economical evaluation is not possible. One day before treatment 2 and 3 an additional section was perforated respectively. Consequently, only treatment 4 can be economically evaluated. This is achieved by comparing the average gas production rate (GR) over X months before and after the stimulation. The following two parameters were calculated:

$$Production\ Improvement\ (\%) = \frac{Post\ stimulation\ GR - Pre\ stimulation\ GR}{Pre\ stimulation\ GR} \times 100\%$$

The results are provided in table A - 12. As can be seen treatment 4 was a technical as well as an economical success. However, none of the treatments can be regarded as a full success, as the gas rate improvement lasted in each treatment only for a short timespan as indicated in fig. 42.

The results of the economical evaluation are in table A - 12.

8 Findings and Conclusion

- The evaluation of data was in certain instances not possible and the subsequent interpretation of the results was subject to error. For example, for some time frames water production was not recorded at all. The calculation of the Injectivity Index by the OMV-intern software program was wrong, as no value for the reservoir pressure was inserted and the unit of the flow rate was liters per minute and not cubic meters per day.
- In none of the treatments a diverting system was used, although the shortest treatment length was 15m and the longest one even more than 159m. The general rule of thumb, explained in the theoretical part, states that treated sections, longer than 6m, benefit from using a diverting system. This is even more crucial in the STR T 5a well, as the treated intervals have high permeability contrasts, as the rocks are naturally fractured carbonates.
- It was only possible to do an economic analysis for the fourth treatment as in the other ones the producing length was different from pre- and post-stimulation.
- Treatments 3 and 4 are the only ones in which the same completion was installed and the same interval was acidized. This made them comparable and based on this, the effects of the acid recipe and the volume of the injected acid system can be investigated.
- Treatment 4 was a success as gas rates improved dramatically afterwards. Treatment 2 failed, as the gas rates even decreased and so the acidizing job must have caused additional damage to the formation.
- In treatment 4 higher acid concentrations were used. But what possibly had a more significant effect was that more than twice the volume was injected (196.8 m^3 compared to 91.6 m^3). Further the fact that 20% acetic acid was used could have added to this success as the high concentration of weak acid acts as a retarder.
- The injected acid probably only flowed along the most permeable fractures because no diverters were used. This is reflected in the production behavior afterwards. The rate increases significantly after the stimulation but drops very fast (1-2 months) to the initial situation before the acid treatment. This is most likely due to the fact that the acid cleaned and partly also etched some fractures. The temporary high production rate afterwards is because the treated fractures have a high conductivity but only a low storage volume for hydrocarbons.
- In the treatments 3 and 4 it was injected with the highest rates, which is of importance as a higher penetration distance and deeper wormholes can be created. This is due to the fact that it was not pumped through coiled tubing, which is rate limited at 300 l/min, but bullheaded instead.
- It seems that only in 2009 the workover or kill fluids had been circulated out of the wellbore. This probably additionally damages the formation.

- The permeability of the formation is very low and the OMV intern decision tree would recommend a fracturing technique. However, in all treatments it was either matrix acidized or acid washed.

9 Recommendations

- Drilling induced damage should be avoided if possible.
- The quality of the data recording must be improved and standardized in order to make a better and easier evaluation of the jobs possible. Further, bottomhole gauges are advised. For example, it would be possible to directly measure the well flowing pressure instead of correlating it, which reduces the amount of possible errors. Additionally, the impact of the acid on the formation can be observed precisely.
- For increasing data quantity and quality, pre- and post-treatment logs, such as PLT runs or temperature logs, are helpful and aid in the evaluation of the acid job.
- As the thesis by Rodriguez Chavez [85] has shown, in order to achieve a successful acid treatment, it is important to circulate the kill fluid out of the borehole, instead of displacing it into the formation. A kill fluid that has remained downhole for some time might chemically react. This alteration could cause troubles in the subsequent acid job. Therefore, the pickling stage is an important contributor to successfully stimulate the well.
- Retardation should be considered to a higher degree as it not only aids in achieving deeper penetration but also creates more wormholes.
- In intervals longer than 6 meters a diversion system is critical in order to achieve a uniform coverage. A standard procedure would be the use of gelled acid which furthermore also retards the acid (higher penetration distance) and improves the fines suspending properties. The viscosity can be further increased by crosslinking the gelled acid. This kind of stimulation treatment was successfully applied in the Warren Unit between New Mexico and Texas, e.g. However, disadvantages are increased pressure losses due to higher friction but also an additional formation damage as a sufficient cleanup might be hard to achieve. An alternative, which is also standard in the oil industry are ball sealers or the use of mechanical packers to selectively stimulate the formation. Drawbacks of ball sealers are that first, it is critical to maintain a constant pressure difference between the treated section of the wellbore and the formation in order to keep the ball sealers in place. Second not all ball sealers might be recovered and third more surface equipment is needed to store the ball sealers. Disadvantages regarding mechanical packers are the long time required for such an operation, which leads to high costs. Further it is in some cases necessary to kill the well in order to release the packer after the stimulation, which damages the formation.

- A new, sophisticated technique is the viscoelastic surfactant acid system, where fibers are added. It combines mechanical and chemical diversion. It has only a high viscosity during the acid reaction, which enhances acid coverage. The pumping of the acid and cleanup is not a problem due to a low viscosity in that stage. Field cases in Kazakhstan have proven that it can also be successfully applied in high temperature (up to 120 °C), high pressure (up to 95 MPa) sour gas wells. The results were very promising as the producing length and the production rate were significantly increased, whereas treatment time and skin were decreased. Further it was shown that this system is superior to common used stimulation designs.
- Foaming the acid is also a possibility for increasing the viscosity and guaranteeing a uniform coverage. They are perfectly suited for low pressure- or gas wells and have several advantages such as being reusable, shear stable and stable over a wide temperature range. However, several field cases have indicated that they are inferior to viscoelastic surfactant acid treatments or water-fracturing.
- Fracturing might be an option as formation permeability is very low. This requires sufficient data gathering as several factors have to be pondered whether an acid fracturing or a propped fracturing treatment would be the better choice.
 - Factors suggesting acid fracturing are:
 - a predominantly naturally fractured carbonate formation, potentially leading to propped-fracture complications
 - a heterogeneous formation, with porosity and permeability streaks, that are conducive to a higher degree of differential acid etching of the fracture walls
 - good formation permeability, but with existing formation damage
 - a well that will not mechanically accept proppant
 - Factors suggesting propped fracturing are:
 - low HCl solubility (<65-75%)
 - a homogeneous carbonate formation (e.g., pure limestones)
 - low acid reactivity (e.g., low-temperature [<66 °C] dolomites)
 - significant softening or creeping of rock under the closure after contact with acid, resulting in poor retention of acid-etched fractures
- In recent years new stimulation techniques without diversion agents emerged. The acid tunneling technique has proven its efficiency in countless field cases worldwide. It can only be used in open-hole completions. No limitations were found and it has also been used at very high temperatures. In order to reduce rapid spending a hydrochloric – acetic blend was pumped. This technique would have been perfectly suited for the open-hole stimulations of the treatments 1 and 5 in Strasshof Tief 5a. Moreover, it was reported that treatment costs are lower than in conventional acid jobs.

References

- [1] F.O. Stanely, SPE; L.N. Portman, SPE; J.D. Diaz, SPE; R.L. Darmawan, SPE; J.P. Strasburg, SPE; J.S. Clark, SPE; M.S. Navarro, BJ Services Company, „Global Application of Coiled-Tubing Acid Tunneling Yields Effective Carbonate Stimulation,“ SPE 135604, Florence, 2010.
- [2] M.A. Siddiqui, KOC, SPE; S.S. Sharma, KOC; M.F. Al-Ajmi, KOC, SPE; M.O Hassan, KOC; F.H. Ashkanani, KOC, SPE; Z.A. Al-Bahar, KOC, SPE; H. Zaki, KOC, SPE; L. Lounas, Baker Hughes, Kuwait, SPE, „Enhance of Oil Production from an Old Well in Thin Carbonate Reservoir through Acid Tunneling,“ SPE 164876, London, 2013.
- [3] R. Arangath, SPE, Schlumberger; K.W. Hopkins, Aral Petroleum Capital; D. Lungershausen, Zhaikmunai LLP; N.T. Bolyspayev, SPE, Schlumberger, "Successful Stimulation of Thick, Naturally-Fractured Carbonates Pay Zones in Kazakhstan," SPE 112419, 2008.
- [4] K.S. Asiri, M.A. Atwi, Saudi Aramco; O.J. Bueno, Pemex; B. Lecerf, A. Pena, T. Lesko, F. Mueller; A. Z.I. Pereira, Petrobras; F. T. Cisneros, „Stimulating Naturally Fractured Reservoirs,“ *Oilfield Review*, Bd. 25, Nr. 3, pp. 4-17, 2013.
- [5] L. Kalfayan, Production Enhancement With Acid Stimulation, Oklahoma: PennyWell Corporation, 2008.
- [6] H.A. Nasr-El-Din, Saudi Aramco; R. Tibbles, Schlumberger; M. Samuel, Schlumberger, „Lessons Learned from Using Viscoelastic Surfactants in Well Stimulation,“ SPE90383, Houston, 2004.
- [7] Nierode, D.E.; Williams, B.B., „Characteristics of Acid Reaction in Limestone Formations,“ Society of Petroleum Engineers, 1971.
- [8] B.B. Williams, Esso; J.L. Gidley, Exxon; R.S. Schechter, University of Texas, „Acid Fracture Fundamentals,“ in *Acidizing Fundamentals*, New York, SPE, 1979, p. 33.
- [9] C.N. Fredd; M.J. Miller, „Validation of Carbonate Matrix Stimulation Models,“ SPE 58713, Lafayette, 2000.
- [10] M.L. Hoefner, H.S. Fogler, „Pore Evolution and Channel Formation During Flow and Reaction in Porous Media,“ *AIChE J.*, Bd. 1, Nr. 34, pp. 45-54, 1988.
- [11] G. Daccord; R. Lenormand; O. Lietard, „Chemical Dissolution of a Porous Medium by a Reactive Fluid,“ *Chemical Engineering Science*, Bd. 1, Nr. 48, pp. 169-189, 1993.

- [12] C.N. Fredd; R. Tija; H.S. Fogler, „The Existence of an Optimum Damköhler Number for Matrix Stimulation of Carbonate Formations; SPE 38167,“ in *SPE European Formation Damage Control Conference*, The Hague, 1997.
- [13] C. Crowe, „Evaluation of Acid Gelling Agents for Use in Well Stimulation,“ *Society of Petroleum Engineers Journal*, 1981.
- [14] Norman, L.R., „Properties and Early Field Results of a Liquid Gelling Agent for Acid,“ in *Society of Petroleum Engineers Production Technology Symposium*, Hobbs, NM, 1978.
- [15] M. Zerboub; K. Ben-Naceur; E. Toubul; R. Thomas, „Matrix Acidizing: A Novel Approach to Foam Diversion,“ SPE 22854, Washington DC, 1992.
- [16] M. Parlar; E.B. Nelson; I.C. Walton; E. Park; V. Debonis, „An Experimental Study on Fluid-Loss Behavior of Fracturing Fluids and Formation Damage in High-Permeability Porous Media,“ SPE 30458, Dallas, 1995.
- [17] F.F. Chang; R.L. Thomas; D.K. Fu, „A New Material and Novel Technique for Matrix Stimulation in High-Water-Cut Oil Wells,“ SPE 39592, Lafayette, 1998.
- [18] R. Arrangath; J.F. Obamba; P. Saldungaray; H. Malonga, „Stimulating High Water Cut Wells: Results from Field Applications,“ SPE 99419, Tulsa, 2006.
- [19] M. Al-Mutawa, E. Al-Anzi, M. Jemmali und M. Samuel, „Polymer-Free Self-Diverting Acid Stimulates Kuwaiti Wells,“ *Oil & Gas Journal*, pp. 39-42, 2002.
- [20] G.R. Coulter; A.R. Jennings Jr., „A Contemporary Approach to matrix Acidizing,“ SPE 38594, San Antonio, 1997.
- [21] R.D. Gdanski; W.S. Lee, „On the Design of Fracture Acidizing Treatments,“ SPE 18885, Oklahoma City.
- [22] A.W. Coulter; C.W. Crowe; N.D. Barrett; B.D. Miller, „Alternate Stages of Pad Fluid and Acid Provide Leakoff Control for Fracture Acidizing,“ SPE 14654, New Orleans, 1976.
- [23] Z. Rahim, H. A. Al-Anazi, A. A. Al-Kanaan, A. H. Habbtar, A. M. Al-Omair, N. H. Senturk, D. Kalinin, „Productivity Increase Using Hydraulic Fracturing in Conventional and Tight Gas Reservoirs – Expectation vs. Reality,“ *Saudi Aramco Journal of Technology*, pp. 28-39, 2012.
- [24] T. Bratton; D. V. Canh and N.V. Que, Cuu Long Joint Operating Company; N.V. Duc, Viet SovPetro; P. Gillspie and D. Hunt, Hydro; B. Li, Ahmadi; R. Marcinew and S. Ray; B. Montaron; R. Nelson, Broken N Consulting; D. Schoderbek, ConocoPhillips; L. Sonneland, „The Nature of Naturally Fractured Carbonates,“ *Oilfield Review*, 2006.

- [25] W. Narr, D. Schechter und L.B.Thompson, Naturally Fractured Reservoir Characterization, Richardson: Society of Petroleum Engineers, 2006.
- [26] R. Nelson, Geological Analysis of Naturally Fractured Carbonates, Houston: Gulf Publishing Co., 2001.
- [27] L. Reiss, The Reservoir Engineering Aspects of Fractured Formations, Houston: Gulf Publishing Co., 1980.
- [28] L. Elkins, „Reservoir Performance and Well Spacing, Spraberry Trend Area of West Texas,“ in *AIME, Trans.*, 1953, pp. 177-195.
- [29] <http://www.naturalfractures.com>, 2014.
- [30] D. Stearns und M. Friedman, „Reservoirs in Fractured Rock,“ in *Stratigraphic Oil and Gas Fields Classification, Exploration Methods and Case Histories*, Tulsa, American Association of Petroleum Geologists, 1972, pp. 82-106.
- [31] A. Yamaji, „Faulting and Brittle Strength,“ in *An Introduction to Tectonophysics - Theoretical Aspects of Structural Geology*, Kyoto, TERRAPUB, 2007, pp. 131-152 .
- [32] T. Engelder, Stress Regimes in the Lithosphere, Princeton: Princeton University Press, 1993.
- [33] D. Pollard und A. Aydin, „Progress in Understanding Jointing over the Past Century,“ Bd. 8, pp. 1181-1204, 1988.
- [34] M. Gross, „The Origin and Spacing of Cross Joints: Examples from the Montgomery Formation,“ *Journal of Structural Geology*, Bd. 6, Nr. 15, pp. 737-751, 1993.
- [35] N.E.Odling, P.Gillespie, B.Bourgnie, C.Castaing, J.P.Chiles, N.P.Christensen, E.Fillion, A.Genter, C.Olsen, L.Thrane, R.Trice, E.Aarseth, J.Walsh und J.Watterson, „Variations in Fracture System Geometry and Their Implications for Fluid Flow in Fractured Hydrocarbon Reservoirs,“ *Petroleum Geoscientist*, Bd. 5, Nr. 4, pp. 373-384, 1999.
- [36] N. James und P. Choquette, Paleokarst, New York City: Springer-Verlag, 1988.
- [37] J. Mylorie und J. Carew, „Unconformities in Carbonate Strata - Their Recognition and the Significance of Associated Porosity, AAPG Memoir,“ in *Karst Development on Carbonate Islands*, pp. 55-76.
- [38] C. Hill, „Origin of Caves in Capitan,“ in *Concepts in Sedimentology and Paleontology: Geologic Framework of Capitan Reef*, 1999, pp. 211-222.

- [39] D.N. Meehan, S. Verma, „Integration of Horizontal Well Log Interpretation in Fracture Reservoir Characterization,“ SPE 24697, Washington DC, 1992.
- [40] R. Nelson, L. Lenox und B. Ward, „Oriented Core: Its use, error, and uncertainty,“ *AAPG Bull.*, Bd. 71, pp. 357-367, 1987.
- [41] D. Ragan, *Structural Geology: An Introduction to Geometrical Techniques*, New York City: Wiley, 1985.
- [42] P. S. M.A. Lackie, „Drill Core Orientation Using Paleomagnetism,“ *Exploration Geophysics*, Nr. 24, pp. 609-614, 1993.
- [43] F. D. E.A. Hailword, „Paleomagnetic Reorientation of Cores and the Magnetic Fabric of Hydrocarbon Sands,“ *Paleomagnetic Applications in Hydrocarbon Reservoir Sands*, Nr. 98, pp. 245-257, 1995.
- [44] B. Kulander, S. Dean und B. Ward, „Fractured Core Analysis: Interpretation, Logging , and Use of Natural and Induced Fractures in Core,“ *AAPG Methods in Exploration*, Bd. 8, 1990.
- [45] D. Haller und F. Porturas, „How to Characterize Fractures in Reservoirs Using Borehole and Core Images: Case Studies,“ in *Core-Log Integration*, London, Geological Society, 1998, pp. 249-259.
- [46] P. S. S.M. Ltuhi, „Fracture Apertures from Electrical Borehole Scans,“ *Geophysics*, Bd. 55, pp. 821-833, 1990.
- [47] K. Beur und R. Trice, „Data Integration and Numerical Fracture Models for Water Flood Management: A Case Study of the Valhall Chalk Reservoir, North Sea,“ *Fractured Reservoirs*, 2004.
- [48] B. Hornby, D. Johnson, K. Winkler und R. Plumb, „Fracture Evaluation Using Reflected Stonely-Wave Arrivals,“ *Geophysics*, Bd. 54, pp. 1274-1288, 1989.
- [49] B. W. D. M.-T. C.G. Dyke, „Advances in Characterizing Natural-Fracture Permeability From Mud-Log Data,“ SPE 25022 PA, 1992.
- [50] C. C. V. C. R. M. G. D. B. F.M. Verga, „Detection and Characterization of Fractures in Naturally Fractured Reservoirs,“ SPE 63266, Dallas, 2000.
- [51] J. Bell, „Investigating Stress Regimes in Sedimentary Basins Using Information From Oil Industry Wireline Logs and Drilling Records,“ Geological Society Spec. Publ., 1990.

- [52] J. C. W. Narr, „Origin of Fracture Porosity: Example from Alamtont Field, Utah,“ *AAPG Bull.*, Bd. 66, pp. 1231-1247, 1982.
- [53] T. Engelder, „Loading Paths to Joint Propagation During a Tectonic Cycle: An Example from the Appalachian Plateau, USA,“ *J. Struct. Geol.*, Bd. 7, pp. 450-476, 1987.
- [54] O. Barkved; B. Bartman; B. Compani; J. Gaiser; R. Van Dok; P. Kristiansen; T. Probert; M. Thompson, „The Many Facets of Multicomponent Seismic Data,“ *Oilfield Review*, Bd. 2, Nr. 16, pp. 42-46, 2004.
- [55] J. Caldwell; P. Christie; F. Engelmark; S. McHugo; H. Özdemir; P. Kristiansen; M. MacLeod, „Shear Waves Shine Brightly,“ *Oilfield Review*, Bd. 11, Nr. 1, pp. 2-15, 1999.
- [56] S. Peralta; C. Barrientos; J.L. Arroyo, „The Specialized Use of the VSP to Define Fracture Orientation and to Help in a Multicomponent Survey Design,“ in *Transactions of the SPWLA 47th Annual Logging Symposium*, Veracruz, 2006.
- [57] W.S. Leaney; C.M. Sayers; D.E. Miller, „Analysis of Multiazimuthal VSP Data for Anisotropy and AVO,“ *Geophysics*, Bd. 64, Nr. 4, pp. 1172-1180, 1999.
- [58] D. Corrigan; R. Wither; J. Darnall; T. Skopinski, „Fracture Mapping from Azimuthal Velocity Analysis Using 3D Surface Seismic Data,“ in *Expanded Abstracts SEG International Exposition and 66th Annual Meeting*, Denver, 1996.
- [59] S.A. Hall; J.M. Kendall, „Constraining the Interpretation of AVOA for Fracture Characterization,“ *Anisotropy 2000: Fractures, Converted Waves and Case Studies*, pp. 107-144, 2000.
- [60] C.M. Sayers, „Misalignment of the Orientation of Fractures and the Principal Axes for P and S Waves in Rocks Containing Non-Orthogonal Fracture Sets,“ *Geophysical Journal International*, Bd. 133, Nr. 2, pp. 459-466, 1998.
- [61] C.M. Sayers; S. Dean, „Azimuth-Dependent AVO in Reservoirs Containing Non-Orthogonal Fracture Sets,“ *Geophysical Prospecting*, Bd. 49, Nr. 1, pp. 101-106, 2001.
- [62] M. Williams; E. Jenner, „Interpreting Seismic Data in the Presence of Azimuthal Anisotropy or Azimuthal Anisotropy in the Presence of the Seismic Interpretation,“ *The Leading Edge*, Bd. 21, Nr. 8, pp. 771-774, 2002.
- [63] V. Grechka; I. Tsvankin, „3-D Description of Normal Moveout in Anisotropic Inhomogeneous Media,“ *Geophysics*, Bd. 63, Nr. 3, pp. 1079-1092, 1998.

- [64] M.A. Perez; V. Grechka; R.J. Michelena, „Fracture Detection in a Carbonate Reservoir Using a Variety of Seismic Methods,” *Geophysics*, Bd. 64, Nr. 4, pp. 1266-1276, 1999.
- [65] L. Bennet; J. La Calvez; D.R. Sarver; K. Tanner; W.S. Birk; G. Water; J. Drew; G. Michaud; L. Eisner; R. Jones; D. Leslie; M.J. Williams; J. Govenlock; R.C. Klem; K. Tezuka, „The Source for Hydraulic Fracture Characterization,” *Oilfield Review*, Bd. 17, Nr. 4, pp. 42-57, 2005/2006.
- [66] B.W. McDaniel, SPE, Halliburton, „How "Fracture Conductivity is King" and "Waterfracs Work" Can Both be Both Valid Statements in the Same Reservoir,” CSUG/SPE 148781, Alberta, 2011.
- [67] O. Baker; F. Kuppe, Epic Consulting Services Ltd, „Reservoir Characterization for Naturally Fractured Carbonates,” SPE 63286, Dallas, 2000.
- [68] J.C. Long, *Construction of Equivalent Discontinuum Models for Fracture Hydro-Geology*, Comprehensive Rock engineer Principles, Practices.
- [69] A.Bitanov; S.Nadezhdin, „Productivity Impact from Matrix Stimulating Long Intervals using a Non Damaging Self Diverting System: A Northwestern Kazakhstan Case Study,” SPE 92831, Barhainm, 2005.
- [70] J. Ely, Ely and Associates of Texas LLC; M.Jacoby, Burnett Oil Company, Inc, „Utilization of Simple Fluids and Proppant Combinedwith Design; Optimization Yields Outstanding Results in New Mexico-San Andres Oil Play,” SPE 146523, Denver, 2011.
- [71] S. Metcalf, SPE; B. Ward, SPE; W. Davis, SPE; D.H. Gray, SPE, BJ Services Company; J. Brienens, SPE; J. Miller, SPE, Conoco Inc., „Acid Fracturing in the Warren Unit of Southwestern New Mexico,” SPE 35228, Midland, 1996.
- [72] J. Becnel, T.A. Fago; Conoco, Inc., „Warren Unit Lease Evaluation,” Conoco, Inc., 1991.
- [73] G. Arzmueller, OMV; S. Buchta, Moravske Naftove Doly; E. Ralbovsky, Slovak Gas Industry, VVNP Research Oil Company; G. Wessely, „The Vienna Basin,” The American Association of Petroleum Geologists, 2006.
- [74] R. Jiricek, „Tectonic Profiles through the West Carpathians,” in *Tectogenetic Development of the Carpathian Arc in the Oligocene and Neogene*, Bratislava, Geologicky ustav D. Stura, 1979, pp. 203-212.
- [75] L. Royden, „The Vienna Basin. A Thin-Skinned Pull-Apart Basin,” *SEPM Special Publication: Strike Slip Deformation, Basin Formation and Sediments*, Bd. 37, pp. 319-338, 1985.

- [76] W. Hamilton, OMV; L. Wagner, OMV; G. Wessely, OMV, Oil and Gas in Austria, Vienna: Mitt. Oesterr. Geo. Ges., 2000.
- [77] J. Kapounek et al., „Die Erdoellagerstaette Schoenkirchen Tief im alpin-karpatischen Beckenuntergrund,“ *Erdoelzeitschrift*, Bd. 80, Nr. 8, pp. 305-317, 1964.
- [78] A. Kroell und G. Wessely, „Neue Ergebnisse beim Tiefenaufschluss im Wiener Becken,“ *Erdoel-Erdgas Zeitschrift*, Bd. 89, Nr. 11, pp. 400-413, 1973.
- [79] W. Hamilton et al., „The Alpine-Carpathian Floor of the Vienna Basin in Austria and CSSR,“ Fed. Geo. Survey, Vienna, Prague, 1990.
- [80] G. Wessely, „The Calcerous Alps below the Vienna Basin in Austria and their Structural and Facial Development in the Aline-Carpathian Border Zone,“ *Geologica Carpathia*, Bd. 43, pp. 347-353, 1992.
- [81] A. Kroll et al., Karten 1:200.000 Ueber den Untergrund des Wiener Beckens und der Angrenzenden Gebiete, Vienna: Geologische Bundesanstalt, 1993.
- [82] OMV, *Processes and Porcedures for: Stimualtion/Acidizing*, Vienna, 2014.
- [83] M.-L. Rodriguez Chavez, „Evaluation and Optimisation of Matrix Acidizing in OMV Fields,“ Mining University of Leoben, Leoben, 2007.
- [84] OMV, *Carbonate Study*, Vienna, 2010.
- [85] J.W. Ely, Ely and Associates, Inc., M.A. Martin, BJ Services Company, U.S.A.; J.J. Duenas, BP America Production Company; J.R. Trythall, BP America Production Company, „Old/New Techniques Translate into Big Savings and Enhanced Stimulation in the Brown Dolomite/Hugoton Fields of Texas and Kansas,“ SPE 80913, Oklahoma City, 2003.
- [86] M.J. Fetkovich; M.E. Vienot; M.D. Bradley; U.G. Kiesow, „Decline Analysis Using Type Curves Case Histories,“ SPE 13169, 1984.
- [87] D.N. Meehan, „Stimulation Results in the Giddings (Austin Chalk) Field,“ SPE 24783, Washington, 1995.

10 Appendix

Table A - 1: Summary of the literature review on stimulation in naturally fractured carbonates

Resource	Country	State	Field Name	HC type	Depth	Pressure	Temperature	Porosity	Permeability	Perforation Interval (total)	Net Pay thickness	Gross Pay Thickness	Frac Method	Frac Type	Proppant	Closure Pressure	Resvr FCPG	Frac Est. Cond.	Additional Information	Paper Conclusions
PINN, Feb2005, Case History OK. ppt	USA	Oklahoma	Carter-Knox	gas	17900 - 18700 ft MD	9000 psi	260 F	2 - 3%	0.05 mD	220 ft	150 ft		Acid	15% HCl neat acid, 10# Linear gel, 5% ZCA, 15%ZCA, 25 # linear gel	0.5 - 1.5 ppg of 100-mesh sand, 0.5-2.0 ppg 30/60		0.563 - 0.69 psi/ft	390 - 1360 md-ft	(1) 2 - 4.5% Sour Gas, (2) High well costs ~\$10MM, (3) Struggle to produce at economic rates, (4) acid treatment w/o prop effectively stim the limestone.	
SPE Production Engineering, May 1992, Vol.7 No.2 - Doc#20973-PA	N. Croatia		Pannonian Basin, Drava depression	gas cond	3300 - 3800 M (10830 - 12470 ft)	45 - 49 Mpa	180 - 195C (356 - 383 F)	4 - 10%	0.003 - 0.2 mD				Linear & Crosslink Gels	80k-528k gal	110k - 1321590 lbm high strength prop	> 50 Mpa (7250 psi)	0.017 - 0.023 Mpa/m		(1) PI's increased from 0.0017 - 0.1 scf/D-psi ² to 0.04 - 1.3 scf/D-psi ² , (2) production fluid is high gravity gas 0.83 - 1.15 to air with up to 22% CO and 48/425, water saturation 30-50%(3) NOT HOMOGENEOUS, anisotropic, naturally fissured, High temp, microfractures, vugs, near vertical fractures, diagenetic	Hydraulic fracture treatments demonstrated that successful stimulation can be done in highly fissured, extreme-temperature formations, although difficulties do exist. Fractures that take into account the production characteristics of tight, heavy-gas-condensate reservoirs must be invariably long. Leakoff control and engineering of the viscosity are crucial elements in obtaining this length. Post-treatment production increases in these wells were generally excellent and this performance was predicted and interpreted.
SPE 58987, February 2000	Mexico		Mata Pionche	gas cond	9350 - 9416 ft	2800 psi	190 F	5% ave	0.11 mD	66 ft	138 ft		acid & ob gel	18000 gal oil base gel & 15% HCl-alcoholic acid		5899 - 5950 psi		4832 md-ft	(1) recomplete using 15%HCl and 18000 gal Oil Base Gel increased production from 0.3 MMCFD to 1.4 MMCFD with CGR of 22 STB/MMCF. Paid back in 22 days and maintained after shut in and reopened. (2) Net pay zone comprises of 90% LS, 1% Sh, 9% QTZ, (3) Fissure closure pressure is 6435 psi.	Combined log analysis, flow efficiency test, frac modeling and well test analysis gives better approach regarding results of fracturing job. From this radial multiple fracture geometry was defined and validated through reservoir simulation. Combined effects of perforation phase, length of perf interval, tortuosity, high leakoff and multiple fractures cause the premature screenout in treatment. screenout not anticipated as step down test not performed. Use of real data extremely important to design and evaluation of fracture treatment. perforation program must be designed for hydraulic fracturing an not for completion. Bottom hole gauge recommended for better definition of perf and near wellbore pressure drops. Fracturing fluid is big source of formation damage; the use of modified fracturing fluid systems should be considered; these fluids could include foams and non-aqueous systems.
SPE 59550, March 2000	USA	New Mexico	Teague	oil	5280 - 5600 ft			< 10%	0.001 mD (eff. @ 1.15-2.09 mD)										(1) Anhydrite is the most common pore and fracture filling material.	Study shows oil can be recovered both with water and CO2 injection. Injectivity studies needed to determine rate that fluid could be injected and if flow would be sufficient and rapid enough to be economical. Air perm indicated two types of perm, matrix and fracture/vug. Even in well mineralized fractures the perm was generally greater than the surrounding matrix. Core was determined to be strongly oil-wet. Tests determined MMP to be higher of 1010 psig or system bubblepoint pressure. Most wells show no change in production that is clearly due to the infill well, indicating that new oil that would not otherwise be produced has been tapped. new perfs in old wells had mixed results.
	USA	Wyoming	Wamsutter	gas	> 15000 ft TVD	> 10000 psi	> 350 F													
SPE 146523, Oct-Nov 2011	USA	New Mexico	Permian Basin	oil										hot acid gelled water, water sand, Waterfrac Sweeps, crosslink gel	(1) Xlink @ 2-8ppg 4000-40000 # w/750-10000 gals, (2) Water Sweep @ 15%HCl, 1500-6750 gals, 40/70 ppg, 1500-12000 #				(1) Waterfrac Sweep treatments for Paddock wells has resulted in 35K barrel increase in ultimate est production over life of well, making it economical in the Blinberry interval.	Use of very simplistic stimulation procedure has both dramatically increased recoverable reserves and improved the economics allowing for production of oil and gas where previously economics didn't work. The process used for the Yeso and Grayburg San Andres has been applied in virtually every other carbonate and naturally fractured reservoir in the US and Canada with similar results.
SPE 140724, March 2011	USA	West Texas	Permian Basin	oil & gas	Spraberry, 6569-8155 ft, Wolfcamp 7749-9701 ft									crosslink gel	100-150k# of 20/40 at max 2-4 ppg		Spraberry (0.517-0.356 psi/ft), Wolfcamp (0.642-0.746 psi/ft)		(1) production response varied due to reservoir quality. A good well will make 100 barrels per day, but initial rates vary from several hundred to 20 barrels a day. (2) proppant type shows to be an important choice affecting production. Higher strength made most improvement.	Crosslinked 15% hydrochloric acid gel treatments were economically and effective; it achieved higher production rates for new well completions compared to sand fracturing and special fluid loss control acid in the Tubb formation. Reservoir quality is the major control parameter; results were similar when changing job size and staging variations in the Drinkard formation. No production enhancement was achieved with heated acid stages or by adding CO2 to the stimulation fluids. Re-stimulation yielded similar results regardless of the type of treatment employed in the Tubb formation. Crosslinked 15% hydrochloric acid gel and gelled acid provided improvement in retardation of reactivity in vugular and naturally fractured dolomite formations and provide better leak-off control than gelled or neat acid.
SPE 35228 - March 1996	USA	New Mexico	Warren Unit	oil & gas	5800 - 6200 ft			Drinkard: 10 - 12% Tubb: 7 - 18%			Tubb: gas - 28 ft oil - 54 ft	200 ft	fracture acidizing	different acid systems are compared					(1) acidizing was key to improved production, (2) leak-off control/frac geom/reaction retardation of HCl also significant parameters in vugular and naturally fractured dolomites, (3) Prod increased with crosslinked acid gel from 28-50 BOPD & 20-189 MCFD to average of 96 BOPD & 111 MCFD, (4) recompletions were on declines of 30% before treatment and 15% after. use of CO2 shows increased improvement to those w/o CO2.	Initial Production rates on new well completions used Crosslinked 15% hydrochloric acid gel treatments and provide an economic and effective stimulation. Job size and staging variations in new well completions indicate reservoir quality is the major control parameter. heated acid stages do not appear to enhance the production and incremental cost of CO2 addition of the stimulation does not appear to contribute to enhanced production. Crosslink 15% HCl and gelled acid provide improvement in retardation of reactivity in vugular and naturally fractured dolomite formations. the crosslinked acid gel provides better leakoff control than gelled or neat acid.
SPE 24783, May 1995	USA	Southeast Texas	Giddings Austin Chalk Field						0,005-0,02 mD			50 - 500 ft	water frac	water, wax bead, 7.5-15% HCl	no				80-90% success rate; horiz. Wells: less success when very low RFI, depleted pressures, no surface build up p, high WC wells; paper discusses 250 vertical- and 150 horizontal wells	1. The "water frac" technique is a complex process with a high rate of success in the Austin Chalk formation for both vertical and horizontal wells. Oil and gas recoveries are substantially increased with this technique. 2. The major mechanisms that explain water frac success (imbibition, gravity swap, pressure maintenance) are characteristic of secondary and/or enhanced recovery. 3. Incremental recoveries associated with water fracs are significantly greater than costs. In many cases second and third cycles usually may yield commercial but diminishing results 4. Additional research to optimize recoveries, accelerate imbibition, improve diversion, etc. is warranted. This technique should also be tried in other low permeability naturally fractured reservoirs.
SPE 80913, March 2003	USA	Texas, Kansas	Hugoton Brown Dolomite	gas	2000-4000 ft	20-500 psi		locally high	locally high				waterfrac	water, sand	no				cost up to 2/3 reduced, production increase higher	treatments not optimized regarding tratment design and equipment yet but still improve in production and reduce in cost
SPE 112419, February 2008	Kazakhstan			oil, gas, condensates		up to 95 MPa	up to 120 °C				up to 1500 m		several systems are compared with VES + fibres	Matrix Acidizing, Acid Washes	no					To minimize skin thick sections must be as uniformly treated as possible Diverting agent for high permeability contrasts crucial Must take chemical reaction physics into consideration to find optimum pump rate Selected treatment technique must allow optimum pump rates CT better than BH without diverters BUT best when BH at high rates and VES diverting agents
SPE 144183, June 2011	Mexico			oil & gas															The paper discusses solutions for the stimulation in high-pressure, high-temperature fractured carbonate reservoirs based on several field cases from Mexico	Acid Fracturing effective in areas with low permeability and low natural fracture density Stimulation near gas cap: use mechanical and chemical diverters Stimulation near gas cap with effective diverters possible Good understanding of reservoir flow units and production mechanisms is essential New wells in exploratory areas have high potential for production improvement if drilling induced damage is removed or bypassed Productivity problems in NFRs increase in frequency and complexity as field matures Removal of formation damage due to organics and inorganic depositions, drilling induced damage and stimulation near the gas cap and the aquifer are the main challenges. To maximize production right diagnose and a fit-for-purpose solution necessary
SPE 135604, September 2010	Worldwide			oil & gas						open-hole			acid tunneling						The relatively new technique "coiled tubing acid tunneling" requires an open-hole completion; it creates multiple drainage holes out into the reservoir pay zone resulting in a negative skin; insensitive - can be applied in all kinds of carbonate rocks, in thick and thin pay zones and also near the water or gas zone; 47 wells in 9 countries utilized acid tunneling that created 299 tunnels and a length of over 10000 ft	Acid can be placed selectively rather than going path of least resistance, penetration up to 100 ft Best case: tunnel reaches a natural fracture -> increases contact of well with reservoir Worst case: increase in inflow potential by placing several tunnels -> still a win Cheaper than matrix- or fracture acidizing; acid can be used more efficiently as the placement can be controlled better Smaller footprint than infill drilling
SPE 118858, January 2009	China	NW	TZ-I Break Slope	gas cond	4800 - 5200 m		130 C	0.2 - 11%	0.08 - 516 mD		30-60 m		acid/prop	40/60 mesh		0.016-0.018 Mpa/m			(1) initially straight acid, however production couldn't reach commercial value or keep stable and declined rapidly. Was found to be due to acid etched fracture is short and can't sustain for long term under high stress. (2) propped fracturing is considered to fulfill the need of reservoir.	Because of serious acid leak off and rapid acid/rock reaction speed, the length of effective acid etched fracture is always restricted and the eff duration of etched fracture is short, esp in deep wells because of high closure stresses. Propped fracturing can create longer length and term conductive fracture. Long fracture was needed in teh low poro and ultra low perm reservoir to enlarge the permeable area and to increase the prob of connecting favorable zone. small size high strength ceramic proppant was selected to fulfill the narrow width of fracture, and prop plugs were utilized to erode the tortuosity of the near wellbore frac path and plug near well multiple hydraulic and natural fractures, which ensured success of propped frac treatment. It was proved by field case that the propped frac was able to dramatically improve well production and was more effective than the acid fracturing in the reservoir.
SPE 110333, November 2007	USA	West Texas	Midland Basin, Welch Field	oil	4800 ft (+3000' lateral)			5-15%	1-10 mD				pinpoint/isolation between intervals						This paper covered Microseismic Monitoring of a Restimulation Treatment in the Permian Basin San Andres Dolomite Horizontal Well.	

Table A - 2: Stratigraphy of Strasshof Tief.

	Age 1	Age 2	Formation	Unit or Layer	Synonyms
Tertiary	Early Tertiary	Late Paleocene	Upper Giesshübl Fm		
	Early Tertiary	Late Paleocene	Mid Giesshübl Fm		
	Late Cretaceous- E.Tert.	Maastr.-Lwr.Paleocene	Lower Giesshübl Fm		
CRETACEOUS	Late Cretaceous	Maastrichtian	Gosau 6		
	Late Cretaceous	Campanian-Maastr.	Nierental Fm	Nierental grau' Fm	
	Late Cretaceous	Coniacian-Lwr. Camp.	Grabenbach Fm		
	Late Cretaceous	Coniacian-Lwr. Camp.	Gosau 3		
	Late Cretaceous	Coniacian-Lwr. Camp.	Gosau 2		
	Late Cretaceous	Coniacian-Lwr. Camp.	Gosau 1		
	Late Cretaceous	Cenoman-Turon.?	Branderfleck Fm	A	
	Late Cretaceous	Cenoman-Turon.?	Branderfleck Fm	B	
	Early/ Late Cretaceous	Albian- Cenom.	Losenstein Fm		
	Gault	Alb	Tannheim Fm		
	Neokomian	Valanghian-?	Schrambach Fm	A	
	Neokomian	Berriasian	Schrambach Fm	B	
	JURASSIC	Malmian	Tithonian	Ammergau Fm	
Malmian		Kimmeridgian	Agatha Fm		Saccococoma Ls
Malmian		Oxfordian	Ruhpolding Fm		Radiolarite
Doggerian		Callovian	Klaus Fm	Globigerina oolithe	
Doggerian		Bathonian	Klaus Fm	Filament Limestone	
Liassic			Hierlatz-Hornstein Fm	A	
Liassic			Hierlatz-Hornstein Fm	B	
Liassic			Hierlatz-Hornstein Fm	C	
Liassic			Hierlatz-Hornstein Fm	D-E	
Liassic			Kirchstein Fm	A	
Liassic			Kirchstein Fm	B	
Liassic?			Kirchstein Fm	"C"	
TRIASSIC	Rhätian		Schattwald Fm	Kössen Fm	
	Norian - Rhätian		Plattenkalk	Plattendolomit	
	Norian - Rhätian		Hauptdolomit		
	Karnian		Opponitz Fm	Anhydrite	
	Karnian		Opponitz Fm	Dolomite	

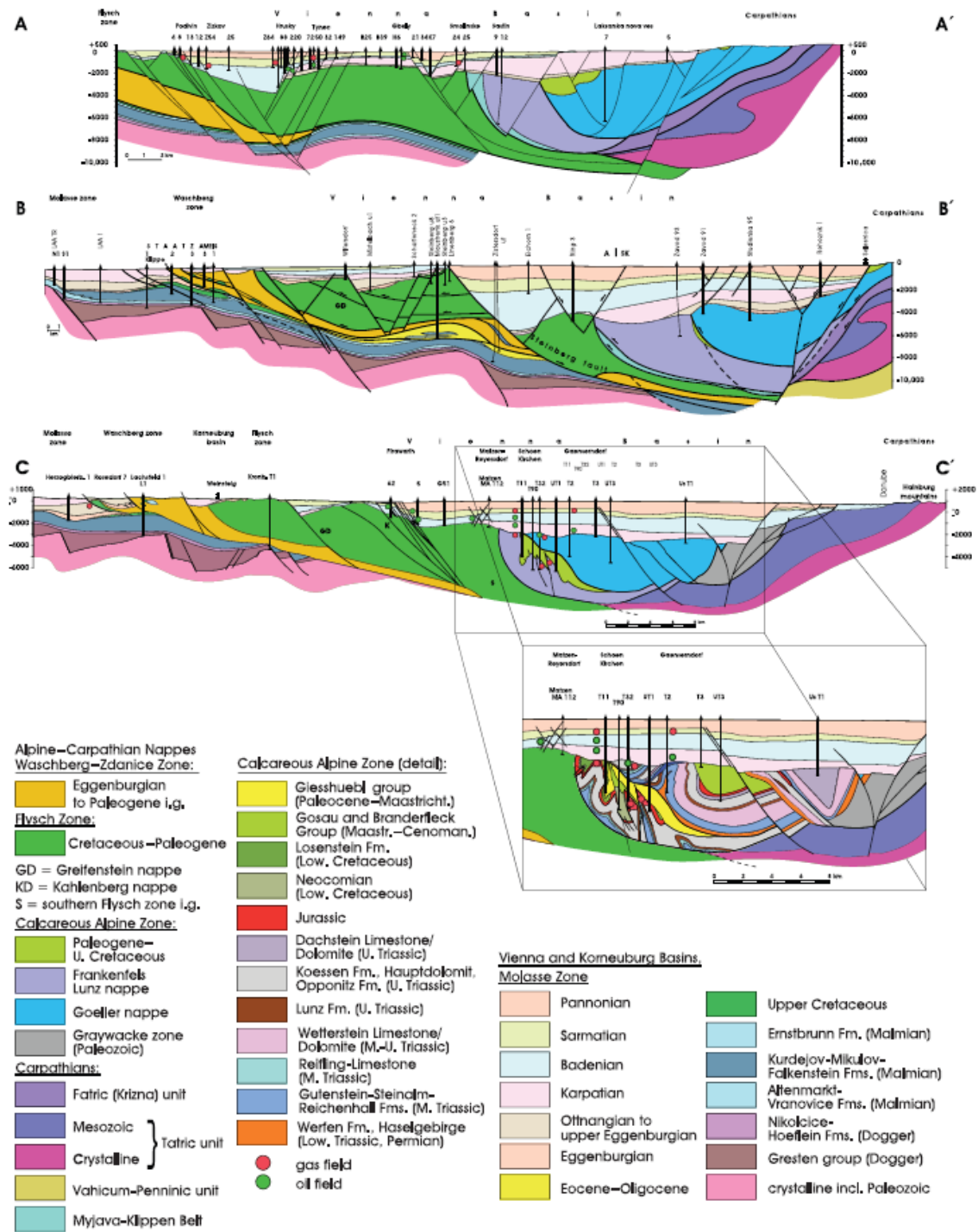


Figure A - 1: Cross-section of the Vienna Basin [73].

Table A - 3: Existing fields including their reservoirs of the Vienna Basin. Only Matzen is still producing [84].

Field	Reservoir	Type	Start of Production
Aderklaa	A019-700-92	oil (H ₂ S)	1962
	A019-800-10	gas (H ₂ S)	1962
	A019-800-20	gas (H ₂ S)	1962
Hirschstetten	A047-800-10	gas (H ₂ S)	1974
Baumgarten	A018-801-10	gas (H ₂ S)	1960
Matzen (H ₂ S)	A015-635-10	gas (H ₂ S)	1968
	A015-700-16	oil (sweet)	2011?
	A015-800-16	gas (H ₂ S)	2008
	A015-800-91	oil (H ₂ S)	1966
	A015-848-91	gas (H ₂ S)	1969
	A015-850-16	gas (H ₂ S)	2009
	A015-850-17	gas (H ₂ S)	2011?
Matzen (sweet)	A015-800-10	oil	1962
	A015-800-12	oil	1966
	A015-800-13	oil	1997
	A015-800-50	gas	2007
	A015-800-14	oil	2010

Table A - 4: Areas of OMV Austria. Area 13 was newly discovered by the Strasshof Tief wells.

AREA	PROD_FIELD_CODE	HOR	PE
Area 1 - North	A001 Goesting		
Area 1 - North	A002 Van Sickle		
Area 1 - North	A004 Maustrenk		
Area 1 - North	A005 St. Ulrich		
Area 1 - North	A007 Scharfeneck		
Area 1 - North	A008 Neulichtenwarth		
Area 1 - North	A010 Althoeflein		
Area 1 - North	A011 Altlichtenwarth		

Area 1 - North	A012 Muehlberg		
Area 1 - North	A013 Bernhardsthal		
Area 1 - North	A014 Rabensburg		
Area 1 - North	A024 Windisch- Baumg.		
Area 1 - North	A028 Paasdorf		
Area 1 - North	A029 Ginzersdorf		
Area 1 - North	A030 Maxbergen		
Area 2 - Matzen	A015 Matzen		
Area 2 - Matzen	A018 Zwerndorf		
Area 2 - Matzen	A052 Marchegg		
Area 2 - Matzen	A058 Duernkrut		
Area 2 - Matzen	A068 Markgrafneusiedl		
Area 2 - Matzen	A069 Seyring		
Area 3 - Sour Gas 1	A015 Matzen	635	10
Area 3 - Sour Gas 1	A019 Aderklaa	700	92
Area 3 - Sour Gas 1	A019 Aderklaa	800	10
Area 3 - Sour Gas 1	A019 Aderklaa	800	20
Area 3 - Sour Gas 1	A015 Matzen	800	90
Area 3 - Sour Gas 1	A015 Matzen	800	91
Area 13 - Sour Gas 2	A015 Matzen(Strasshof Tief)	700	16
Area 13 - Sour Gas 2	A015 Matzen(Strasshof Tief)	800	16
Area 13 - Sour Gas 2	A015 Matzen(Strasshof Tief)	848	16
Area 13 - Sour Gas 2	A015 Matzen(Strasshof Tief)	850	16
Area 4 - Hochleiten	A009 Niedersulz		
Area 4 - Hochleiten	A006 Hohenruppersdorf /Erdpress		
Area 4 - Hochleiten	A016 Hochleiten		
Area 4 - Hochleiten	A017 Pirawarth		
Area 5 - South	A019 Aderklaa		
Area 5 - South	A021 Fischamend		
Area 5 - South	A022 St. Marx		
Area 5 - South	A023 Oberlaa		
Area 5 - South	A025 Himberg		
Area 5 - South	A036 Breitstetten		
Area 5 - South	A040 Orth		
Area 5 - South	A047 Hirschstetten		
Area 5 - South	A050 Wienerherberg		
Area 5 - South	A057 Ludersdorf		
Area 5 - South	A059 Moosbrunn		

Area 5 - South	A060 Favoriten		
Area 5 - South	A066 Wiesen		
Area 6 - Hoeflein	A056 Hoeflein		
Area 7 - West	A027 Wildenduernbach		
Area 7 - West	A031 Ameis		
Area 7 - West	A037 Hagenberg		
Area 7 - West	A046 Roseldorf		
Area 7 - West	A048 Klement		
Area 7 - West	A051 Stockerau		
Area 7 - West	A053 Stockerau-Ost		
Area 7 - West	A054 Altprerau		
Area 7 - West	A055 Merkersdorf		
Area 7 - West	A061 Neulengbach		
Area 7 - West	A062 Pottenhofen		
Area 7 - West	A064 Waschberg		
Area 7 - West	A065 Neuruppersdorf		
Area 8 - Upper Austria	A038 Piberbach		
Area 8 - Upper Austria	A039 Harmannsdorf		
Area 8 - Upper Austria	A041 Wirnzberg		
Area 8 - Upper Austria	A044 Thann/Teufeldgr.		
Area 8 - Upper Austria	A045 Steyr		
Area 8 - Upper Austria	A049 Wels		
Area 8 - Upper Austria	A063 Gruenau		
Area 8 - Upper Austria	A067 Molln		

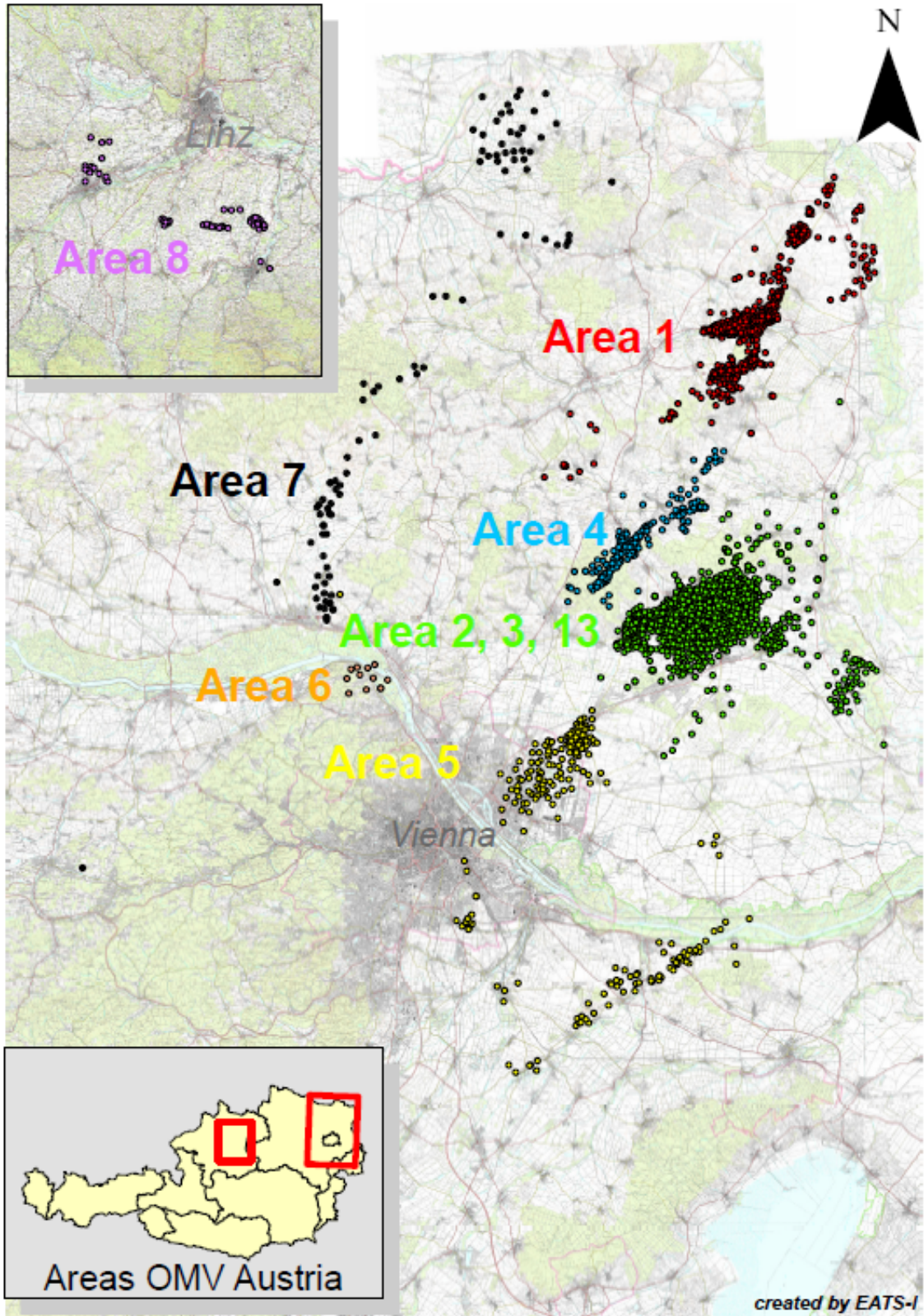


Figure A - 2: Geographical location of the areas.

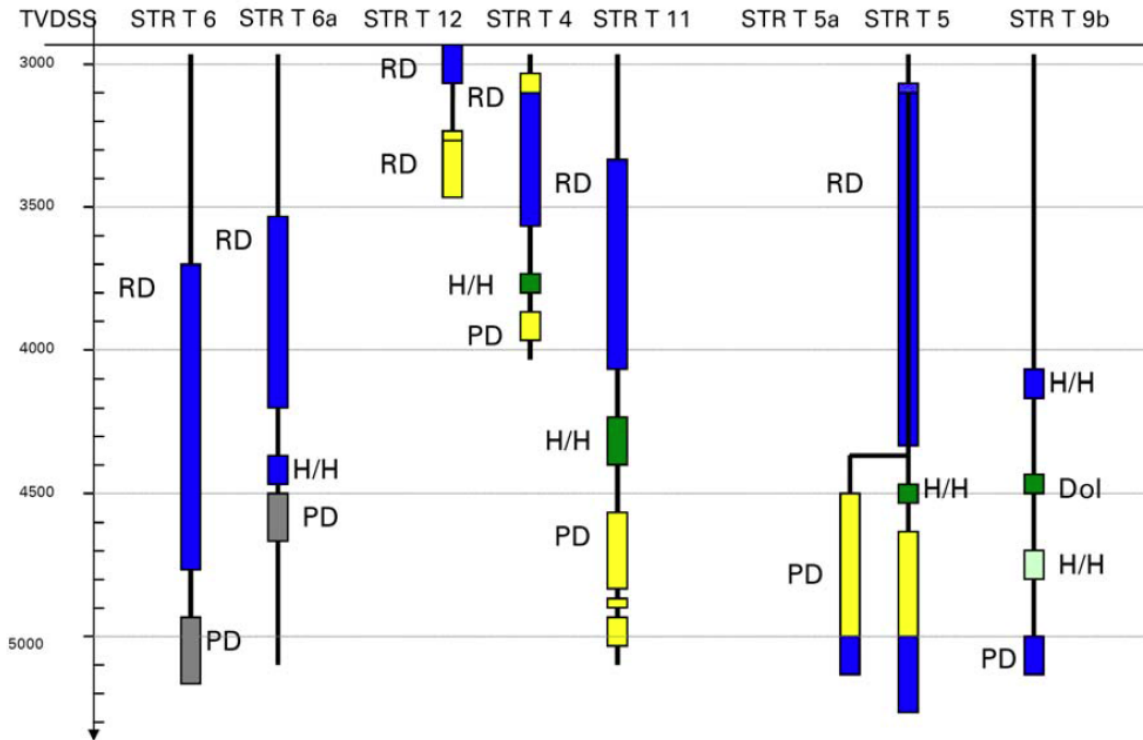


Figure A - 3: Horizons and fluid content of the Strasshof Tief wells. The horizons are Perchtoldsdorfer Dolomite (PD), Hierlatz – Hornsteinkalk (H/H) and Reyersdorfer Dolomite (RD). The blue color is used for water, green for oil, yellow for gas and grey is a tight formation [84].

Table A - 5: Lithological profile of Strasshof Tief 5.

Sediment. Cyde - Tectonic Unit	Age	Age 2	Formation	Unit/ Layer	Synonym	Top	Isopach	upright/ inverse
						m MD (log)	m	
Gosau Giesshübl	Maastr.-Paleocene		Unt. Giesshübl Fm (?)			2771	19	normal
Gosau Giesshübl	Campanian-Maastr.		Nierental Fm			2790	12	normal
Gosau Giesshübl	Coniacian-Lwr. Camp.		Grabenbach Fm			2802	7	normal
NCA - Reyersdorf	Neokomian	Berriasian	Schrambach Fm	A		2809	32	?
NCA - Reyersdorf	Lwr.-Upp.Cretaceous	Albian- Cenom.	Losenstein Fm			2841	45	normal
NCA - Reyersdorf	Gault	Alb	Tannheim Fm			2886	9	normal
NCA - Reyersdorf	Malmian	Kimmeridgian	Agatha Fm.		Seccoc. Ls	2895	3	?
NCA - Reyersdorf	Gault	Alb	Tannheim Fm			2898	46	normal
NCA - Reyersdorf	Neokomian	Berriasian	Schrambach Fm	A		2944	117	normal
NCA - Reyersdorf	Lwr.-Upp.Cretaceous	Albian- Cenom.	Losenstein Fm			3061	88	normal
NCA - Reyersdorf	Gault	Alb	Tannheim Fm			3149	54	normal
NCA - Reyersdorf	Neokomian	Valanghian-?	Schrambach Fm	A		3203	13	normal
NCA - Reyersdorf	Malmian	Kimmeridgian	Agatha Fm.		Seccoc. Ls	3216	17	inverse
NCA - Reyersdorf	Malmian	Tithonian	Ammergau Fm		Celpio. Ls	3233	7	inverse
NCA - Reyersdorf	Neokomian	Berriasian	Schrambach Fm	B		3240	9	inverse
NCA - Reyersdorf	Norian - Rhätian		Hauptdolomit			3249	364	?
NCA - Reyersdorf	Malmian	Kimmeridgian	Agatha Fm.		Seccoc. Ls	3613	2	normal ?
NCA - Reyersdorf	Norian - Rhätian		Hauptdolomit			3615	99	normal ?
NCA - Reyersdorf	Karnian		Opponitz Fm			3714	86	norm./inv.?
NCA - Reyersdorf	Norian - Rhätian		Hauptdolomit			3800	685	inverse ?
NCA - Percht./ Rey	Neokomian	Valanghian-?	Schrambach Fm	A		4485	78	norm./inv.
NCA - Perchtoldsdorf	Neokomian	Berriasian	Schrambach Fm	B		4563	40	normal
NCA - Perchtoldsdorf	Malmian	Tithonian	Ammergau Fm		Celpio. Ls	4603	6	normal
NCA - Perchtoldsdorf	Malmian	Kimmeridgian	Agatha Fm.		Seccoc. Ls	4609	3	normal
NCA - Perchtoldsdorf	Malmian	Oxfordian	Ruhpolding Fm		Redio.	4612	10	normal
NCA - Perchtoldsdorf	Liassic		Hierlatz-Homstein Fm	A od B		4622	1	normal
NCA - Perchtoldsdorf	Liassic		Hierlatz-Homstein Fm	C		4623	5	normal
NCA - Perchtoldsdorf	Liassic		Hierlatz-Homstein Fm	B		4628	15	normal
NCA - Perchtoldsdorf	Liassic		Hierlatz-Homstein Fm	C, + traces D-E		4643	5	normal
NCA - Perchtoldsdorf	Liassic		Kirchstein Fm	A		4648	3	normal
NCA - Perchtoldsdorf	Liassic		Kirchstein Fm	B		4651	9	normal
NCA - Perchtoldsdorf	Liassic?		Kirchstein Fm	"C"		4660	13	normal
NCA - Perchtoldsdorf	Norian - Rhätian		Plattenkalk			4673	11	normal
NCA - Perchtoldsdorf	Liassic		Kirchstein Fm	B		4684	11	normal
NCA - Perchtoldsdorf			Hierlatz-Homstein Fm	D-E		4695	40	normal
NCA - Perchtoldsdorf	Liassic		Kirchstein Fm	B		4735	38	normal
NCA - Perchtoldsdorf	Liassic?		Kirchstein Fm	"C"		4773	5	normal
NCA - Perchtoldsdorf	Rhätian		Schattwald Fm			4778	15	normal
NCA - Perchtoldsdorf	Norian - Rhätian		Plattenkalk			4793	87	normal
NCA - Perchtoldsdorf	Rhätian		Kössen Fm			4880	104	normal
NCA - Perchtoldsdorf	Norian - Rhätian		Hauptdolomit			4984	451	normal
				TD Standard		5435		

Table A - 6: Lithological profile of Strasshof Tief 5a.

Str T5a New Fm-Tops (12.02.2014 - RS, GA, UH)								
Sediment. Cycle - Tectonic Unit	Age	Age 2	Formation	Unit/ Layer	Synonym	Top	Isopach	upright/ Inverse
						m MD (log)	m	
					KOP	4520		
NCA - Percht./ Rey	Neokomian	Valanghian-?	Schrambach Fm	A		4520	43	normal
NCA - Perchtoldsdorf	Neokomian	Berriasian	Schrambach Fm	B		4563	36	normal
NCA - Perchtoldsdorf	Malmian	Tithonian	Ammergau Fm		Calp. Ls	4599	5	normal
NCA - Perchtoldsdorf	Malmian	Kimmeridgian	Agatha Fm.		Secoc. Ls	4604	11	normal
NCA - Perchtoldsdorf	Malmian	Oxfordian	Ruhpolding Fm		Radol.	4615	4	normal
NCA - Perchtoldsdorf	Uassic		Hlerlatz-Hornstein Fm	D-E	Scheibelbergkalk	4619	8	normal
NCA - Perchtoldsdorf	Uassic		Kirchstein Fm	A		4627	4	normal
NCA - Perchtoldsdorf	Uassic		Kirchstein Fm	B		4631	6	normal
NCA - Perchtoldsdorf	Uassic ?		Kirchstein Fm	"C"		4637	2	normal
NCA - Perchtoldsdorf	Rhathian		Schattwald Fm			4639	6	normal
NCA - Perchtoldsdorf	Norian - Rhatian		Plattenkalk			4645	51	normal
NCA - Perchtoldsdorf	Norian - Rhatian		Plattendolomit			4696	71	normal
NCA - Perchtoldsdorf	Uassic ?		Kirchstein Fm	"C"		4767	20	normal
NCA - Perchtoldsdorf	Norian - Rhatian		Hauptdolomit			4787	613	normal
				TD Standard		5400		

Table A - 7: Memory gauge data from the welltest 2006.

Gauge measuring depth	4,666.42 m MD = 4659.72 m TVD
Bottom hole temperature	138 °C
Initial shut-in pressure	490bar-g
Final Flowing Pressure On 28/64" Adjustable choke	275bar-g (also with MDT)
Final shut-in pressure against closed tester valve	427 bar-g (still increasing)

Table A - 8: Comparison of the gas compositions of Strasshof 4, 5 and 5a [84].

Component Perforation / OH interval	STR T 5a 4985-5144m MD	STR T 5a 4656-4689m MD	STR T 5 5050-5060m MD 5068-5080m MD	STR T4 4335-4350m MD 4375-4395m MD
Date	13.11.2006	14.08.2006	02.06.2006	29.03.2006
H2S	2.06%	0.64%	2.14%	1.51%
CO2	11.94%	4.32%	11.62%	7.02%
N2	0.85%	0.64%	0.84%	0.82%
Methane	84.24%	93.37%	84.36%	89.71%
Ethane	0.5%	0.59%	0.53%	0.54%
Propane	0.12%	0.14%	0.14%	0.14%
Isobutane	0.03%	0.03%	0.04%	0.03%
n-Butane	0.06%	0.06%	0.07%	0.07%
Isopentane	0.03%	0.02%	0.03%	0.03%
n-Pentane	0.03%	0.03%	0.03%	0.03%
C6+	0.14%	0.16%	0.20%	0.10%
Σ	100%	100%	100%	100%
Density [kg/m ³]	0.9021	0.7948	0.9016	0.8349
Rel. density (air=1)	0.6977	0.6147	0.6974	0.6457

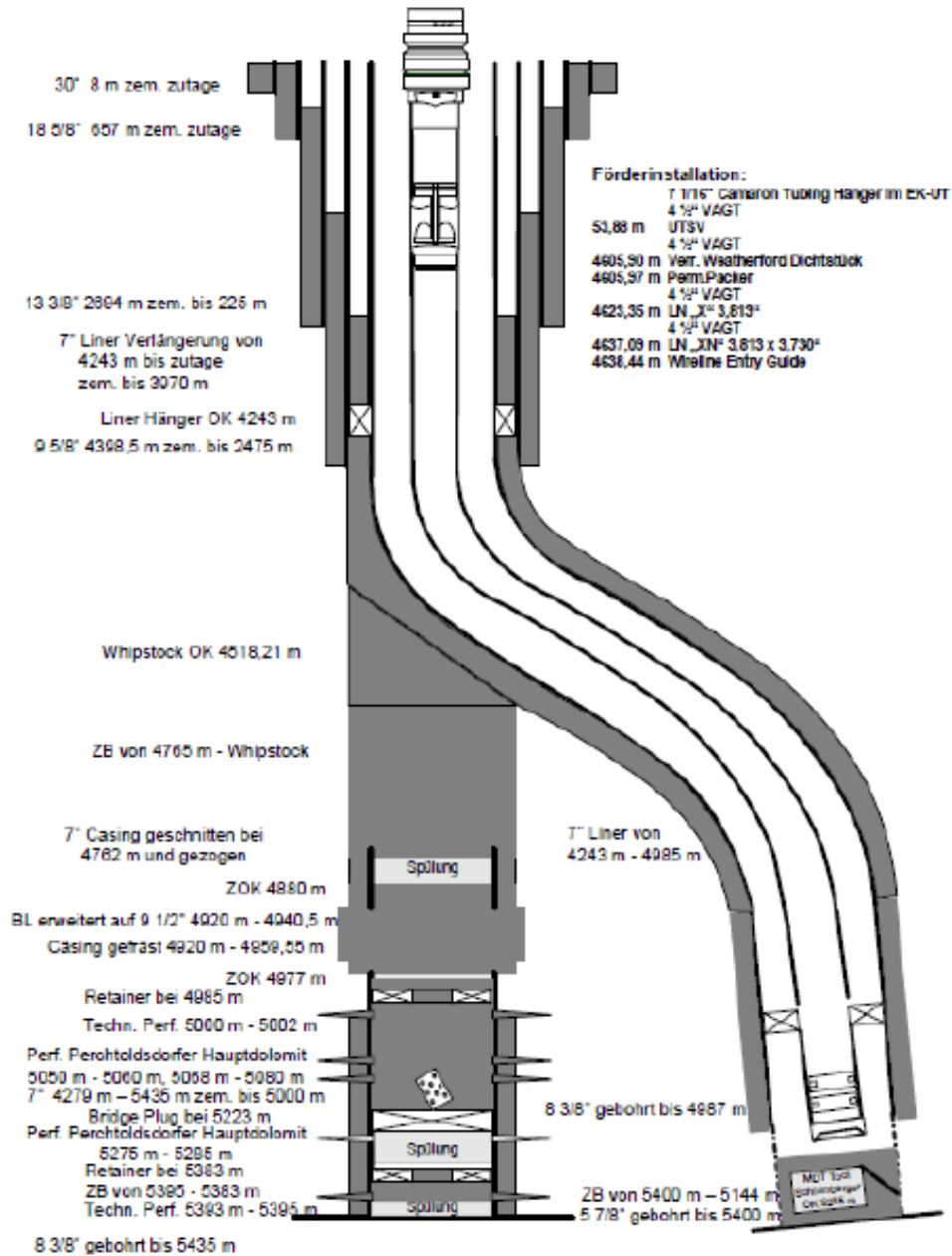


Figure A - 5: Completion after extending STR T 5a to its final depth [84].

Straßhof Tief 5a - Trajectory Top View

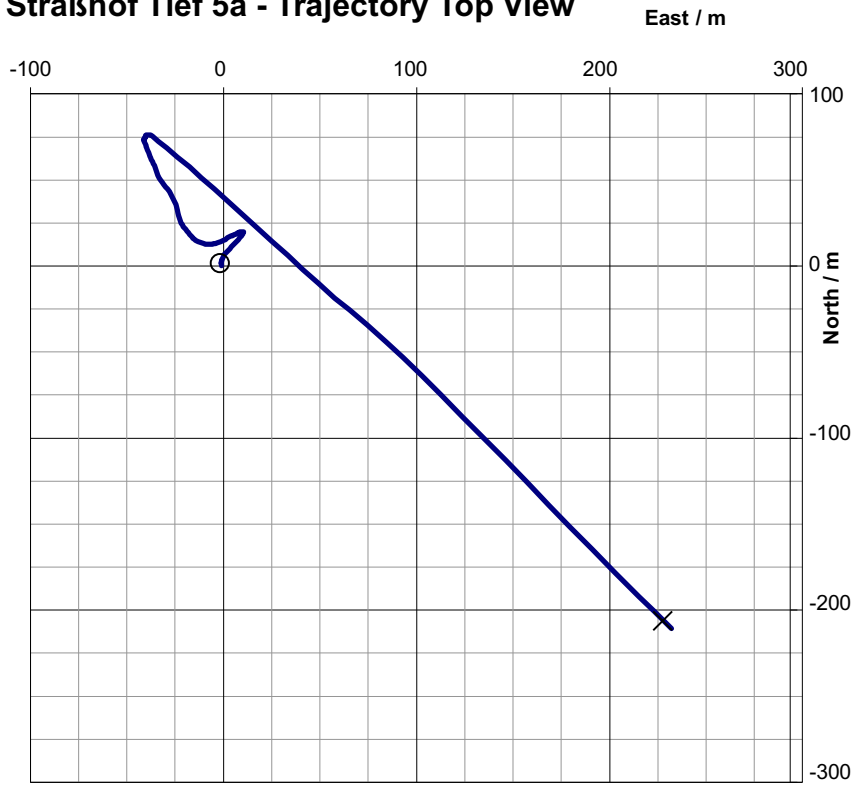


Figure A - 6: Top view of the STR T 5a trajectory.

Straßhof Tief 5a - Trajectory from South



Figure A - 7: Side view from the south of the STR T 5a trajectory.

Straßhof Tief 5a - Inclination Plot

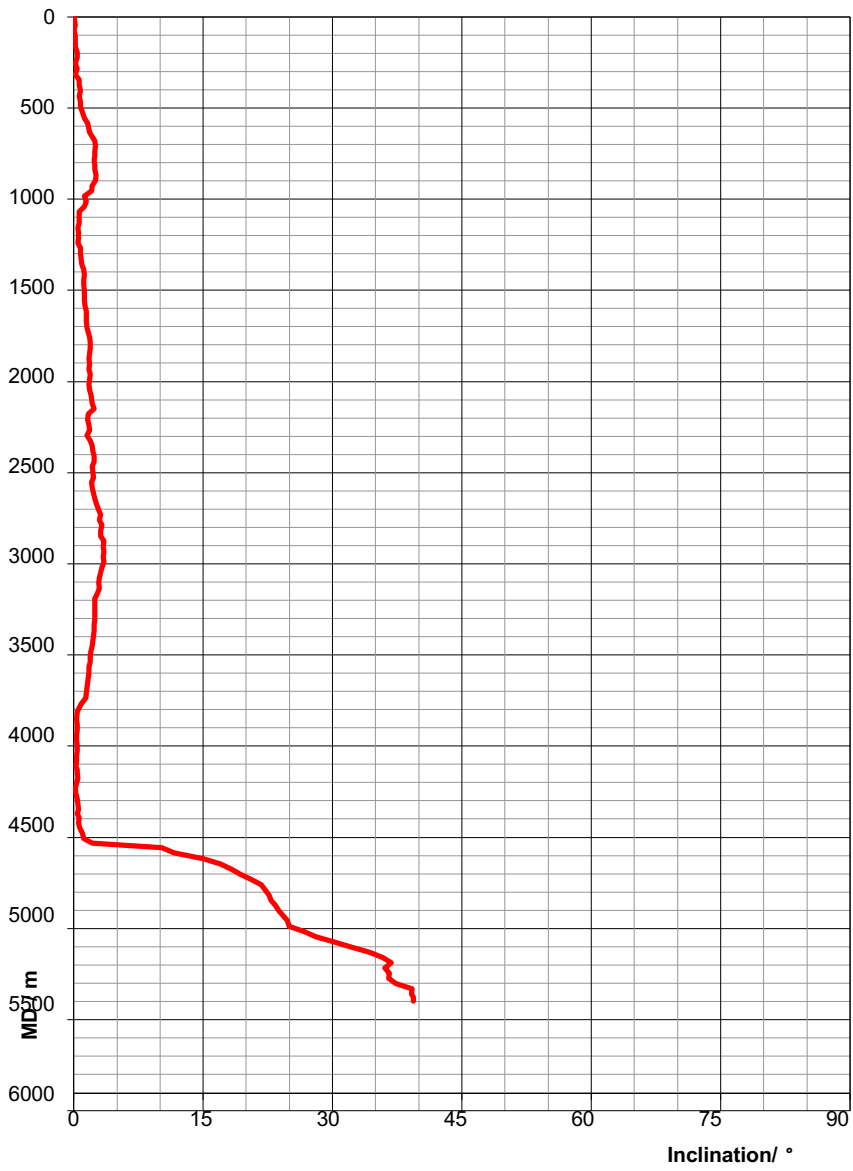


Figure A - 8: Depth vs inclination of STR T 5a.

Straßhof Tief 5a - Dogleg Plot

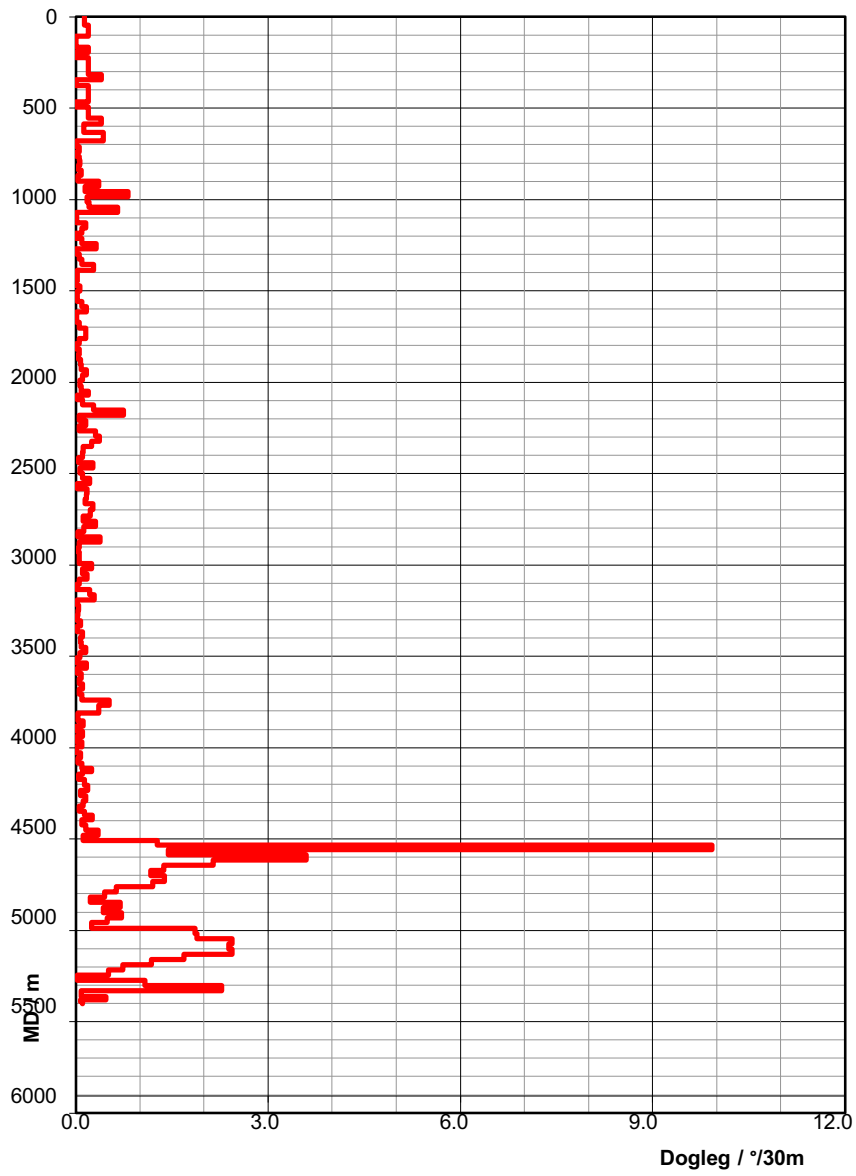


Figure A - 9: Depth vs Dogleg of STR T 5a.

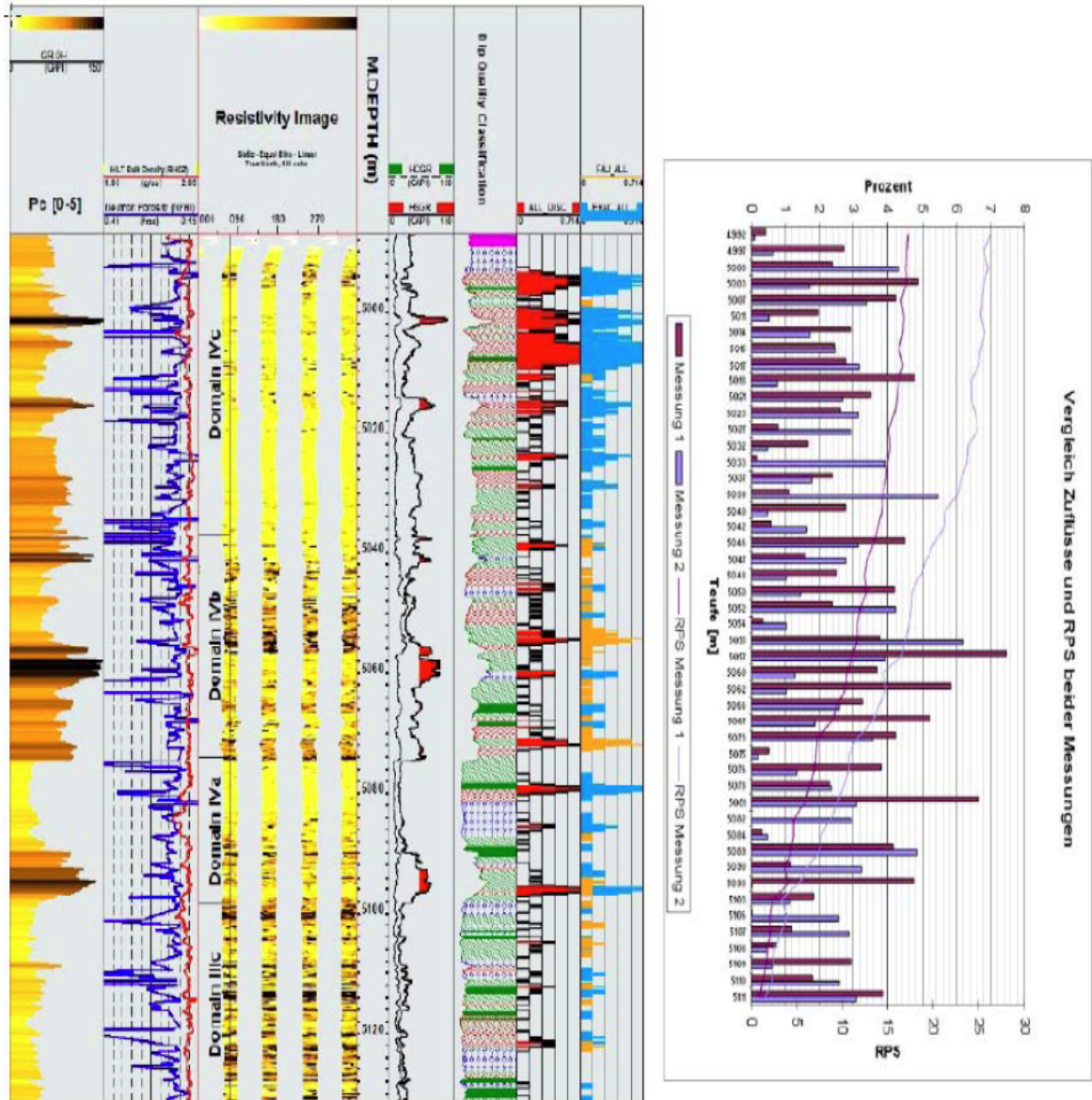


Figure A - 10: On the left the logs for fractures detection are shown, on the right the inflow in dependence of depth, measured by the production logging tool [84].

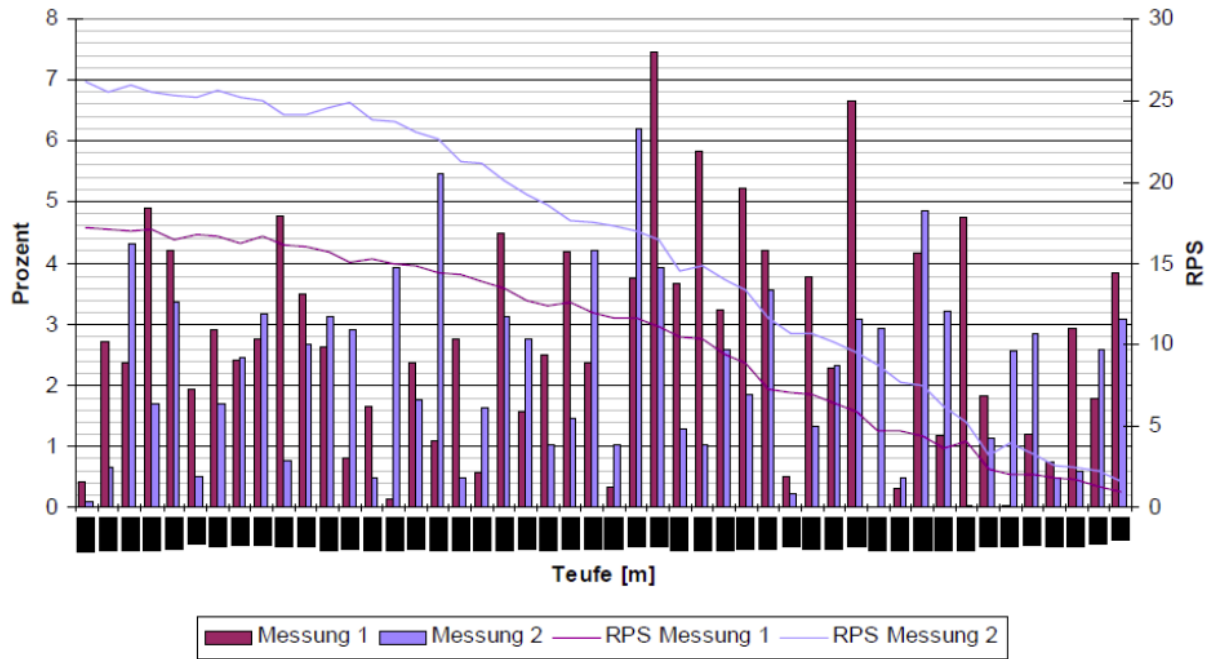


Figure A - 11: The two measurements of the inflow in dependence of depth detected by the PLT runs [84].

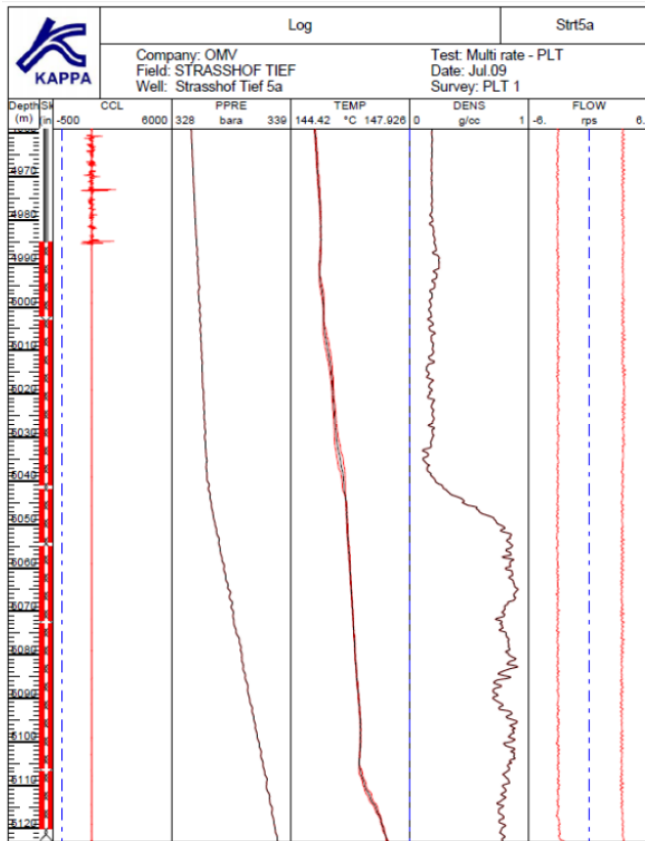


Figure A - 12: Result from the PLT run made in 2009. The sudden decrease in density at 5040 m MD indicates the GWC. To a smaller degree this can also be observed with the PPRE and the temperature log [84].

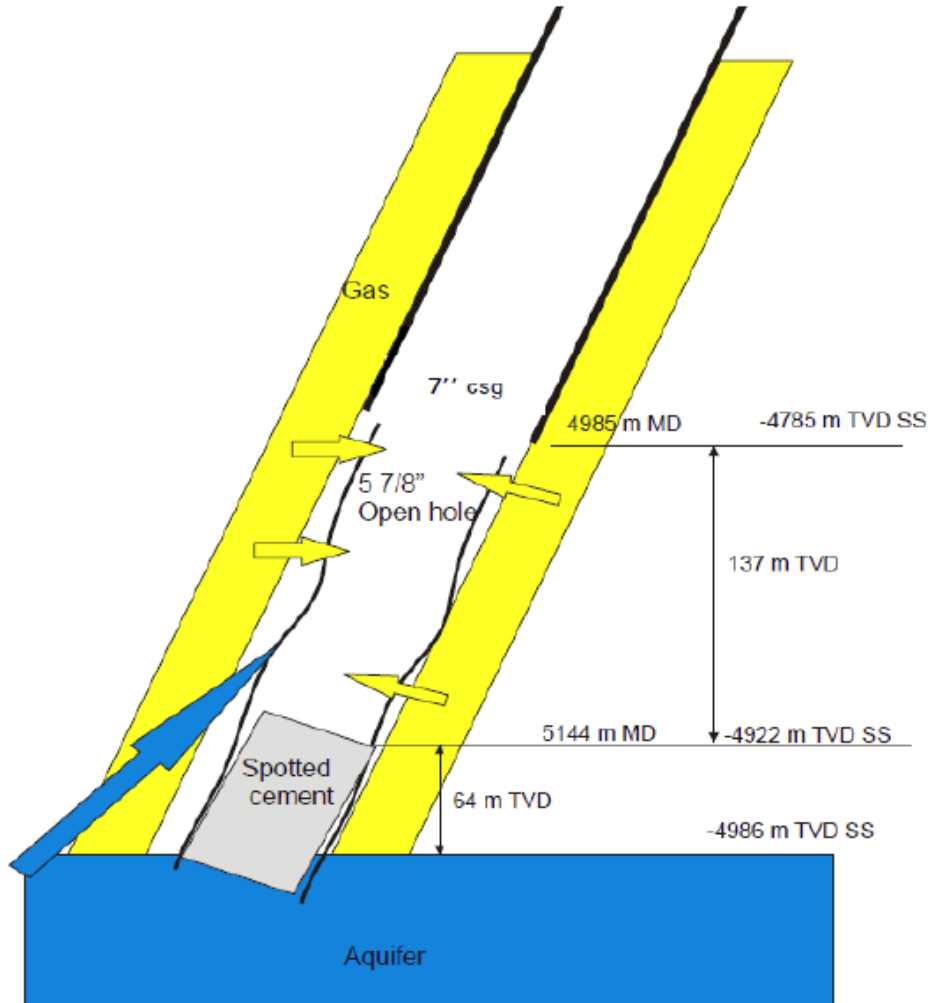


Figure A - 13: Scheme of STR T 5a. The cement was used to reduce water production. However, water coning still occurred, as the fractures connected the wellbore with the aquifer [84].

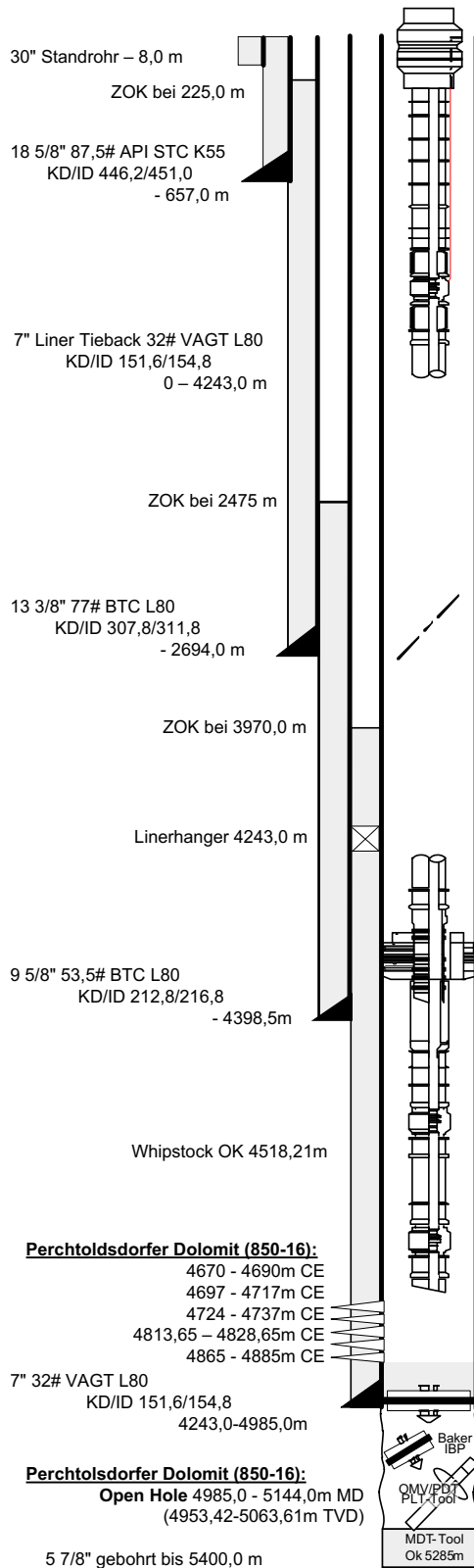


Figure A - 14: Cased-hole completion from June 2010 till end of 2013.

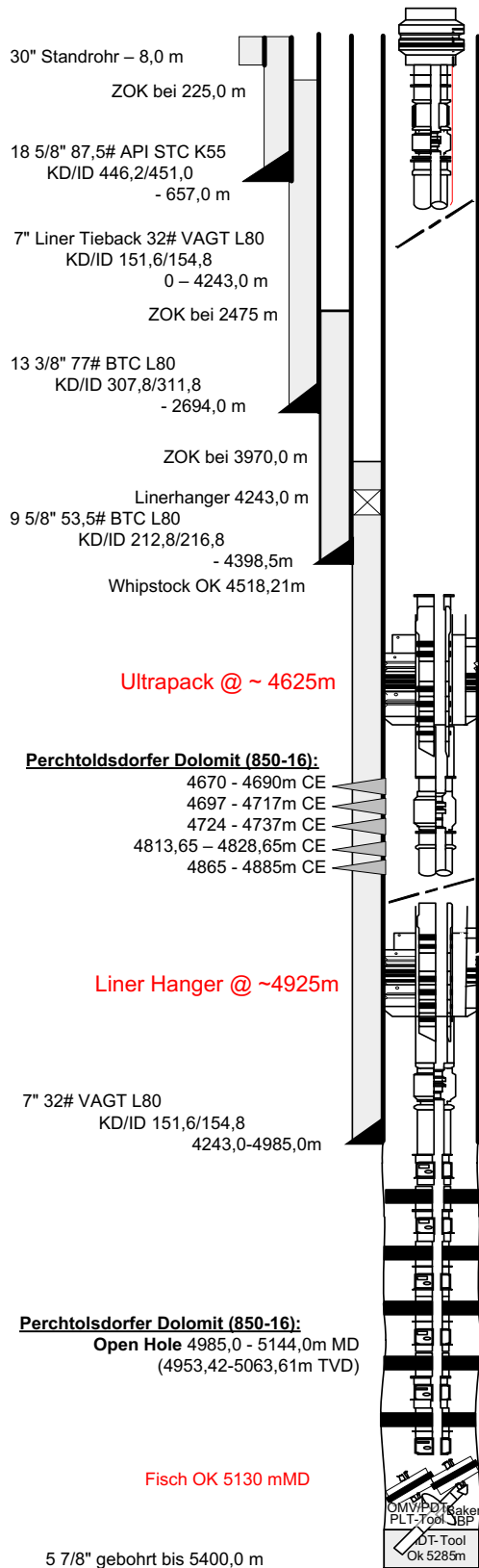


Figure A - 15: Current open-hole completion with 4 zones, isolated by swellable packers.

Table A - 9: Reservoir parameters

MPWHP [bar]	375
BHP [bar]	435
BHT [°C]	145
Production intervals [m]	Logging depth 4985-5000 (SSD4: 4991) 5003-5074 (SSD3: 5025) 5101-5074 (SSD2: 5077) 5104-5144 (SSD1: 5107)
H2S	2%
CO2	12%

Table A - 10: Wellbore parameters

Minimum ID	57 mm at WLRSV 50 m		
Total Depth	5400 m, plug back to 5144m (TOC) but Wiper Plug set at 5129 m		
	ID	Depth	Volume
4.5" Tubing	100.5 mm	4930 m	40 m3
3.5" Tubing	75.9 mm	98 m	0.95 m3
Wellhead Connection	4-1/16" 10000 psi		

Table A - 11: Perforation history

Date	Perforated interval [m MD]	Gun type	Shot density [shots/foot]	Phasing [°]
07.10.2009	4670-4690 4697-4717 4724-4737	TCP	6	60
10.06.2010	4813-4828 4865-4885	TCP	6	60

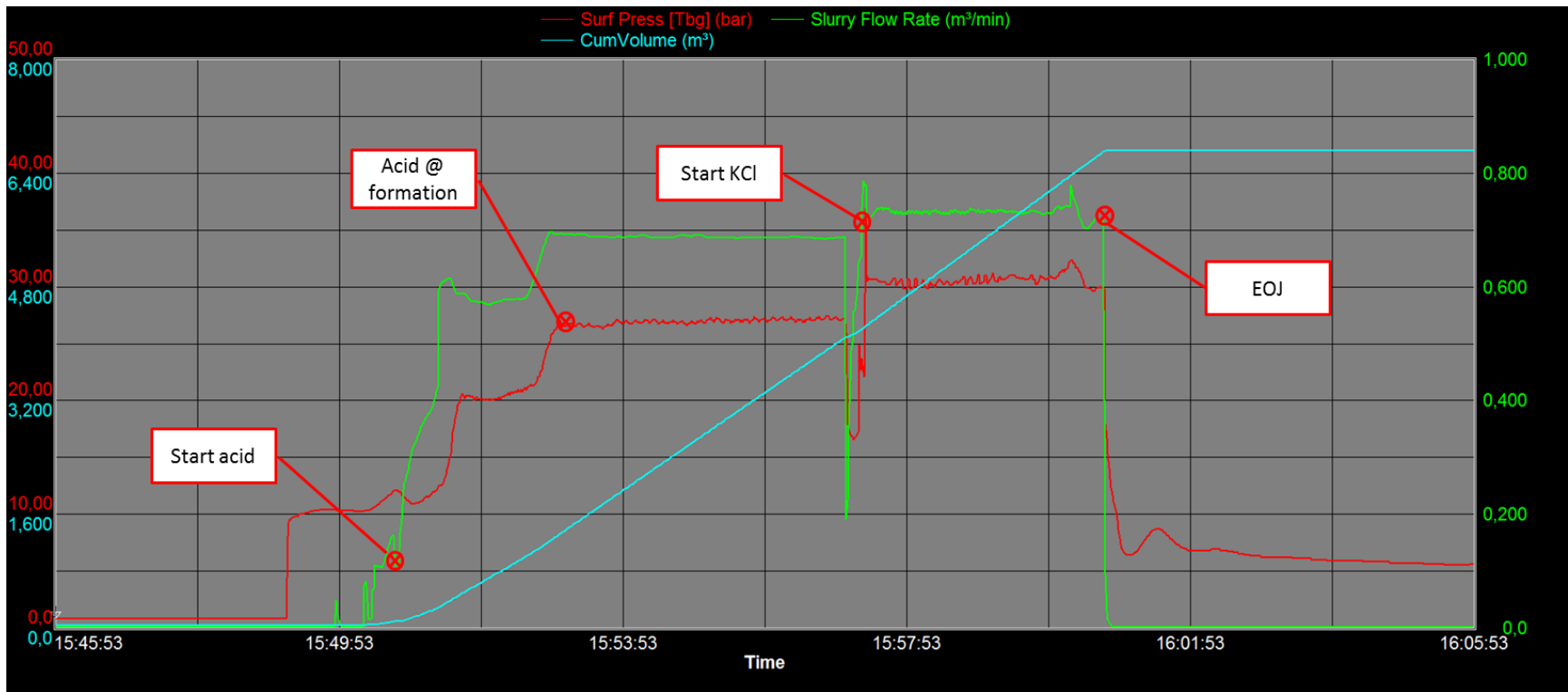


Figure A - 17: Graph treatment 1. The well flowing pressure was calculated with the software "Prosper".

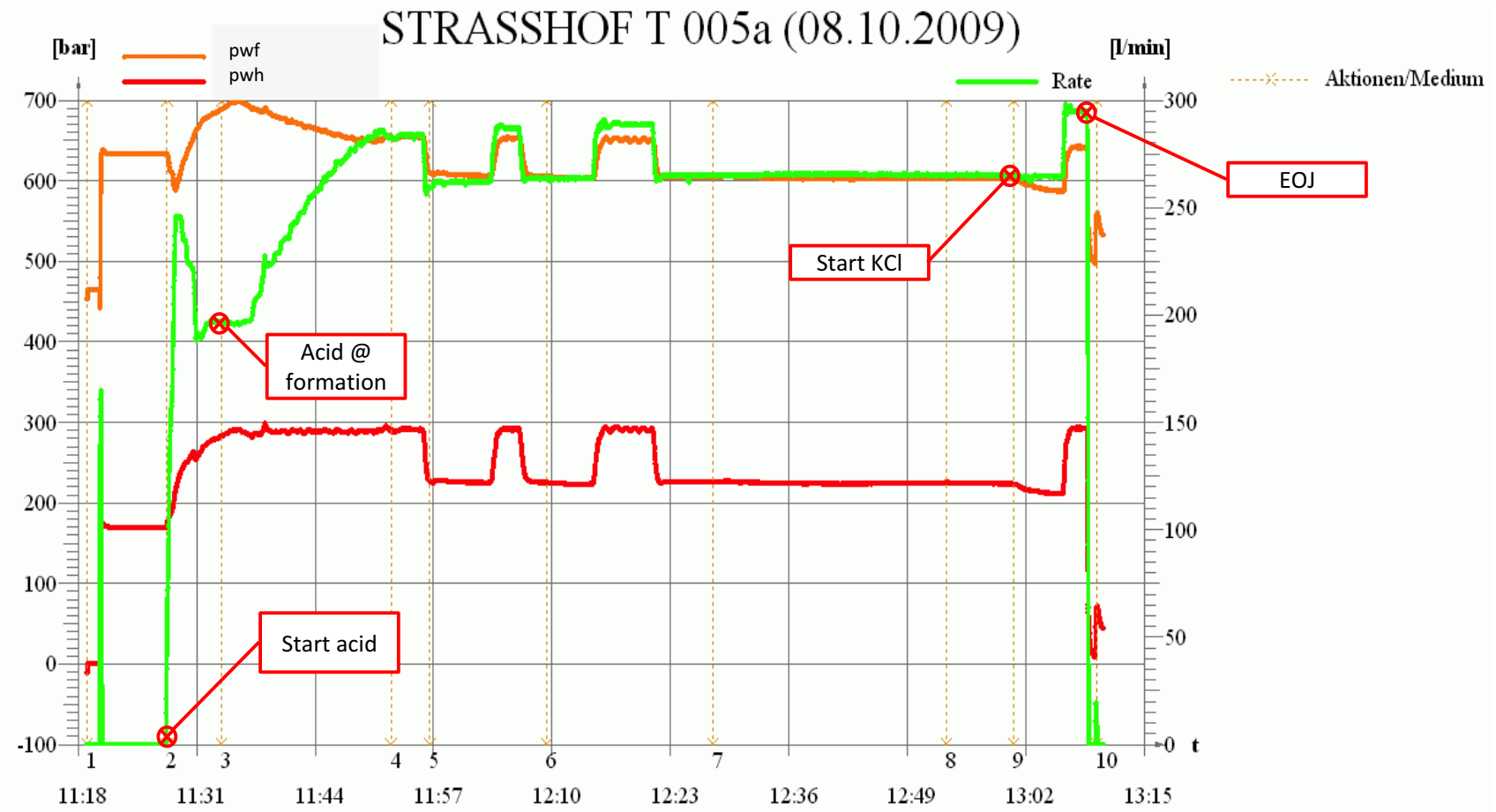


Figure A - 18: Graph treatment 2

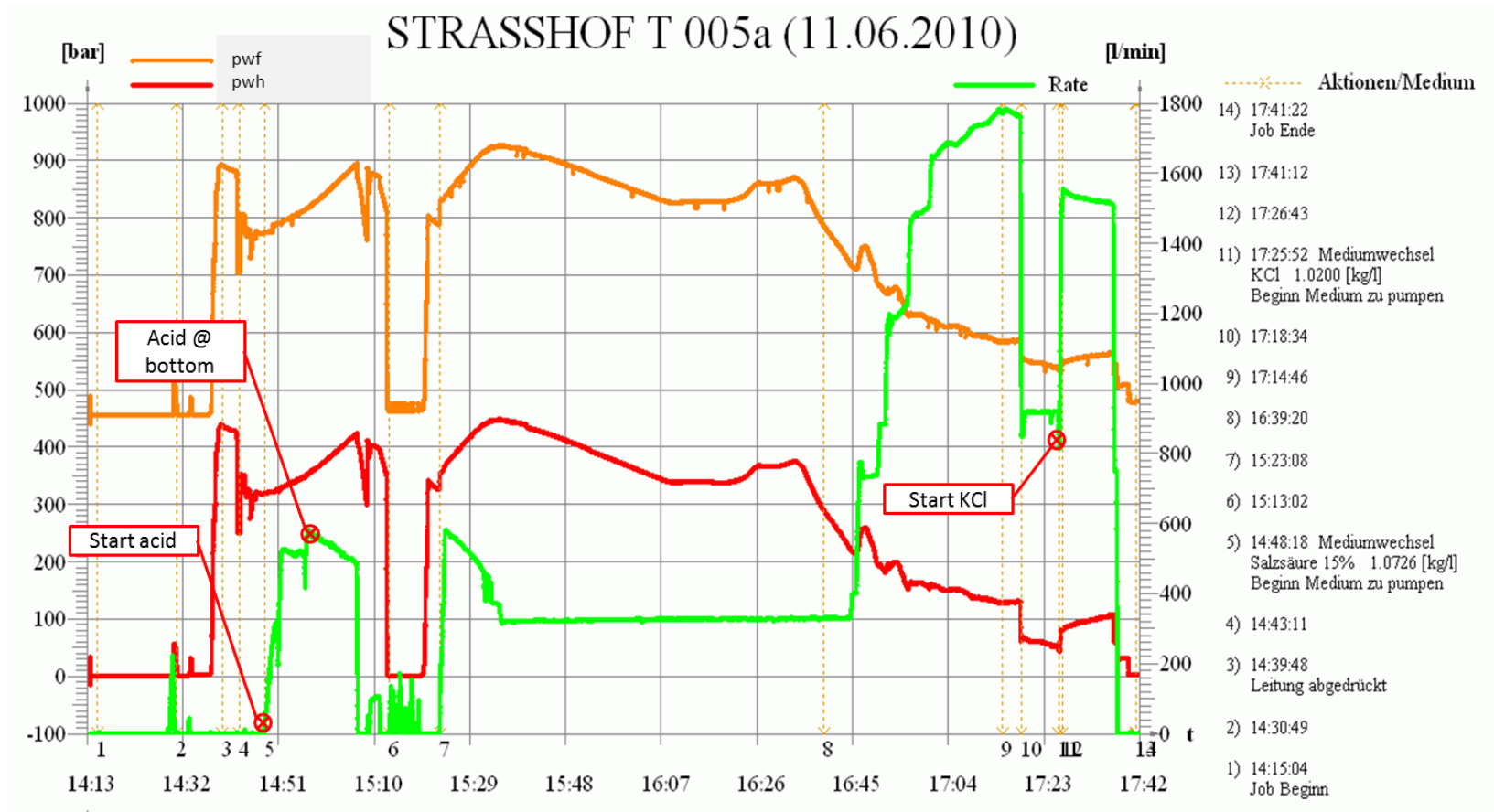


Figure A - 19: Graph treatment 3

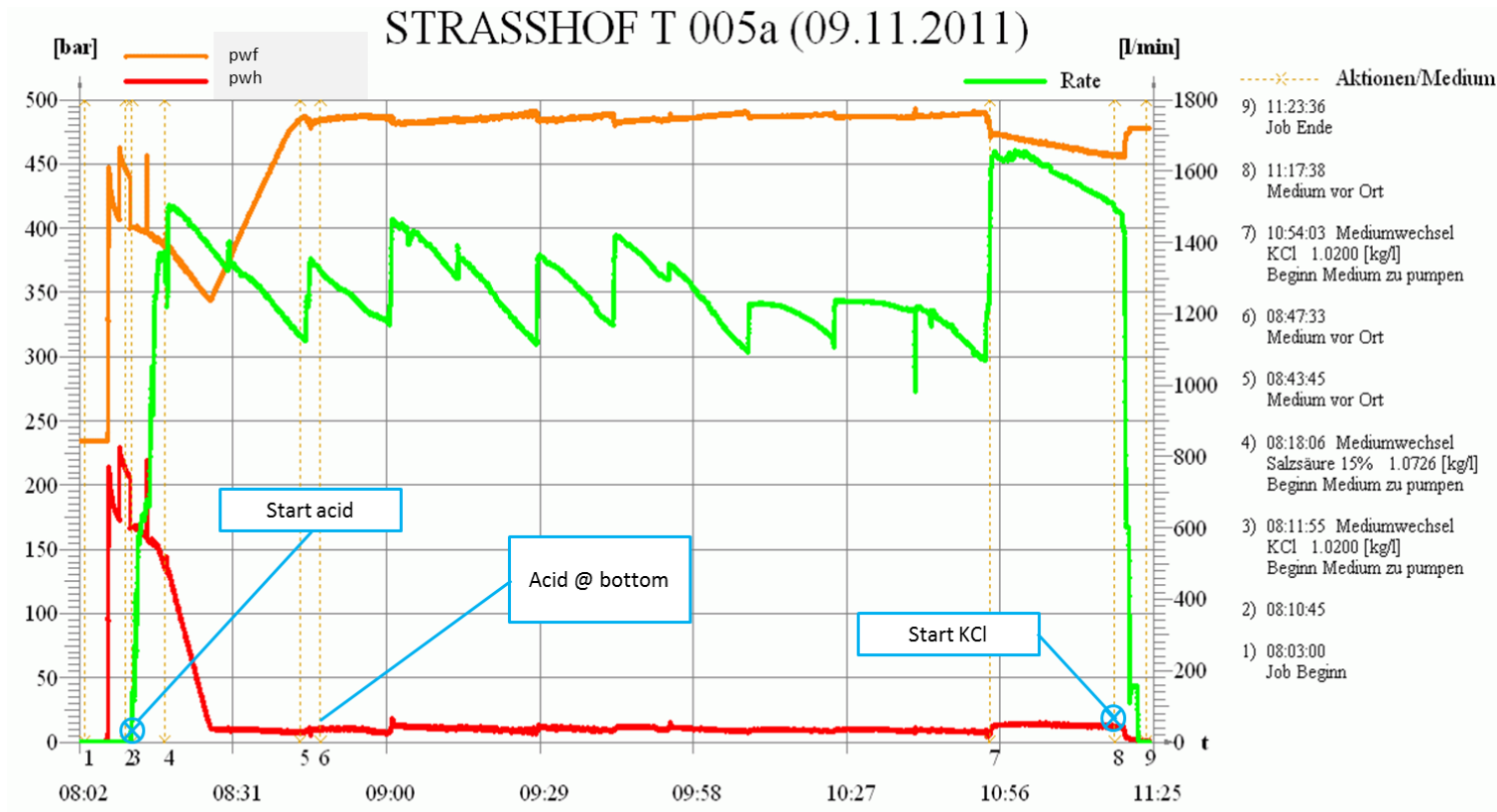


Figure 43: Graph treatment 4

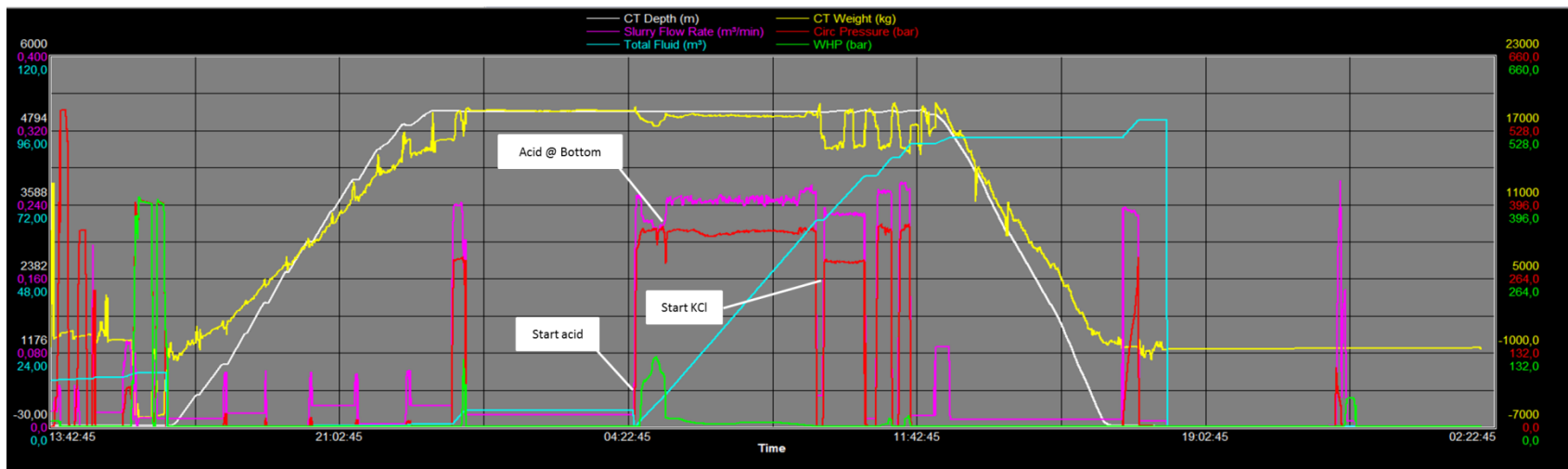


Figure A - 20: Graph treatment 5 SSD 1. The well flowing pressure was calculated with the software "Prosper".

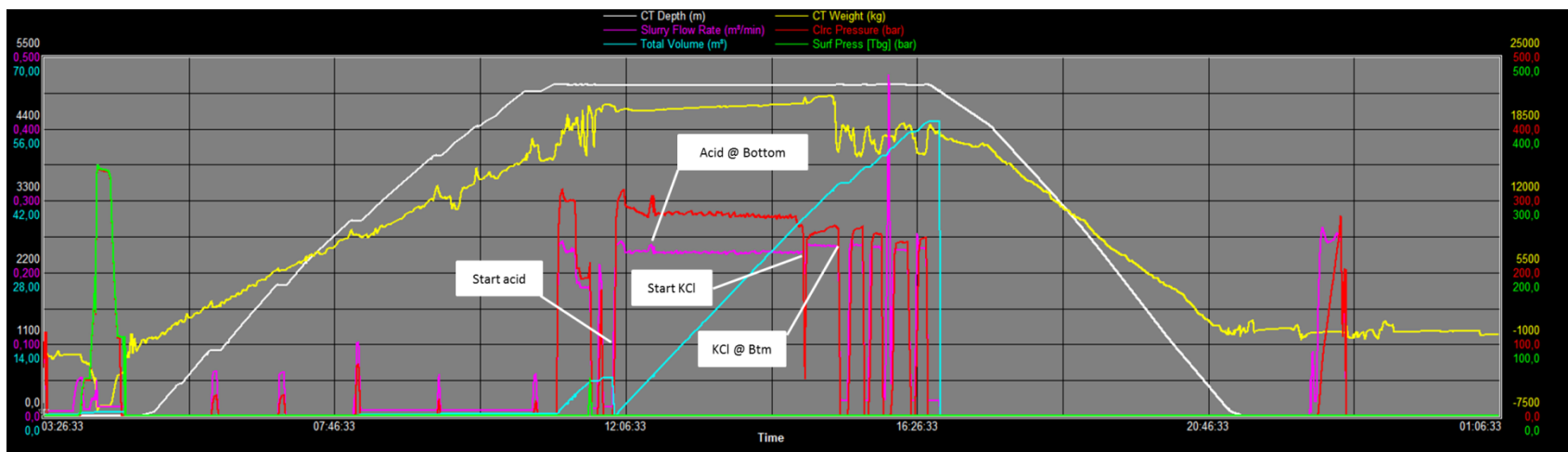


Figure A - 21: Graph treatment 5 SSD 2. The well flowing pressure was calculated with the software "Prosper".



Figure A - 22: Graph treatment 5 SSD 3. The well flowing pressure was calculated with the software "Prosper".

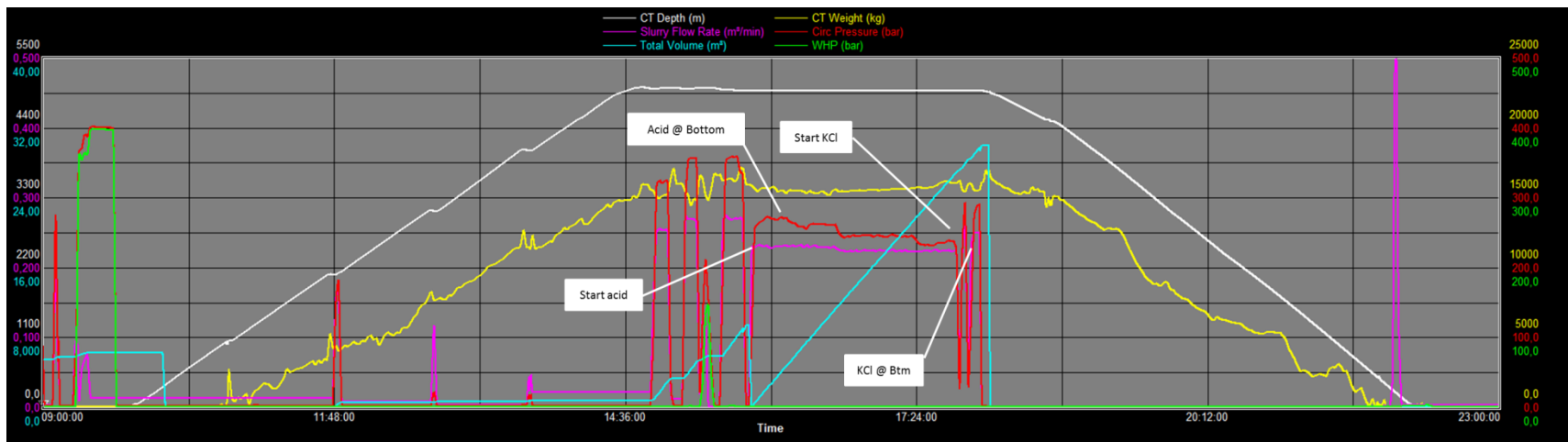


Figure A - 23: Graph treatment 5 SSD 4. The well flowing pressure was calculated with the software "Prosper".

Table A - 12: Stimulation results

Stimulation date	Stimulation Interval [m]	Kind of formation	Kind of interval	Flow Conduit	Pressure initial (bar)	Pressure final (bar)	Injection rate initial (l/min)	Injection rate final (l/min)	pres [bar]	II_initial	II_final	Improvement Injectivity [%]	Change in producing interval	Gas rate [m3/day] before	Gas rate [m3/day] after	Production Improvement [%]
28.10.2006	4985 - 5144	Hauptdolomite	OH	CT	828	820	250	270	483	1,0434783	1,153709199	11	first time from OH	-	500.000	-
08.10.2009	4670 - 4690 4697 - 4717 4724 - 4737 4985 - 5144	Plattendolomite Plattendolomite Plattendolomite	CH CH CH OH	CT	690	600	200	265	465	1,28	2,826666667	121	additionally perforated	-	125.000	-
11.06.2010	4670 - 4690 4697 - 4717 4724 - 4737 4813 - 4828 4865 - 4885	Plattendolomite Plattendolomite Plattendolomite Hauptdolomite Hauptdolomite	CH	BH	820	550	580	1500	435	2,1693506	18,7826087	766	additionally perforated	-	100.000	-
09.11.2011	4670 - 4690 4697 - 4717 4724 - 4737 4813 - 4828 4865 - 4885	Plattendolomite Plattendolomite Plattendolomite Hauptdolomite Hauptdolomite	CH CH CH OH CH	BH	485	455	1300	1500	435	37,44	108	188	no change	40.000	60.000	50
13.01.2014	5104 - 5144	Hauptdolomite	OH	CT	826	829	249	260	435	0,9170332	0,950253807	4	OH re-opened	-	-	-
15.01.2014	5074 - 5101	Hauptdolomite	OH	CT	765	790	228	29	435	0,9949091	0,117633803	-88	OH re-opened	-	-	-
16.01.2014	5003 - 5052	Hauptdolomite	OH	CT	844	745	220	245	435	0,7745721	1,138064516	47	OH re-opened	-	-	-
17.01.2014	4985 - 5000	Hauptdolomite	OH	CT	739	718	232	225	435	1,0989474	1,144876325	4	OH re-opened	-	-	-